NASA Technical Memorandum 104613

Spacecraft Attitude Determination Accuracy From Mission Experience

D. Brasoveanu
J. Hashmall
Computer Sciences Corporation
Lanham, Maryland

D. Baker
Goddard Space Flight Center
Greenbelt, Maryland

National Aeronautics and
Space Administration

Goddard Space Flight Center
Greenbelt, Maryland 20771
1994

This publication is available from the NASA Center for AeroSpace Information,
800 Elkridge Landing Road, Linthicum Heights, MD 21090-2934, (301) 621-0390.

Preface

This document was prepared with the content standard for Technical Memorandums.

Questions concerning this document or proposed changes shall be addressed to

E. Ketchum
J. Koppersmith
Code 553
Goddard Space Flight Center
Greenbelt, Maryland 20771

Abstract

This document presents a compilation of the attitude accuracy attained by a number of satellites that have been supported by the Flight Dynamics Facility (FDF) at Goddard Space Flight Center (GSFC). It starts with a general description of the factors that influence spacecraft attitude accuracy. After brief descriptions of the missions supported, it presents the attitude accuracy results for currently active and older missions, including both three-axis stabilized and spin-stabilized spacecraft. The attitude accuracy results are grouped by the sensor pair used to determine the attitudes. A supplementary section is also included, containing the results of theoretical computations of the effects of variation of sensor accuracy on overall attitude accuracy.

Keywords: accuracy, AE, AEM/HCMM, AEM/SAGE, attitude, CTS, DE, ERBS, EUVE, GOES, GRO, IMP, ISEE, IUE, MAGSAT, SAMPEX, SAS, satellite, SEASAT, sensor accuracy, sensor pair, SIRIO, SMM, spin-stabilized, SSS, three-axis stabilized, TOPEX/POSEIDON, UARS

Contents

Figures

Tables

Section 1. Executive Summary and Conclusions

This section describes the organization and content of the document and provides a description of how it might be used. A brief sensor performance and attitude determination accuracy summary review are included to provide general mission planning guidelines.

This report is a compendium of information about the attitude determination accuracy that can be expected from using a given sensor complement. The report is based on flight data available to the Attitude Section of the Flight Dynamics Division (FDD) at Goddard Space Flight Center (GSFC). It is expected to be useful in the early mission planning and design stages of future spacecraft.

1.1 Document Organization

Section 2 of this report provides a general description of the factors that influence attitude determination accuracy. This description is based on attitude principals and broad mission experience rather than on the experience with particular missions and is useful as background in understanding the specific mission experience in later sections. It explains the factors that influence the accuracies presented in later sections.

Section 3 provides brief mission descriptions, including their sensor complements and goals. The section is divided into subsections describing three-axis-stabilized spacecraft and spin-stabilized spacecraft. For each mission, the description includes the mission profile, the sensors flown, their orientations, their accuracies (especially of any mission-specific or unusual sensors), and any other factors that influence attitude accuracy.

Section 4 contains information on the attitude determination accuracies obtained by the various missions arranged according to the pair of sensors used in the solution. It is divided into subsections for three-axis-stabilized and spin-stabilized spacecraft. Section 4 also contains a number of graphs that display in an easily understandable visual format the relative attitude accuracies. Separate graphs that display a summary of the results for all sensor pairs described are provided.

Section 5 contains supplemental studies performed using the Attitude Determination and Error Analysis System (ADEAS). These studies provide theoretical estimates of attitude uncertainty determination where the actual mission data are unavailable. They use sensor pairs in the configurations and mission profiles of specific missions. The theoretical results are designed to provide guidance for attitude determination accuracy where the actual mission data are unavailable. They show how the overall attitude determination accuracy varies as the measurement accuracy of the sensors is systematically changed from nominal values.

1.2 Document Use

The document can be used by mission planners and designers as, among other things, an aid in determining what attitude hardware is needed for a mission, how it will be placed, and what data rates should be used for the attitude sensors.

The document's use is best illustrated with an example. Suppose a mission planner is given certain attitude determination accuracy requirements (usually to meet science data processing needs) for a three-axis-stabilized spacecraft and must equip the spacecraft with attitude sensors to meet these requirements. The planner should look first to Figure 4-6 which summarizes the approximate attitude determination accuracies for past three-axis-stabilized missions using various sensor combinations. This figure should give the mission planner an idea of which sensor combinations could realistically meet mission requirements. The mission planner would then review the subsections in Section 4 corresponding to these sensor combinations to obtain more detailed information. Sections 2 and 3 would alert the planner to various factors that could influence the attitude determination accuracy for the mission. If these factors can be characterized numerically in terms of degradation in the individual sensor measurement accuracies, then the theoretical results, presented in Section 5, may be used to scale the attitude determination accuracy results of old missions to the expected attitude determination accuracies for the new mission.

1.3 Overview

The attitude sensors used on board three-axis-stabilized spacecraft included in the survey are (see Section 2): the fixed head star tracker (FHST) (References 8 and 11), the charge coupled device star tracker (CST), the fine Sun sensor (FSS) (References 1, 2, 5, and 8), the fine-pointing Sun sensor (FPSS) (Reference 11), the digital Sun sensor (DSS) (References 2, 3, and 4), the horizon scanner (HS) (References 2, 3, 4, and 8), the static Earth sensor (SES), and the three-axis magnetometer (TAM) (References 2, 3, 4, and 7). For three-axis-stabilized missions the sensor accuracies ranged from 0.001 to approximately 0.7 deg (1σ). The most accurate sensor is the CST (3 arc sec measurement accuracy, 1σ), followed by the FPSS (5 arc sec, 1σ), the FHST (10 arc sec, 1σ) and the FSS (60 arc sec, 1σ). The DSS has a measurement uncertainty of no less than approximately 0.15 deg. Using an Earth infrared emission model, the HS measurement can attain an uncertainty of 0.2 to 0.3 deg. The SES can attain approximately 0.1 deg. Due to current Earth magnetic field modeling limitations TAMs can attain an accuracy of no better than 0.3 deg to 0.4 deg. Further Earth magnetic field modeling refinements can significantly reduce this uncertainty since the instrument design itself does not impose such a poor accuracy limit.

The attitude sensors used on board spin-stabilized spacecraft included in the document are (see Section 2): the single-axis FSS (Reference 18), the single-axis DSS (References 3, 4, 15, 16, 17, 20, and 21), the V-slit Sun sensor (References 22, 23, and 26), the single- and multiple-slit star scanner (Reference 3), the body-mounted horizon scanner (BHS) (References 3, 4, 12, 18, 19, 20, 21, 22, 23 and 26), and the TAM (Reference 25). Their accuracies range from 0.02 to approximately 1 deg. The most accurate sensors are the single-axis FSS (60 arc sec, 1σ) and the multiple-slit star scanner (0.033 deg, 1σ). Like the two-axis DSS, the single-axis DSS can achieve no better than approximately 0.15 deg. The BHS is similar in performance to the HS, attaining an accuracy of about 0.2 to 0.3 deg. The single-slit star scanner achieved approximately 0.3 deg. The TAM achieved approximately 0.7 deg.

The listed accuracies can be achieved only after calibration and in optimum circumstances. Various error sources can be present and degrade the accuracy. The most important error sources are: stray light and bright objects, the South Atlantic Anomaly (SAA), the measurement time uncertainty, the star magnitude, the near neighbor interference, the Earth atmosphere

temperature variation, the Earth atmosphere refraction, the telemetry data precision, the Earth magnetic field, and bit flipping. Stray light can disable an FHST. Stray light can induce errors of several arc sec in FPSS measurements. The error induced in single-axis and two-axes FSS measurements can exceed one arc min. The error induced in HS and SES measurements can attain 0.4 deg. The SAA can induce errors of more than 20 arc sec in FHST position measurements. The measurement time uncertainty can produce errors of 30 arc sec or more in FHST, of 0.003 deg in single- and two-axis FSS, and 0.01 deg in multiple-slit star scanners. Dim star measurements can have random errors of up to 11 arc sec. Near neighbor stars induce FHST and CST measurement errors of up to 7 arc sec. The Earth atmosphere temperature variation can induce errors of up to 0.1 deg in SES measurements, and up to 0.3 deg in HS and BHS measurements. The Earth atmosphere refraction can produce errors of up to 0.1 deg in single- and two-axis FSS and DSS measurements, as well as in multiple-slit star scanners. The current telemetry data precision is responsible for errors of up to 8 arc sec in FHST measurements, 0.003 deg in single- and two-axis FSS measurements, 0.13 deg in single- and two-axis DSS measurements, 0.005 deg in BHS measurements, and up to 0.2 deg in TAM measurements. The Earth magnetic field model errors can induce errors of up to 0.4 deg in the TAM measurements. Bit flipping can affect any sensor and the errors can be very large.

The common mitigating techniques used for FHST and CST are: using sunshades; avoiding pointing the instrument near Sun, Earth, or Moon; removing observations if target star is near a planet or when the instrument is occulted by Earth; when the spacecraft is in the SAA, limiting the star reference catalog to brighter stars; removing any catalog star with bright neighbors; correcting sample time for spacecraft rotation; and not using data if target star image is near the Earth limb. For FSS and single-axis FSS, the analyst should look for anomalous data and not use them, and correct measurement times for spacecraft rotation. The analyst should also discard data if the Sun is near the Earth limb, should correct sample time to reduce the measurement time uncertainty effect, and use a large number of observations. For HS and BHS look for anomalous data and do not use them; use an Earth radiance model, or atmosphere temperature measurements, and use correct Earth oblateness model. In addition, the SES can benefit from avoiding measuring in the quadrant where error sources are present by changing the operation mode. DSS measurements taken near Earth limb should not be used. TAMs should not be used in the SAA, and the most accurate available Earth magnetic field model should be used for calibrating them. TAM calibration should also consider coupling with magnetic torquers and TAMs should be placed as far away as possible from instruments that generate magnetic fields. Star scanner measurements taken near Sun, Moon, and Earth limb should not be used, while time corrections and a large number of observations can reduce the effect of measurement time uncertainty. All anomalous sensor data should be discarded, and the usage of large amounts of data is always recommended.

Neither a single sensor producing a single observation vector (the Earth vector or the Sun vector, for example) nor parallel observation vectors (the Sun and Earth magnetic field) provide enough information to determine all three axes; therefore, the sensor complements include at least two instruments, preferably oriented and scheduled to minimize parallel viewing. For three-axis-stabilized missions, the most accurate sensor complements are two CSTs, CST plus FPSS, FHST plus FPSS, two FHSTs, CST plus FSS, and FHST plus FSS. In general, three-axis-mode sensors provide two angular measurements. Spin mode sensors normally provide only one, either the arc length separation between the spin axis and a known reference vector, or a rotation angle

between two known vectors. Therefore, in order to determine the orientation of the spin axis, two measurements provided by different sensors are needed. For spinning missions the most accurate complement consists of a single-axis FSS and a V-slit star sensor. The attitude accuracies attained by the missions included in this survey are summarized in a plot in Figure 4-6 and Figure 4-13 (see Section 4 for more details). Three-axis-stabilized mission attitude determination accuracies per axis ranged between 3 arc sec and 2 deg (1σ). The most accurate attitude determinations were achieved by the Extreme Ultraviolet Explorer (EUVE) (3 arc sec per axis) using two FHSTs, and by the Solar Maximum Mission (SMM) (5 arc sec) using an FHST and an FPSS. The spinning missions achieved spin axis attitude determination accuracies in the 0.1 to 1 deg range (1σ). Among spinning spacecraft, the best attitude determination accuracies belong to the Italian Industrial Operations Research Satellite (SIRIO) and the Geostationary Operational Environmental Satellite-5 (GOES-5) (approximately 0.1 deg) using a V-slit Sun sensor and an Earth sensor. Missions using two FHST sensor complements attained accuracy in the 3 to 20 arc sec range per axis. Spacecraft using an FHST and an FPSS attained accuracies between 5 and 10 arc sec. The FHST plus FSS sensor complement attained accuracies in the 10 to 40 arc sec range. Missions using an FHST and an HS achieved accuracies of approximately 20 arc sec. Those using an FHST and a TAM achieved between 12 and 80 arc sec. Spacecraft using an FSS and an HS achieved accuracies in between 0.08 deg and 0.15 deg. The missions using FSS and TAM achieved accuracies between 0.15 and 0.4 deg. The DSS plus HS sensor complement attained accuracies in the 0.2 to 0.3 deg range. The single mission equipped with a DSS and a TAM included in the survey attained approximately 0.5 deg. The single spacecraft using an HS and TAM pair attained an accuracy of approximately 0.3 deg. The TAM only accuracies were between 0.25 and 1.6 deg. Spinning satellites using a multiple-slit Sun sensor and a BHS attained attitude determination accuracies in the 0.1 to 1 deg range. The only mission equipped with a multiple-slit star scanner and a single-axis DSS attained approximately 0.3 deg. The only spinning mission included in the survey that used a single-axis FSS and a BHS attained approximately 1 deg. Those using a single-axis DSS and a BHS attained between 0.15 and 0.6 deg. The only satellite surveyed that used a single-slit star scanner and a single-axis DSS attained approximately 1 deg.

Maximum attitude determination accuracy is attained when the instrument boresights are perpendicular, since the uncertainties depend on the sine of the angle between the observations. The attitude determination accuracy also depends on the attitude determination algorithm and the amount of data used. Single-frame solutions provide less accuracy than multiple-frame methods such as the batch least-squares and the Kalman filter. Multiple-frame methods require data propagation; therefore, the gyro errors must be also analyzed.

The three-axis-stabilized missions included are: the Application Explorer Mission-1/Heat Capacity Mapping Mission (HCMM), Ocean Studies Satellite-1 (SEASAT-1), the Application Explorer Mission-2/Stratospheric Aerosol and Gas Experiment (SAGE), Magnetic Satellite Mission (MAGSAT), SMM, Dynamics Explorer-2 (DE-2), Earth Radiation Budget Satellite (ERBS), Gamma Ray Observatory (GRO), the Upper Atmosphere Research Satellite (UARS), Extreme Ultraviolet Explorer (EUVE), Solar, Anomalous, and Magnetospheric Particle Explorer (SAMPEX), and Ocean Topography Experiment (TOPEX/POSEIDON). The spin-stabilized missions included are: the Communications Technology Satellite (CTS), DE-1, Small Scientific Satellite-1 (SSS-1), Interplanetary Monitoring Platform-8 (IMP-8), International Sun-Earth

Explorer (ISEE-3), International Ultraviolet Explorer (IUE), GOES-3, GOES-5, Atmospheric Explorer-3 (AE-3), Small Astronomy Satellite-2 (SAS-2), and SIRIO (see Section 3).

Under the influence of various error sources, the attitude determination accuracy is degraded (see Section 5). A brief discussion of the effect of error sources on the most accurate sensor complements follows (for more details see Section 5). In a typical case, for a two-FHST sensor complement, the attitude determination uncertainty due solely to sensor noise can exceed 15 arc sec when the accuracy of one sensor is degraded to 100 arc sec. This is the measurement uncertainty of an uncalibrated FHST, or the worst value observed in the middle of the SAA. Similar attitude determination uncertainties result for the FHST and FSS complement, if the FHST accuracy is degraded to 100 arc sec, or the FSS measurement uncertainty attains 0.05 deg. Due to insufficient data, the CST was not included in this study. For spin-stabilized spacecraft, considering an angle between sensor boresights of at least 30 deg, the attitude uncertainty is roughly proportional to the inverse of the square root of the number of observations.

1.4 Conclusions and Recommendations

The attitude determination accuracy survey included 11 spin-stabilized and 12 three-axis-stabilized missions. The sensors used by the three-axis-stabilized missions include FHST, FSS, DSS, Earth sensor, and magnetometers. Most of the recent three-axis-stabilized missions use gyros to propagate measurement data. The attitude sensors used by the spin-stabilized missions surveyed include single- and multi-slit star scanners, single-axis DSSs, single-axis FSSs, body-mounted Earth sensors, and magnetometers.

The overall accuracy of spin-mode sensors used ranges from 0.05 to about 1 deg. For the three-axis-stabilized missions the accuracy ranges from 0.001 to about 1 deg. The most accurate sensors used on board the three-axis-stabilized missions are the FHST, the related charge-coupled device (CCD) star trackers, and the FSS. These instruments achieve high accuracy but at high cost.

Because sensors commonly used on three-axis-stabilized missions are more accurate than those used on spin-stabilized missions, the best attitude determination accuracies come from three-axis-stabilized missions. For spinning missions, the attitude determination accuracy ranged from 0.1 to 1 deg. For three-axis-stabilized missions the attitude determination accuracy ranged from 0.001 to 2 deg.

To reduce the cost, 1-revolution-per-orbit (rpo) missions that do not require an attitude determination accuracy of less than 0.2 deg could use DSSs and an HS. To attain the same accuracy, inertial missions could use DSSs and magnetometers. For attitude determination accuracies of less than 0.1 deg, FHSTs or CSTs are required. If an attitude determination accuracy of less than 5 arc sec is required, CSTs and FPSSs are recommended. Spin-stabilized missions that require an accuracy no better than 0.2 deg could use HSs and DSSs. If a spin-axis determination accuracy of better than 0.2 deg is required, a multi-slit star sensor and a single-axis FSS should be used. Missions that require an attitude determination accuracy no better than 0.4 deg could use magnetometers only (to achieve these levels three-axis-stabilized missions must also be equipped with gyroscopes).

Section 2. Influences on Attitude Accuracy

This section contains a discussion of the factors influencing the attitude determination accuracy that can be obtained using a given sensor complement. These factors include the following:

- Sensors used in the attitude determination and their properties
- Geometry of these sensors on the spacecraft
- Accuracy of the sensor calibration
- Algorithms used for attitude determination
- Amount and quality of data used for attitude determination

This section provides a basis for the discussion of accuracies that have been attained by the various missions presented in Sections 3 and 4.

2.1 Sensor Complement

The most important factor limiting attitude determination accuracy is the choice of sensors. As a rule of thumb, if there is sufficient data and observability to reduce random errors, the accuracy of attitudes determined with a set of sensors cannot be much more accurate than the accuracy of the most accurate sensors.

In order to determine a three-axis attitude, at least three independent data items are required. These data can be obtained from two nonparallel unit vector measurements. Most sensors generate two angles—corresponding to a unit vector—so either two sensors, a single sensor measuring more than one target, or a single sensor with multiple measurements at different times (propagated to the same time) are used. In general, missions are designed so that two sensors suffice to meet attitude accuracy requirements.

For commonly used sensors, approximate sensor measurement accuracy limits are given in Table 2-1 for three-axis-stabilized satellites and Table 2-2 for spin-stabilized spacecraft. The sensors used for these two types of spacecraft are generally different and even in cases (such as horizon scanners) where the same type of measurement can be used in both types of spacecraft, the implementation often results in different errors.

These numbers should be viewed as approximate best-case measurement accuracy limits for the specified sensors assuming optimum calibration. In addition to sensor design, the actual accuracy of a single-sensor measurement depends on many other factors, such as sensor calibration accuracy, spacecraft attitude motion, position of a target in the sensor field of view (FOV), and spacecraft environment.

Table 2-1. Approximate Limits of Measurement Accuracy for Attitude Sensors Frequently Used on Three-Axis-Stabilized Satellites

Sensor	Limit of Achievable Sensor Accuracy (1σ)(deg)
CST	~0.00083 (3 arc sec)
FHST	~0.0028 (10 arc sec)
FSS	~0.017 (60 arc sec)
SES	0.1
DSS	0.2
HS	~0.25
TAM	~0.5

Table 2-2. Approximate Limits of Measurement Accuracy for Common Attitude Sensors Usually Used on Spin-Stabilized Satellites

Sensor	Limit of Achievable Sensor Accuracy (deg)
Single-axis FSS	0.015
V-slit star sensor	0.033
V-slit Sun sensor	~0.15
Single-axis DSS	0.25
BHS	0.25

Some spacecraft have been equipped with special sensors designed to meet particular mission attitude requirements. An example of such a sensor is the digital fine Sun sensor (DFSS) flown on the SMM, which was considerably more accurate than a standard FSS. This sensor is also sometimes referred to as an FPSS.

A summary of the estimated in-flight measurement accuracies of a number of common attitude sensors is given in Tables 2-3 and 2-4. The table contains data for only those missions for which explicit values have been published; these published values are presented without revision. Except where noted, the values represent estimates of the uncertainties after in-flight calibration has been performed (see Section 2.3).

For each sensor in this table, the missions in which it was flown and estimates of the random and systematic contributions to sensor uncertainty (e.g., noise and misalignments, respectively) are given in addition to the overall sensor uncertainty. The sensors are designated by the

Table 2-3. Measured Sensor Accuracies From In-Flight Data (1σ)—Three-Axis-Stabilized Missions (1 of 2)

Sensor (typical manufacturer)	Mission	Axis	Systematic Errors (deg)	Random Errors (deg)	Total Sensor Error (deg)	Reference
FHST (BECD)	SMM	pitch and yaw	0.0139	0.0042	0.014	11
	MAGSAT	pitch, roll, and yaw	0.003	0.003	0.004	8
FSS (Adcole)	MAGSAT	pitch and roll	0.006	N/A	N/A	8
		yaw	0.005	0.003	0.006	
	SEASAT-1	pitch	0.12	0.015	0.12	5
		roll	0.15	0.015	0.15	
		yaw	0.26	0.023	0.26	
	DE-2	all axes	0.1	N/A	N/A	12
DSS (Adcole)	AEM-1/HCMM	pitch	<0.05	0.14	0.14	2,3
		roll	<0.04	0.09	0.09	
	AEM-2/SAGE	pitch	0.2	0.14	0.25	4
		roll	0.2	0.09	0.22	
		yaw	0.2	0.23	0.3	
HS (Ithaco)	AEM-1/HCMM	pitch	0.45(1)	0.11	0.56(1)	2,3
		roll	1.2(1)	0.09	1.3(1)	
	AEM-2/SAGE	pitch	0.05	0.15	0.16	3,4
		roll	0.03	0.15	0.15	
	MAGSAT	pitch	<0.05	0.15	0.15	3,4,8
		roll	<0.2	0.5	0.5	

TABLE 2-3. Measured Sensor Accuracies From In-Flight Data (1σ)—Three-Axis-Stabilized Missions (2 of 2)

Sensor (typical manufacturer)	Mission	Axis	Systematic Errors (deg)	Random Errors (deg)	Total Sensor Error (deg)	Reference
	SEASAT-1	pitch	0.1	0.09	0.13	3,4,5
		roll	0.1	0.048	0.11	
	DE-2	pitch	0.1	<0.15	<0.2	3,12
		roll	0.05	<0.2	<0.2	
TAM (Schoenstedt)	SMM	all axes	N/A	0.7	0.7	11
	HCMM	all axes	~0.4	~0.35	~0.5	2
	SAGE	all axes	~0.4	1.1	1.2	3,4,7
NOTE (1) Before in-flight alignment						

Table 2-4. Measured Sensor Accuracies From In-Flight Data (1σ)—Spin-Stabilized Missions

Sensor	Mission	Systematic Errors (deg)	Random Errors (deg)	Total Sensor Error (deg)	Reference
Multi-slit star sensor	SAS-2	N/A	N/A	0.017	3
Single-axis FSS	ISEE-3	0.05	0.004	0.05	18
Single-axis DSS	CTS	0.12	0.08	0.14	15,16
	DE-1	0.2	N/A	0.1	4,12
	IMP-8	0.5	0.5	0.7	3
	IUE	0.25	0.25	0.35	20,21
	SSS-1	N/A	0.2	N/A	17
V-slit Sun sensor	GOES-3	0.15	0.2	0.25	22
	GOES-5	0.1	0.1	0.15	23
	SIRIO	0.1	0.003	0.1	26
BHS	CTS	0.12	0.02	0.12	15,16
	DE-1	0.2	0.05	0.2	4,12
	IMP-8	0.5	negligible	0.5	3
	IUE	0.5	0.8	1.0	20,21
	ISEE-3	0.25	0.25	0.35	18,19
	GOES-3	0.05	0.25	0.25	22
	GOES-5	0.09	0.05	0.1	23
	SIRIO	0.04	0.1	0.11	26
TAM	SAS-2	≈0.5	0.4	0.7	25

common names with which they are usually specified. This terminology is not standard and in some missions sensors may be referred to by names other than those given here. Some description of the sensors themselves is presented in Section 4. The references from which the data were obtained are also given. For descriptions of the missions referred to in this table, the reader is directed to the mission descriptions in Section 3 and to the glossary for the names of the satellites.

Each sensor has advantages and disadvantages in attitude determination. Examples of these are given in Table 2-5 for three-axis-stabilized satellites and Table 2-6 for spin-stabilized satellites.

The output of attitude sensors may be in one of several forms. Star trackers and Sun sensors provide angular displacements between the sensor boresight and detected targets. These displacements are processed to provide unit vectors in the direction of the target. Target position vectors are usually corrected for velocity aberration to provide maximum accuracy. Many CSTs will be capable of tracking more than one target at a time and

Table 2-5. Advantages and Disadvantages of Some Common Attitude Sensors Usually Used on Three-Axis-Stabilized Satellites

Sensor	Advantages	Disadvantages
CST	Accuracy, ability to provide information for complete three-axis attitude with one sensor	Small FOV, possible Earth, Moon, Sun interference, computational overhead of star identification, little mission experience available to determine the evolution of sensor properties in flight
FHST	Accuracy	Small FOV, complex calibration function, interference from Earth, Moon, Sun, computational overhead of star identification
FSS	Moderate accuracy, moderately wide FOV	Single target (Sun), Earth occultation, horizon distortion
SES	No target acquisition needed, attitude measurement can be obtained at any point in orbit	Same as HS but smaller perturbations, less interference, greater accuracy, and greater sensitivity to deviations from design attitude and orbit
DSS	Wide FOV	Limited accuracy, Single target (Sun), Earth occultation, horizon distortion
HS	No target acquisition needed, attitude measurement can be obtained at any point in orbit	Incomplete compensation for seasonal and latitude perturbations to infrared horizon height, limited accuracy, Sun interference, provides attitude data only when near design attitude and orbit
TAM	Attitude measurement can be obtained at any point in orbit, ability to provide information for complete three-axis attitude with one sensor	Very limited accuracy (mostly due to inaccurate Earth magnetic field model), bias often of significant magnitude that must be removed correctly

Table 2-6. Advantages and Disadvantages of Some Common Attitude Sensors Usually Used on Spin-Stabilized Satellites

Sensor	Advantages	Disadvantages
Multislit star sensor	Accuracy, wide coverage, angle and phase measurements	Few targets, interference by Earth, Sun, and Moon
Single-axis FSS	Wide coverage, moderate accuracy	Single target, Earth occultation
Single-axis DSS	Wide coverage	Single target, Earth occultation
V-slit Sun sensor	Wide coverage, angle and phase measurements	Single target, Earth occultation
BHS	Wide coverage, target always visible	Interference by Sun and Moon

will provide corresponding vectors for each target. Attitude determination using star or Sun vectors requires knowledge of the actual position of the star (from a star catalog) or the Sun (from a model of the Earth's orbit about the Sun). If high accuracies are needed, compensation for velocity aberration on the positions of the Sun and stars may be applied using relative velocities from Earth and spacecraft ephemerides.

Earth horizon sensors provide measurements of the Earth width, the angle between the Earth limb and an index in the sensor or (in the case of some Earth sensors on spin-stabilized satellites) times of Earth limb crossing. These data are often converted into spacecraft pitch and roll angles (yaw data are not available) but may also be converted to a nadir vector. Attitude determination using Earth horizon sensors requires knowledge of the spacecraft position and a model of the effective horizon height at which the sensor detects the Earth limb.

TAMs provide a complete vector directly. This vector includes the magnitude of the magnetic field as well as its direction. Attitude determination using TAMs requires knowledge of the spacecraft position and a model of the Earth's magnetic field as a function of position.

Slit sensors (on spin-stabilized satellites) provide measurements of the times at which targets are observed and often the angle between a target vector and the spin axis. Observation times provide spin rate information, while angle data can provide the spin axis direction.

Although they are attitude rate sensors rather than attitude direction sensors, the availability of gyroscopic inertial reference unit (IRU) data greatly affects both the manner in which attitudes are computed and the accuracy of the solutions. In the absence of IRU data, rate information can also be computed from differences in attitude sensor output at different times or from dynamic modeling. This computed rate information is generally less accurate than that derived from IRU measurements (which are normally extremely accurate) and results in less accurate attitudes. The attitude determination accuracies presented in Sections 4 and 5 assume that accurate gyro data are available, except where explicitly stated otherwise.

Without rate information or an accurate model with which to propagate attitudes, single-frame attitudes (attitudes using a set of sensors at a single time) and average attitudes may be determined. Multiframe batch methods have been used to produce average attitudes, even in the absence of rate information, but such methods must employ assumptions about the rates (e.g., constant rates, zero rates) and the attitude accuracies may be limited by the validity of these assumptions. Single-frame attitudes are generally limited in accuracy by the random error of the sensors which is usually (for a single measurement) larger than the systematic error. A series of single-frame solutions may also be averaged over a timespan to provide a more accurate average attitude.

If rate information or an accurate propagation is available, sensor measurements at various times can be propagated to give equivalent vectors at a single time. This procedure statistically reduces the random component of sensor error and allows more accurate attitudes to be determined. In addition, attitudes may be determined accurately for periods during which no sensor data are available by propagating attitudes determined with sensor data to the times in which sensor data are absent. Dynamic propagation models are rarely accurate for three-axis-stabilized satellites but may be quite accurate for spin-stabilized satellites.

2.2 Sensor Placement

Most sensors provide measurements of angles relative to the sensor position on the spacecraft. For many sensors (especially those on three-axis-stabilized spacecraft) enough angle data are provided to define a unit vector in the direction of a target. The direction of a target vector provides no information about the rotation angle around the target vector. For knowledge of spacecraft attitude in all three axes, observations of at least two different target vectors are needed, and if those two observations are generated by separate sensors, as is commonly the case, the combined attitude determination accuracy is sensitive to the mounting angle between the sensors.

In general, because the attitude accuracy depends on the sine of the angle between observation vectors, the more parallel the observation vectors from the two sensors are, the less accurate the attitude obtained from the measurements will be. Although mounting sensors at right angles to each other would appear to provide maximum accuracy, mission design considerations often preclude this choice. Sensor placement must not only provide for direct attitude determination accuracy requirements but must also consider indirect effects such as the number of observations that will be generated by the sensors with the spacecraft operating in various mission modes.

TAMs represent a somewhat different situation than do the sensors discussed above. TAMs are really composed of three independent sensors, each measuring one component of the magnetic field. The resulting magnetic field vector potentially has equal accuracy in all three directions and can be used for single-sensor attitude determination. Due to changes in spacecraft position as it traverses its orbit, TAM measurements at different times correspond to different target vectors. Because of this, TAM measurements may be used, in combination with rate information from IRUs or a dynamic propagation model, to determine three-axis attitudes without the use of information from any other sensors.

The TAM should be, and usually is, mounted as far as possible from other instruments that generate magnetic fields. Many spacecraft contain magnetic torquer assemblies (MTAs) to dump accumulated momenta into the Earth by coupling with the Earth's magnetic field. MTAs are expected to interfere with TAMs, and this effect should be considered when sensor placement is specified.

Earth sensors can also be used to provide single-sensor attitudes, but a spacecraft ephemeris must be used with the sensor measurements to completely specify the sensor-pointing vector. Earth sensor output corresponds to a nadir vector, and single measurements provide no information concerning the spacecraft rotation about the Earth vector; but use of several measurements, together with knowledge of the spacecraft position at the time of each measurement (and attitude rate information provided by gyroscopes) can provide three-axis information of the orientation of the spacecraft.

FHSTs can also produce measurements of different targets at different times if the spacecraft is rotating such that different stars pass through the FOV or if the sensor is commanded to scan through the FOV. Although these measurements could be used to produce single-tracker, three-axis attitudes, this has not, in general, been done. FHSTs are used when high attitude accuracies

are required, and in these cases, pairs of FHSTs, separated by a significant angle, are usually used. If the spacecraft is inertial, the single-tracked star cannot be used to determine a single-tracker, three-axis attitude.

The new generation of star trackers—CSTs—using CCDs as detectors can track more than one star at a time and can provide enough information for a single-frame attitude. This attitude will be less accurate around the boresight of the tracker than in other directions. The degradation of accuracy will be by approximately a factor of the sine of the angle between the target vectors and, since the FOVs of these star trackers may be small, pairs of sensors may still be needed if attitude determination accuracy requirements are high. For example, for the Submillimeter Wave Astronomy Satellite (SWAS) that has a single CST (with an 8-deg square FOV), the CST will be used alone for attitude determination. For the Solar and Heliospheric Observatory (SOHO) with redundant CSTs (with 3-by-4-deg FOV), one of the CSTs will be used to supplement an extremely accurate Sun sensor. For the X-Ray Timing Explorer (XTE), a pair of CSTs (with 8-deg square FOVs) will be used together to satisfy stringent attitude requirements.

2.3 Sensor Calibration

The potential measurement accuracy of any sensor is usually attained only after calibration has been performed to remove systematic components of the error. Two general types of calibration may be performed on sensors: alignment calibration and transfer function calibration. Transfer function calibration determines the constants in a transfer function. This information is used to transform the sensor output into physical quantities in a sensor reference frame. Alignment calibration determines the relationship of the sensor reference frame to a defined attitude reference frame. Attitudes are specified as the relationship between the attitude reference frame and an external reference frame, such as the geocentric inertial (GCI) frame or an orbital coordinate system (OCS). Although transfer functions often contain terms that represent alignments, any calibration that results in transfer function coefficients is referred to as a transfer function calibration in the discussion below, even if it also results in alignment parameters.

In general, both alignment and transfer function calibration are performed before launch and on-orbit. Alignments change significantly (often on the order of 0.1 deg) at launch, and for missions with attitude determination accuracy requirements on this order or greater, it is necessary to determine the alignments on-orbit. On-orbit changes in transfer function constants appear to have a much smaller effect on the accuracy of most sensors, and although attempts have been made to perform such calibration on-orbit, the results, with the exception of determination of FHST scale factors, have not been significant. The exception is in determining IRU biases and scale factors.

Of sensors that have been commonly used, FHSTs are usually the most accurate on missions requiring high attitude determination accuracy. Their alignment calibration is, therefore, critical. For the most accurate possible alignment calibration of FHSTs, stars used for calibration should be observed at many points in the FOV of each FHST to minimize the effect of FOV calibration variation at specific points in the FOV. Through the use of this strategy, the EUVE mission was

able to determine alignments of the FHSTs to about 4 arc sec, which may be the greatest alignment accuracy possible for these sensors.

For accurate FSS FOV calibration, observations should be taken from points that span the FOV. Even with these data, neither EUVE nor UARS were able to improve on the prelaunch FOV calibration. The existence of regular patterns in the postcalibration sensor residuals, however, indicates that the transfer function used, although sufficient to attain the manufacturer's specifications, leaves some effects uncompensated.

SMM and UARS were equipped with similar FSSs that were successfully calibrated. SMM had a FSS of similar design but with a smaller FOV and greater accuracy. UARS had a second FSS similar to that used for SMM and mounted on a gimballed platform. Both of these FSSs were calibrated using data obtained during attitude maneuvers during which the Sun's position in the FOV was moved to cover the entire FOV. In both of these cases the on-orbit calibration resulted in a significant decrease of sensor measurement error.

In some recent missions—the Hubble Space Telescope (HST), UARS, EUVE, and the Compton Gamma Ray Observatory (GRO)— apparent deviations from the FOV calibration of FHSTs were detected. GRO, UARS, and EUVE personnel compensated for the deviations by performing a partial FOV calibration to obtain corrections corresponding to changes in scale factors, alignment changes, and (in the case of EUVE) quadratic and cubic distortions. Of these, the scale factor changes were most evident and had the largest effect on the measured star position. FHST FOV calibration has not only corrected postlaunch scale factor drifts but also has (in the case of EUVE) improved homogeneity of observation errors across the FOV to better than the manufacturer's specifications.

The effect on attitude determination accuracy of FHST scale factor errors depends on the way in which attitudes are determined and on the spacecraft attitude motion. For rotating spacecraft, stars traverse the FOV, resulting in many observations of each star from different positions across the FOV, and thus many stars are observed and used for attitude determination in any orbit. In ground attitude solutions using a batch least-squares method, deviations in one direction from one star in a portion of the FOV will be effectively canceled by observations of the same star and/or other stars in portions of the FOV on the other side of the boresight. In rotating spacecraft such as UARS (one rpo) and EUVE in survey mode (3 rpo), except for large scale-factor changes, the ground attitude solution is not greatly affected by these scale factor changes. In contrast, for spacecraft with inertial attitudes such as GRO and EUVE in spectroscopy mode, changes in scale factors and even FOV homogeneity can significantly affect attitude determination accuracy.

The onboard computer (OBC) attitude is usually computed with a Kalman filter. Each star as it enters the FOV must be identified before it is used to update the filter. Usually, repeated identification is performed before the star is used. For rotating spacecraft this repeated identification means that the star has traversed a substantial portion of the FOV before it is used. All observations of a single star, taken together, tend to be on one side of the FOV, and the scale factor effect is not canceled; therefore, some error remains. This error is amplified by the

fact that the limited processing capability of the OBC prevents it from updating the Kalman filter with all the data used in the ground solution. Also, because the Kalman filter updates attitudes sequentially for each observed star, errors due to scale factor changes on the observations of one star cannot be fully compensated by errors in the opposite direction of another, subsequently observed, star.

For spacecraft operating in inertial mode, all observations of the stars used for attitude determination will be from the same approximate position in the FOV. As a result, FHST scale factor changes will decrease the attitude determination accuracy regardless of the attitude determination algorithm.

The output of HSs is usually produced as a pitch and a roll angle. Alignment determination for HSs can therefore be viewed as equivalent to determinations of biases on the pitch and roll axes. The limitation on calibration of HSs is due to inherent variability in the radiance of the stratosphere.

HSs measure the angles at which a rotating telescope, sensitive in the infrared, detects the edge of the Earth. The light detected by these telescopes comes from black body radiation of the atmosphere and is temperature dependent. Normally, the apparent Earth edge (called the "limb") is at about 35 km above the mean sea level, but this altitude varies with the atmospheric temperature near this height. Variation in atmospheric temperature results in errors on the order of 0.3 deg in the measurement of pitch and roll angles by HSs on near-Earth-orbiting spacecraft.

Variation in the apparent Earth limb altitude has a seasonal and latitudinal component, as well as a component that depends on day-to-day atmospheric conditions. The predictable seasonal and latitudinal variation represents about half of the total horizon radiance variability. These predictable components can be modeled and removed to improve the sensor accuracy to about 0.2 deg in both axes. An FDD software package, the Horizon Radiance Modeling Utility (HRMU), which predicts and compensates for the atmospheric temperature variation, has been run for some missions to improve the accuracy of ground attitudes that use HSs.

Even if the HRMU is used to correct horizon heights, variations in stratospheric radiance due to effects that are presently unpredictable cause significant attitude effects. In addition to daily meteorological phenomena, there are occasional major changes in stratosphere temperatures called sudden stratospheric warming (SSW) events. Such events occur about once a year in a winter hemisphere and last as long as 2 months. Major SSW events occur in the northern hemisphere about once every 2 years. Stratospheric warming during major SSW events can increase the northern hemisphere stratosphere to the same temperature as that of the southern hemisphere. This warming produces results with opposite sign and magnitudes comparable to or larger than the variations that are compensated for in the HRMU and so eliminate much of the potential benefit of the HRMU.

SESs are Earth sensors with a different design from that of HSs. They generally have several detectors that view different portions of the horizon. Because these portions are separated by greater angular distances than are the regions detected by HSs, and because they are generally

larger in area than the HS detectors, SESs are less sensitive to local stratospheric temperature variations and oblateness effects, exhibiting attitude uncertainty of about 0.1 deg due to atmospheric temperature effects.

TAM data can be corrupted by several phenomena, the effects of which can be minimized through calibration. Residual magnetization of spacecraft components, although kept to a minimum during the design phase through choice of materials and demagnetization procedures, generally results in a bias on TAM measurements. The operation of electrical components on board, especially that of MTA, produces time-varying magnetic fields, which can lead to errors in measured magnetic fields.

The effect of TAM biases can be removed either by including them in the attitude determination state vector or through separate calibration. MTA coupling can be removed through determination of a coupling matrix, which multiplies the commanded MTA magnetic fields to produce a correction to the magnetic field on each axis of the TAM.

TAM calibration beyond bias determination is generally not needed, but TAM scale factors and misalignments have been determined for UARS, and these parameters plus MTA coupling matrices have been determined for EUVE.

2.4 Attitude Determination Algorithms

Three general types of algorithms are regularly used in the FDD to determine attitudes of three-axis-stabilized spacecraft: single-frame solutions, sequential filters, and batch least-squares methods. Of these, only single-frame methods are generally used without attitude rate measurements or assumptions about the attitude change through the period being considered. All of these methods attempt to estimate the state of the system, which, for attitude algorithms, includes the attitude but which may also include other parameters such as gyro biases.

2.4.1 Single-Frame Algorithms

Single-frame solutions, such as the quaternion estimator (QUEST), use a set of sensor data at a single time to determine the best estimate of attitude. The only statistical compensation that can be used for random variations in sensor measurements arises from the availability of more than two independent, simultaneous observation vectors. If QUEST were used with CST observations, the availability of several star vectors at the same time could improve the QUEST attitude accuracy. With only pairs of sensor observations these methods are usually limited in attainable accuracy. They are most often used for rapid determination of coarse attitude in situations where speed is more important than accuracy or where rate data are unavailable.

2.4.2 Sequential Filter Algorithms

Sequential filters, such as the commonly used Kalman filter, supplement sensor data at any time with attitude estimates from the previous solution, propagated to the time of the sensor data measurement using rate data or a rate model. A gain is computed at each time step and used as

an effective weight of the observation residuals on the state update. If this gain is small, the prior state estimate is updated only slightly to correct for sensor residuals. The gain is computed from the sensor uncertainties, the gyro noise and the previous estimate of the attitude accuracy (usually given as a covariance matrix.) Sensor uncertainties are specified separately for each sensor and their values determine the relative importance of the sensors on the solution. The filter is initialized with an estimate of the state (often of low accuracy) and improves the accuracy of the estimated state with each sensor measurement. The major limitations of the improvement are the accuracy of the previous estimate, the accuracy of propagation from the previous time to the current time, and the accuracy of the sensor data and of the assumed statistics.

Soon after a filter is initialized, the largest error arises from the error in the previous attitude estimate. Sensor data generally improve this estimate at each observation until the attitude determination accuracy reaches a limit, due primarily to the sensor data accuracy. The time needed to converge on this limit depends on the relative weight given to the sensor data and to the propagated attitude. If the input parameters are set so that the gain is small, sensor data will have a small effect in changing the attitude, and the filter will converge slowly. If sensor data are given high weight, anomalous sensor measurements (or noise) will erroneously alter the computed attitude. Sequential filters must usually be "tuned" to obtain the best choice of gain and sensor weights. Tuning is achieved by varying the assumed process noise, measurement noise, and initial state covariance.

Sequential filters that use IRU data as a source of rate information often solve for IRU biases along with attitude. IRU biases are offsets to the commonly observed rates. These biases, which usually change slowly over a period of weeks, affect the attitude propagation, and their calculation improves attitude determination accuracy. If IRU biases change rapidly, their computation by the filter is essential to obtaining the best possible attitudes.

Sequential filters estimate the attitude at any given time by combining current sensor measurement residuals with previous attitude estimates. Effective weights of the measurements and prior attitude estimates are functions of sensor uncertainties and rate data uncertainties. The filter algorithm has an inherent fading memory so that older data are used with a lower effective weight than new data.

Filters require tuning. The relative uncertainties of the sensors and of the gyros that are used by the filter must be adjusted to obtain optimum results. If the filter is not properly tuned, attitude changes, rate bias changes, sensor noise, and rate noise may influence each other improperly and therefore, result in inaccurate results. This effect is exacerbated if periods of colored noise are encountered because this noise can be interpreted by the filter as changes in the state vector. Since even truly white noise may appear colored over a short data span, sequential filters may show small, short-term deviations from the true attitude and rate bias.

2.4.3 Batch Least-Squares Algorithms

Batch least-squares methods for three-axis-stabilized spacecraft attitude determination use rate data either to propagate sensor measurements to a common time or propagate an epoch attitude to each measurement time. They then determine deviations between observations and reference vectors and find the attitude at the epoch time that minimizes the root mean square (rms) measurement residuals. As with using a sequential filter, IRU biases are usually determined as part of the same state function as the attitude, and the sensor observations are weighted relative to each other.

Batch least-squares methods and sequential filters should give identical results in the limit of large data spans with only white noise. With less than ideal data, the results of the methods will differ due to the different ways in which they treat the data.

Batch least-squares methods use data from the entire period for which attitudes are needed. They propagate either sensor observation residuals to an epoch time using rate data or an epoch attitude to each measurement time, solve for the attitude at the epoch, and propagate that attitude over the entire period using rate data. The weight given to any measurement is typically taken as the inverse of the measurement uncertainty. Often, the measurement uncertainty is assumed to be the sensor noise without consideration of the propagation error arising from rate data noise. This assumption results in attitudes that are accurate at the epoch (assuming large data quantities and white noise) but which generate incorrect attitude covariances.

A separate assumption normally made in batch least-squares methods is that a constant bias may be used to accurately describe the state. If the rate bias is not constant, the propagation steps needed for attitude solutions may introduce considerable error.

2.5 Data Quantity and Quality

For measurements from any single sensor used for attitude determination by an algorithm using multiple measurements, increasing the quantity of measured data usually decreases attitude uncertainty by decreasing the contribution to attitude uncertainty due to any zero-mean measurement errors. Increasing the data quantity cannot reduce uncertainty due to systematic deviations, such as misalignments or constant biases. A statistical rule of thumb is that the uncertainty of the mean of a group of randomly distributed data is proportional to the inverse of the square root of the number of data points up to the limit at which the contributions from systematic errors becomes significant. This rule serves as a guideline for attitude determination accuracy but not as an exact formula because of the ways the data are used to determine attitudes.

Removal of systematic errors from sensor data leads to more accurate attitudes. In addition to biases and misalignments that can be removed by proper calibration, sensors often have characteristic data anomalies that can degrade the quality of a portion of available data. Data exhibiting these anomalies should be removed from processing either automatically or manually and not used in determining attitudes. Tables 2-7 and 2-8 contain a number of common attitude sensors and the sorts of error sources that can affect the sensors, the approximate magnitude of

Table 2-7. Error Sources and Common Mitigation Techniques for Three-Axis-Stabilized Spacecraft (1 of 2)

Error sources	Sensor Affected	Error Size	Mitigation Technique	
Star magnitude (dim stars less accurate than bright)	FHST	11 arc sec	Limit catalog to brighter stars	
Near neighbor star interference	FHST	7 arc sec	Remove from catalog any stars with bright near neighbors	
Star catalog errors	FHST	2 arc sec	Usually negligible. Catalog must be carefully validated.	
Temperature	FHST	4 arc sec	Use temperature correction terms in FOV calibration function	
	IRU	0.0008 deg/sec	If this error is significant, calibrate bias and/or scale factor changes with temperature	
Stray light and bright objects	FHST	Could disable sensor	From Sun, Moon, or lit Earth	Usually eliminated by sunshade, bright object sensor, and target suppress; avoid pointing FHST near Sun, Earth, or Moon
			From lit objects on dark Earth	Eliminate observations when FHST is occulted by Earth
			From planet	Remove observations if target star is near planet (rare)
	FSS	0.0015 deg	Look for anomalous data, and do not use them	
	HS	0.4 deg		
	SES	<0.4 deg	Change mode to not use data from affected quadrant	
SAA	FHST	<29 arc sec	Do not use data when spacecraft is near SAA	
Earth magnetic field	FHST	1 arc sec	Use magnetic field correction terms in FOV calibration function	
	TAM	1 Mg (model errors)	Use most accurate available Earth magnetic field model with current coefficients	

Table 2-7. Error Sources and Common Mitigation Techniques for Three-Axis-Stabilized Spacecraft (2 of 2)

Error sources	Sensor Affected	Error Size	Mitigation Technique
SPACECRAFT residual magnetic field	TAM	5 Mg if not calibrated	Calibrate bias and MTA coupling, place TAM as far as possible from instruments that create magnetic fields
Earth atmospheric refraction	FHST, FSS, DSS	0.1 deg	Do not use data if target image is near Earth limb
Earth atmosphere temperature variation	HS	0.3 deg	Use HRMU or temperature measurements of atmosphere (causes smaller effect on SES)
	SES	0.1 deg	
Earth oblateness modeling errors	HS,SES	0.02 deg	Use correct Earth oblateness model
Measurement time uncertainty	FHST	<29 arc sec	(Only occurs on rotating spacecraft) Correct sample time for average time, use large numbers of observations, use pattern-matching algorithm
Bit flipping in sensor output	All	varies	Examine sensor data for points with large anomalous values, and do not use them
Telemetry data precision	All	Telemetry dependent	Use large amounts of data

Table 2-8. Error Sources and Common Mitigation Techniques for Spin-Stabilized Spacecraft

Error sources	Sensor Affected	Error Size	Mitigation Technique	
Stray light and bright objects	Star scanner	(Can disable sensor)	From Sun, Moon, or lit Earth	Remove star from catalog when it is located near the Sun, Earth, or Moon
			From planet	Remove star from catalog when it is near planet (rare)
	FSS	0.0015 deg	Look for anomalous data, and do not use it	
	BHS	<0.4 deg		
Earth atmosphere refraction	Star scanner, FSS, DSS	0.1 deg	Do not use data with target image within about 10 deg of Earth limb	
Earth atmosphere temperature variation	BHS	0.3 deg	Use HRMU or temperature measurements of atmosphere	
Earth oblateness modeling errors	BHS	<0.02 deg	Use correct Earth oblateness model	
Measurement time uncertainty	Star scanner	0.01 deg	Correct sample time for average time; use large numbers of observations	
	FSS	0.003 deg		
Bit flipping in sensor output	All	Varies	Examine sensor data for points with large anomalous values, and do not use them	
Telemetry data precision	All	Telemetry dependent	Use large amounts of data	

the error due to the source where applicable, and usual ways the effects of lower quality data can be mitigated. The CSTs and the V-slit Sun sensors were not included due to insufficient flight data analyses.

The effects of the sensor error sources on attitude determination accuracy for the various sensor combinations covered in this study may be obtained from the theoretical (from ADEAS) results given in Section 5. In Section 5, the accuracy level of particular sensors is varied and the resulting attitude error computed. By using the observed sensor errors in the tables of this section in combination with the results of Section 5, the attitude errors due to the anomalies treated here may be estimated.

The quantity of data used for attitude determination depends on the timespan of data used and on the rate at which the data are sampled and telemetered. A high sampling rate generally decreases the statistical error in the data, but if the sampling rate exceeds the sensor measurement rate the data samples will not be independent. Long timespans also decrease the statistical error in the data but can introduce (in batch least-squares methods) propagation errors that increase with increasing data timespans and can become the dominant error source.

2.6 Mission Design

Mission design encompasses a number of factors that can significantly influence attitude determination accuracy. Although mission design parameters are determined by spacecraft science and health and safety requirements, they can also affect attitude determination accuracy.

The parameters that affect data quality and quantity include

- Planned attitude motion and rates
- Desired pointing directions
- Planned attitude maneuvers
- Data rates for attitude sensors and IRUs
- Spacecraft orbit
- Launch time
- Sun constraints (heating and illumination)
- Communications constraints

Section 3. Mission Descriptions

This section describes the various spacecraft included in this attitude accuracy study. Included are brief descriptions of scientific goals, attitude, orbit, and attitude determination hardware used. Section 3.1 describes the three-axis-stabilized spacecraft, and Section 3.2 presents a similar description for spin-stabilized spacecraft.

In this document, spin-stabilized spacecraft are those that rotate at a rapid rate (on the order of 10 to 100 of revolutions per minute). These spacecraft seldom use gyros. Their pointing stability depends on the gyroscopic effect of the spinning spacecraft itself. Attitudes for spinning spacecraft are most often represented as the pointing direction of the spin axis (often as right ascension and declination) and a phase of rotation about the spin axis.

Three-axis-stabilized spacecraft are those that are inertially pointed or rotate slowly (on the order of several revolutions per orbit). These spacecraft often have gyros to measure attitude rates. Attitudes for three-axis-stabilized spacecraft are represented by a transformation between GCI and body coordinates. This transformation may be parameterized as a transformation matrix, a quaternion, or as an Euler sequence of rotations. Euler rotations are the most easily visualized of these possibilities and are used in this document.

Some three-axis-stabilized spacecraft are Earth oriented. These spacecraft generally rotate at a 1 rpo rate to keep some instruments pointed at the Earth. For these spacecraft, the attitude is represented by a transformation between the orbital coordinate system (OCS) and body coordinates. The OCS is a coordinate system that rotates with the spacecraft as the spacecraft progresses in its orbit. One axis is generally pointed toward the Earth, a second toward the orbit normal, and the third is the cross product of the first two. The OCS is defined with respect to the geocentric inertial coordinate system (GCI) at each point in the spacecraft orbit, so the spacecraft attitude is completely defined by the attitude with respect to OCS coordinates and the spacecraft ephemeris.

3.1 Three-Axis-Stabilized Spacecraft

The three-axis-stabilized missions for which data have been gathered in this attitude accuracy analysis are summarized in Table 3-1. This table also includes the attitude sensors available to each mission. Any unusual mission characteristics are identified.

3.1.1 Applications Explorer Mission-1/Heat Capacity Mapping Mission

The Applications Explorer Mission-1/Heat Capacity Mapping Mission (AEM-1/HCMM) spacecraft was launched on April 26, 1978.

Table 3-1. Summary of Three-Axis-Stabilized Missions Studied

Mission	Launch Date	Attitude Hardware Available						Required Accuracy (arcsec 1σ)	Comments
		FHST	FSS	DSS	HS	TAM	IRU		
HCMM	4/26/78			2	1	1		2,520	roll
								1,800	pitch
								7,200	yaw
SEASAT-1	06/27/78		4		2	1		720	
SAGE	02/18/79			5	2	1		2,520	roll
								1,800	pitch
								7,200	yaw
MAGSAT	10/30/79	2	1	1	1	1	1	20	
SMM	02/14/80	2	2				1	360	roll
								5	pitch and yaw
DE-2	7/31/81		2		1			3,600	
ERBS	10/05/84		2	2	2	1	2	300	roll, pitch, and yaw
GRO	4/91	2	2			2	1	28.8	
UARS	9/12/91	2	1		2	2	1	20	
EUVE	6/7/92	2	1			2	1	5.8	pitch and yaw in survey mode and all axes in spectroscopy mode
								9.0	roll in survey mode
SAMPEX	7/3/92			1		1		7,200	
TOPEX	8/10/92	2	1		2	2	1	70	The FHSTs were HDOS CCD star trackers tracking 1 star at a time

The HCMM was designed to conduct thermal mapping of the North American continent, particularly the United States, with primary emphasis on applications related to the availability of Earth resources (Reference 1).

HCMM had a circular orbit with an altitude of 600 km and an inclination of 98 deg.

AEM-1 was a three-axis-stabilized spacecraft. The HCMM instruments were nadir pointing (Reference 1). The attitude determination hardware consisted of three two-axis DSSs manufactured by Adcole, one BHS manufactured by Hughes, and a TAM (Reference 1).

The required attitude determination accuracies, 1σ, were roll 0.7 deg, pitch 0.5 deg, and yaw 2.0 deg in operational mode (References 1 and 2).

The main attitude sensors were the DSS and the infrared HS. Magnetometer data were used mainly for yaw determination when Sun data were not available.

The definitive attitude was determined using a batch least-squares method.

3.1.2 Ocean Studies Satellite-1

SEASAT-1 was launched on June 27, 1978. SEASAT-1 was part of the Earth and Ocean Dynamics Applications Program of the National Aeronautics and Space Administration (NASA) Office of Applications (OA). The primary experimental objective of the SEASAT-1 mission was to study the world's oceans and to determine whether microwave instruments scanning the oceans from space could provide useful scientific data for oceanographers, meteorologists, and commercial seafarers.

SEASAT-1 had a circular orbit with an altitude of 790 km and an inclination of 108 deg.

SEASAT-1 was a three-axis-stabilized, Earth-referenced spacecraft. The instrument module was nadir pointing (References 3 and 4).

The definitive attitude determination hardware consisted of two Ithaco HSs, four Adcole two-axis FSSs, and a TAM.

The required attitude determination accuracies, 1σ, were 0.2 deg in pitch, roll, and yaw (References 3 and 4).

The HSs were normally used together to determine pitch and roll; however, either instrument could provide pitch and roll with degraded accuracy by replacing the signal from the second scanner with a constant voltage. The FSSs were used to provide yaw data and the HS biases. The TAM were used to provide coarse attitude data. The definitive attitude was determined using a batch least-squares method (Reference 5).

3.1.3 Applications Explorer Mission-2/Stratospheric Aerosol and Gas Experiment Mission

The AEM-2/SAGE spacecraft was launched on February 18, 1979.

The SAGE mission was to determine the spatial distribution of stratospheric aerosols and ozone by measuring the attenuation of solar radiation at four distinct wavelengths during occultations (Reference 6).

SAGE had a circular orbit with an altitude of 600 km and an inclination of 50 deg.

SAGE was a three-axis-stabilized spacecraft. The SAGE instrument boresights were pointing toward the horizon.

The attitude determination hardware consisted of five Adcole two-axis DSS, two Hughes HS scanners, and a TAM (Reference 6).

The required attitude determination accuracies were roll 0.7 deg, pitch 0.5 deg, and yaw 2.0 deg in operational mode (References 3 and 7).

Usually the attitude determination was based on input from one Sun sensor and from one horizon sensor. Magnetometer data were used mainly for yaw determination when Sun data were not available. The definitive attitude was determined using a batch least-squares method.

3.1.4 Magnetic Satellite Mission

The MAGSAT was launched on October 30, 1979. MAGSAT was a cooperative effort between NASA and the United States Geological Survey (USGS) as part of the Earth and Ocean Dynamics Applications Program in the NASA OA. The mission objective was to update the USGS worldwide magnetic field model and to compile a crustal anomaly map (References 8, 9, and 10). MAGSAT reentered the Earth's atmosphere on June 11, 1980.

MAGSAT had an elliptic orbit with a 325 km perigee, a 550 km apogee, and an inclination of 97 deg.

MAGSAT was a three-axis-stabilized spacecraft. The nominal MAGSAT attitude was such that the body X-axis pointed at the Earth, the body Y-axis pointed in the flight direction, and the body Z-axis pointed at the negative orbit normal.

The attitude determination hardware consisted of a spinning-mode Adcole digital Sun sensor, a coarse Sun sensor, a magnetometer, an Ithaco scan wheel HS, an Adcole FPSS, a pitch gyro, and two Ball Brothers Research Corporation (BBRC) CT-401 star trackers.

The required attitude determination accuracies, 1σ, were 20 arc sec in roll, pitch, and yaw (Reference 3 and 4).

The sensor pairs used for coarse attitude determination were HS and coarse Sun sensor (CSS), and HS and TAM when Sun data were not available, the HS providing roll and pitch data. Fine attitude determination was based on FPSS and FHST data. The requirements were 0.33 deg for coarse attitude and 20 arc sec for fine attitude determination. The definitive attitude was determined using a batch least-squares method.

3.1.5 SMM

The SMM spacecraft was launched on February 14, 1980, by a two-stage Delta rocket. The primary experimental objective of the mission was to study the solar-flare phenomena at a peak in solar activity. Of particular interest were the storage and release of flare energy, particle acceleration, formation of hot flare plasma, and mass ejection (Reference 11). SMM was repaired in 1984 and its FHSTs replaced.

SMM had circular orbit with an altitude of 560 km and an inclination of 28.5 deg.

SMM was a three-axis-stabilized spacecraft. The spacecraft axes were nominally aligned with the Sun coordinate axes.

The attitude determination hardware consisted of two Ball Aerospace Division (BASD) FHSTs, two TAMs, two CSSs, one Adcole FPSS, one standard DSS (never used), and one IRU.

The required attitude determination accuracies, 1σ, were 0.1 deg in roll about the sunline, and 5 arc sec in pitch and yaw (Reference 3).

Coarse pitch and yaw solutions were obtained using CSS and magnetometer data corrected for magnetometer biases, whereas only magnetometer data could be used for roll. Definitive attitude was determined using FHST and FPSS data. The definitive attitude was determined using a batch least-squares method.

3.1.6 Dynamics Explorer-2

The DE-2 was launched on July 31, 1981, together with the DE-1. The DE-2 mission was to study the physical processes of the Earth's upper atmosphere, ionosphere, and magnetosphere (Reference 12).

DE-2 had an elliptic orbit with a 275-km perigee, a 1200-km apogee, and an inclination of 90 deg.

DE-2 was a three-axis-stabilized spacecraft for normal mission operations. For some particular scientific purposes and for calibration, DE-2 was used as a spin-stabilized spacecraft. In three-axis-stabilized mode, its X-axis was pointing along the spacecraft velocity vector, its Z-axis along the positive normal orbit, and the Y-axis completed a right-handed reference system.

The DE-2 Attitude Determination System (ADS) consisted of a wheel-mounted HS and two Adcole FSSs. The HS was used to determine the pitch and roll, and its mirror traced out a 50-deg half-angle cone about the negative Z-axis of the spacecraft. The FSSs were mounted with both boresights lying in the X, Z plane and at angles of 47 deg and 60 deg, respectively, with respect to the $+Z$ axis.

In three-axis-stabilized mode the definitive attitude determination accuracy requirements, 1σ, were 0.16 deg pitch, 0.25 deg roll, and 0.03 deg yaw. The definitive attitude was determined using a batch least-squares method.

3.1.7 ERBS

The Earth Radiation Budget Satellite (ERBS) was launched on October 5, 1984 by Space Transportation System 41_G (Space Shuttle Challenger). It was released the same day at an altitude of approximately 352.5 km and was subsequently raised to a nominal mission altitude of 603 km by the spacecraft hydrazine propulsion system between October 7 and October 10, 1984 (Reference [1]). The orbit inclination is 57 degrees, and the eccentricity 0.000951. To maintain good sunlight exposure on the solar array throughout the mission a 180-degree yaw maneuver was performed every 35 days on average as the orbit plane precesses past the Sun.

The major scientific goal of the ERBS mission was to support the Earth Radiation Budget Experiment and the Stratospheric Aerosol and Gas Experiment (Reference [2]). Measurements from ERBS are very important for NASA's climate study program. ERBS carries three scientific instruments: the Earth Radiation Budget Experiment Scanner, the Earth Radiation Budget Experiment Non-Scanner, and the Stratospheric Aerosol and Gas Experiment-II. The mission nominal period was 1 year, the operational goal was 2 years. So far, ERBS has exceeded 8 years.

ERBS is an Earth-pointing mission. The ERBS is referenced to a geodetic nadir unit and the spacecraft velocity unit vector. The geodetic X direction points toward nadir, the Y direction is given by the cross product between the nadir and the velocity unit vectors, and the Z direction by the cross product between the X and Y unit vectors. The body orientation with respect to this frame is given in terms of pitch, roll, and yaw angles. The required definitive attitude determination accuracy (roll, pitch, and yaw) is 0.083 deg (1σ), except at night when the requirements are less stringent.

In order to attain this accuracy ERBS was equipped with two Ithaco Scanwheel HS assemblies, two Adcole two-axis Sun sensors containing coarse and fine grids, a Schoenstedt TAM, and two IRUs (Reference 14).

The scan cone axis of each HS is in the Y-Z plane of the spacecraft body axes and is tilted 10 degrees from the $+Y$ and $-Y$ spacecraft body axes. To avoid sensor performance degradation, the instruments are disabled when the Sun angle drops to approximately 5 degrees.

The Sun sensors boresight orientations are defined by an Euler 3-2-3 sequence from spacecraft frame. For the first instrument, the nominal Euler angles are: 18 degrees, 98 degrees, and 0 degrees. For the second, the nominal Euler angles are: 78 degrees, 98 degrees, and 0 degrees. As a result of this geometry, there is an overlap of 4 degrees between the Sun sensors FOVs in the X-Y plane.

The three magnetometers composing the Schoenstedt TAM unit are mounted parallel to the spacecraft axes.

The two redundant IRUs will be nominally aligned along the spacecraft axes with an uncertainty of approximately 0.1 degree on each axis.

The ERBS mission requires definitive attitude for annotation of scientific data and near-real-time attitudes for monitor and control support. The ERBS mission design calls for definitive attitude determination to be performed on board the spacecraft using a Kalman filter. Normally, the attitude is controlled by OBC. If onboard determination cannot be performed successfully or the bias values need to be updated, definitive attitudes are to be determined on the ground using telemetry data. On the ground, definitive attitudes are determined over periods for which valid HS and gyro data are available selected from 24-hour blocks using a batch method. HS biases and gyro biases are determined on the ground periodically and the new values are uplinked to the spacecraft.

3.1.8 GRO

GRO was carried into space aboard the shuttle Atlantis on the Space Transportation System-37 (STS-37) mission on April 6, 1991. It was released on April 7, 1991, and moved into a nearly circular orbit at altitude 455 km, inclination 28.48 deg, and eccentricity 0.0004708. The initial mission profile included periodic orbit adjust maneuvers but, because of propulsion system problems discovered early in the mission, orbit adjusts were postponed until the orbit had decayed to about 350 km.

The major scientific goal of the GRO mission is to provide astronomical observations over a wide energy range (from 0.1 to 30,000 million electron volts (MeV)). To accomplish this goal, GRO contains four scientific instruments.

GRO attitude is periodically adjusted to point the scientific instruments at specific targets. It remains inertially fixed at these attitudes for periods of about 2 weeks. While inertially fixed GRO was required to maintain its attitude with a knowledge accuracy of 0.024 deg (3σ).

In order to achieve these requirements GRO was equipped with an attitude control system containing two Ball Electro-optics/Cryogenics Division (BECD) FHSTs, two Adcole FSSs, a Teledyne IRU, and two Schoenstedt TAMs (Reference 15).

The boresights of both FHSTs lie in the body *XY* (Roll/Pitch) plane at 45 deg angles from the $-X$-axis. The FHST1 boresight points on the $+Y$ side while the FHST2 boresight points on the $-Y$ side. The FHST *Y*-axes also lie in the body *XY* plane.

The two FSS boresights lie in the body *XZ* plane. The FSS1 boresight lies 30 deg from the body *Z*-axis in the $+X$ direction and the FSS2 boresight lies 2 deg from the body *X*-axis in the $-Z$ direction. The FSSs which have 32 by 32 deg FOVs thus cover the all angles from 34 deg from the *X*-axis in the $-Z$ direction to 2 deg from the *Z* axis in the $-X$ direction. Their FOVs overlap by 2 deg in the body *XY* plane. As a result of this geometry the Sun is seldom in both FSSs at the same time (Reference 16).

The attitude was controlled by an OBC which determined the attitude using a Kalman filter that estimated the spacecraft attitude and gyro biases. The ground fine ADS used the same data in a batch least-squares method that determined the attitude but not the gyro biases. Input gyro biases for the ground ADS are obtained using separate software and are updated weekly. They are assumed to be constant throughout the week.

After launch the gyro biases drifted for several weeks making calibration difficult. During the mission (long after postlaunch calibration was complete), increases in attitude errors were observed. These were traced to a drift in the FOV calibration of FHST2. After considerable work a calibration method was found for this drift and continued drift was subsequently monitored. The drift was corrected for OBC processing by shifting the positions of guide stars sent to the OBC to compensate for the position shift caused by the scale factor drift. The ground attitude was computed using the computed scale factors and the correct star positions.

3.1.9 UARS

UARS was carried into space aboard the shuttle Discovery on the Space Transportation System-48 (STS-48) mission on September 12, 1991. It was released on September 15, 1991, and moved into a frozen orbit at altitude 585.72 km, inclination 56.9 deg, and eccentricity 0.00139. Throughout the mission, this orbit was maintained by periodic orbit adjust maneuvers.

The main scientific goals of the UARS mission are to study the properties of the upper atmosphere and provide information on upper atmospheric chemistry. To meet these goals, most of the UARS science instruments are oriented to view the Earth limb at specific altitudes. The actual altitude at which the science instruments view the atmosphere depends strongly on the spacecraft attitude.

UARS attitude is controlled to rotate the spacecraft at 1 rpo about its pitch axis to keep the scientific instruments pointing always at the Earth limb. The attitude knowledge requirement is 60 arc sec (3σ) on each axis.

To achieve this requirement, UARS was equipped with a Modular Attitude Control System (MACS) module containing two BECD FHSTs, an Adcole FSS, a Teledyne IRU, two Schoenstedt TAMs, and two Ithaco Earth sensor assemblies (ESAs)—also referred to as HSs.

It also was equipped with a set of CSSs, which were used for attitude acquisition but not for attitude determination. Attitude control was provided with a set of reaction wheels, and accumulated momentum was managed with an MTA.

UARS was equipped with a pair of additional Sun sensors mounted on a gimballed platform called the Solar-Stellar Pointing Platform (SSPP). These sensors, called the platform Sun sensors (PSSs), were similar to the MACS FSS but with a 2-by-2-deg square FOV and correspondingly greater accuracy than the FSS. The PSSs were nominally coaligned with science instruments, and in normal mission mode the SSPP gimbals tracked the Sun, keeping it at the center of the PSS and science instrument FOV. Although provisions were made to use the PSSs as attitude instruments, they were never so used because the uncertainty of the gimbal alignment calibration degraded the accuracy of the PSS observations in the body frame to about the same level as that of the FSS. The PSS observations were used as extremely accurate references for the SSPP science instruments.

UARS performs a 180-deg yaw maneuver approximately every 5 weeks to maintain the Sun on one side of the spacecraft. A few small-amplitude (about 10 deg) roll maneuvers were performed early in the mission, but no other maneuvers have been performed or are planned.

Calibration of the UARS sensors included determination of alignments of the FHSTs to about 6.5 arc sec, the FSS to about 33 arc sec, and HSs to about 1 arc min. The IRU alignments, biases, and scale factors were also determined.

3.1.10 EUVE

The EUVE was launched on June 7, 1992, aboard a Delta II expendable launch vehicle. It was released in a near circular orbit with an altitude of about 527 km and an inclination of 28.5 deg. Its mission is to survey the sky in the extreme ultraviolet region of the spectrum (80 - 900 Angstrom) and to make detailed spectroscopic observations of any interesting features found. The survey phase is scheduled to last 6 months and the spectroscopy phase an additional 30 months. During its survey phase, it is to maintain its X-axis pointing away from the Sun and rotate about this axis at a rate of 3 rpo. After the 6-month survey is completed, it is to point its X-axis at targets of interest within 30 deg of the anti-Sun direction. During this spectroscopy phase, short periods of survey activities will also be performed to fill in any gaps in the all-sky map obtained in the first 6 months.

EUVE has two FHSTs, an FSS, and an IRU containing three two-axis gyros as attitude sensors. These sensors are mounted in a multimission modular spacecraft (MMS) configuration similar to that flown on UARS. The two FHSTs are placed so that a vector halfway between their boresights is perpendicular to the body X-axis, and the plane containing the two boresights also contains the X-axis. The FSS boresight is tilted 15 deg from the $-X$ axis in both the $+Y$ and $+Z$ directions. The angle between the boresights of FHST1 and the FSS is 145 deg, while that between FHST2 and the FSS is 73 deg. Thus, in inertial mode, attitudes using the FSS and FHST2 are likely to have greater accuracy than those using the FSS and FHST1 because observation pairs from FHST2 and the FSS are nearer 90 deg apart than those from FHST1 and

the FSS. At 3 rpo, observations of stars from many different directions are used in the attitude determination. Because the FHST observations are more accurate than FSS observations, the FHST observations dominate the attitude accuracy and either FHST will produce attitudes of high accuracy.

EUVE attitude requirements, 5.7 arc sec (1σ) for pitch and yaw and 9 arc sec (1σ) for roll, were the most severe of any FDF-supported satellite. Calibration of great accuracy was required to meet these requirements. To achieve these accuracies, 11 orbits of data were used for alignment calibration. Attitudes were chosen for these 11 orbits so that the same stars appeared at points distributed throughout the FOV at different times in the data. This choice of data reduced the contributions of FOV-position-dependent errors to alignment errors. Estimated postcalibration alignment accuracy for the EUVE FHSTs was 4 arc sec per axis (1σ). Calibration of the IRUs and FSS FOV were also performed but had no effect on the attitude accuracy.

After launch, attempts were made to improve EUVE attitude accuracy. A method was developed to reduce the error in the FHST FOV from about 4 to about 2 arc sec (1σ) for a single observation. It was also determined that use of the IRU in low-rate mode (possible only while the spacecraft was in its inertial-pointing phase of the mission) reduced gyro contributions to attitude errors from as much as 15 arc sec to about 5 arc sec over a one-orbit data span.

In survey phase, the rotation of the spacecraft results in a position error of star observations due to the uncertainty in FHST measurement time relative to FHST sampling time. This uncertainty can be represented as a uniform distribution with a range of ± 50 msec corresponding to a position range of ± 20.3 arc sec. It is reduced in ground attitude determination through the use of about 200 samples of star position to approximately 1/14 of the single measurement uncertainty. On board, it is reduced by a time-pattern matching algorithm to about 1/3 of the single measurement uncertainty.

3.1.11 Solar, Anomalous, and Magnetospheric Particle Explorer

SAMPEX was launched on July 3, 1992, on a Scout expendable launch vehicle. Its mission was to measure the properties of several types of energetic particles, including cosmic rays and relativistic electrons trapped in the Earth's magnetic field. It was placed in a 580-km near-circular orbit with an inclination of 82 deg.

Because about 90 percent of SAMPEX's scientific measurements are made by instruments pointing near the zenith while the spacecraft is near the magnetic pole, in its nominal attitude mode the spacecraft is required to maintain the Z-axis within 15 deg of zenith while the spacecraft is over the poles. It rotates once per orbit about the Sun direction.

For attitude determination, SAMPEX was equipped with a two-axis DSS and a TAM. No attitude rate sensors were present. The least significant bit of the DSS output is 0.5 deg, resulting in a uniform error distribution of ± 0.25 deg. Such a distribution corresponds roughly to a normal error of 0.204 deg (1σ).

3.1.12 Ocean Topography Experiment/POSEIDON

TOPEX was launched on August 10, 1992, on an Ariane-42P expendable launch vehicle. Its orbit was near-circular with a mean altitude of 1336 km and an inclination of 66 deg. Its mission is to map the world's ocean surface elevation to great accuracy.

Throughout the mission, the spacecraft Z-axis (yaw) is pointed to the nadir with an attitude accuracy requirement of about 70 arc sec (1σ). To achieve this accuracy TOPEX was equipped with an MMS, including two Hughes Danbury Optical Systems (HDOS) CSTs referred to as Advanced Star Trackers (ASTRA) -A and -B, one FSS, two HSs, and an assembly of three two-axis IRUs. The star trackers can follow one star at a time and have a nominal measurement accuracy of 10 arc sec. They are mounted so that the mean of their boresights lies in the Y-Z plane, and each boresight is 19.5 deg from the Y-axis in the $-Z$ direction. The FSS boresight is in the X-Y plane and points 15 deg from the $-X$ direction toward the $-Y$ direction.

About 6 months after launch, the protective shield of the ASTRA-B failed, disabling the instrument, and attitudes were thereafter determined using ASTRA-A and the FSS. The failure was due to a bit flip in the electronics controlling the cover. The ASTRA-B was shielded when no bright object was present, and unshielded only when a bright object was sensed. The FSS itself experienced problems attributed to Solar reflections off the spacecraft body. These problems were reduced, but not eliminated, by restricting Sun data for use in attitude determination to a central region of the FOV.

TOPEX attitude determination and calibration are performed at the Jet Propulsion Laboratory (JPL), so complete mission data for this satellite are not readily available to FDF. TOPEX calibration was not completed until after ASTRA-B failed. As a result, TOPEX attitude accuracy measurements were obtained using only the FSS and one star tracker. Attitude accuracy measurements with these sensors were estimated at JPL by comparison of the sensor-derived spacecraft attitude with the nadir direction determined by one of the high-accuracy radar altimeters used by TOPEX for its scientific studies. These measurements give estimates of pitch and roll attitude errors.

3.2 Spin-Stabilized Spacecraft

The spin-stabilized missions for which data have been gathered for attitude accuracy analysis are summarized in Table 3-2. This table also includes the attitude sensors available to each mission. Any unusual mission characteristics are identified.

3.2.1 Communications Technology Satellite

The CTS was launched on January 17, 1976. The goal of the CTS mission was to advance the technology of spacecraft-mounted and related ground-based devices and systems applicable to future satellites (References 17 and 18), including high efficiency 12 GHz traveling wave tube (TWT) and associated power processor; functional demonstration of an unfurlable flexible solar cell array with over 1 Kw of power; design, development, and space operation of an accurate

Table 3-2. Summary of Spin-Stabilized Missions Studied

Mission	Launch Date	Attitude Hardware Available						Spin Axis Required Accuracy (deg, 1σ)	Comments
		VSS	FSS	DSS	HS	TAM	Star Sensors		
CTS	01/17/76			2	2			1.0	Highly eccentric orbit
DE-1	07/31/81			2	2			0.1	Highly eccentric orbit
SSS-1	11/71			1	1		1	1.0	Highly eccentric orbit perigee height = 250 km
IMP-8	10/73			1	1			0.5	Perigee height = 190000 km
ISEE-3	08/12/78		2		1			1.0	Aphelion = 1.007 AU Perihelion = 0.973 AU
IUE	02/14/78			1	1			1.0	
GOES-3	04/09/75	2			5			1.5	Highly eccentric transition orbit
GOES-5	05/22/81	2			2			0.7	Highly eccentric transition orbit
AE-3	12/16/73			1	3	1		0.67	AE-3 had 2 HSs and 1 BHS

attitude stabilization system with large, flexible appendages; color television broadcast to small, low-cost, Earth terminals; audio broadcast to very small Earth terminals; two-way voice communications; and wide-band data transmission and data relay.

The final orbit was geosynchronous with 0.1 deg inclination. During the first operation phase, before the final geosynchronous orbit was reached, CTS was spin-stabilized. The attitude determination hardware used in spin-stabilized mode consisted of two Adcole spinning-mode DSSs and two BHSs. The two spinning Sun sensors were mounted rigidly on the spacecraft on opposite sides. They spanned a sky band with a width of 128 deg. Within a width of 40 deg they could work in high-accuracy mode providing measurement uncertainties of no more than 0.1 deg. The BHSs had an FOV of 26 by 26 deg. The scan plane was tilted so that the scan paths were slightly offset from the Earth center. The sensor geometry was chosen so that either instrument provides the angular error about both the pitch and roll axes (Reference 17). The system provided redundant output over a ± 2.8 deg linear range. The specified sensor accuracy is 0.05 deg with a 0.01 deg least significant bit.

The required spin axis attitude determination accuracy was 1.0 deg (1σ), and the required spin rate uncertainty was 0.02 rpm (1σ).

The attitude was computed using several single-frame analytic methods. The single-frame attitude solutions were then averaged. Single-frame attitude determination was performed using methods employing the following combinations of input data: the Sun angle/Earth-in rotation angle, Sun angle/Earth-out rotation angle, Sun angle/Earth width, Sun angle/midscan dihedral angle, Earth width/midscan dihedral angle, and Sun angle/Earth-nadir angle (Reference 17).

3.2.2 DE-1

The DE-1 was launched on July 31, 1981, together with the DE-2. The mission of DE-1 was to study physical processes of the Earth's upper atmosphere, ionosphere, and magnetosphere (Reference 12).

DE-1 had a highly elliptical orbit with a 275-km perigee and a 23918-km apogee. The inclination was 90 deg.

DE-1 was a spin-axis-stabilized spacecraft. It was placed in a polar orbit and had the spin axis within 1 deg of the orbit normal. The perigee altitude was 683 km, the apogee altitude was 24875 km. The DE-1 attitude determination hardware consisted of two RCA BHSs and two Adcole single-axis DSSs. In nominal mode the BHS-1 line of sight made an angle of 81 deg with the spin axis; the BHS-2 line of sight made an angle of 99 deg with the spin axis. Both instruments had an FOV of 2.5 by 2.5 deg. The single-axis DSSs were similar in design and estimated performance to those flown by CTS. In nominal mode the first DSS boresight was directed at 73 deg from the spin axis and that of the second instrument was directed at 107 deg from the spin axis. The Sun sensors had FOVs of 128 deg. In nominal mode the Sun direction was within 40 deg of each sensor boresight, i.e., in the high accuracy (0.1 deg) range of their FOVs.

The required spin axis determination accuracy was 0.1 deg (1σ). The required spin rate was 10 $\pm$0.1 rpm.

The attitude was computed using single-frame analytic methods. The single-frame attitude solutions were then averaged. Single-frame attitude determination was performed using methods employing the following combinations of input data: Sun angle/Earth-in rotation angle, Sun angle/Earth-out rotation angle, Sun angle/Earth width, Sun angle/midscan dihedral angle, Earth width/midscan dihedral angle, Sun angle/Earth-nadir angle, and similar data and combinations of data in which Earth measurements were replaced by similar Moon measurements (Reference 3).

3.2.3 Small Scientific Satellite-1

SSS-1 was launched in November 1971. The primary objective of the SSS-1 was to investigate and study the dynamic processes that occur in the inner magnetosphere near the magnetic equator. A secondary objective was to flight demonstrate the performance of a lightweight, general-purpose scientific satellite (Reference 19).

SSS-1 had highly elliptical orbit with a 222-km perigee and a 28876-km apogee. The inclination was 3 deg.

The SSS-1 was a spin-stabilized mission. The spacecraft spin axis was positioned within 10 deg of the equatorial plane. The satellite had a low-inclination, high-eccentricity orbit with an apogee height of 27,000 km and a perigee height of 250 km. The attitude determination hardware consisted of a single-slit star sensor, a BHS, and a DSS.

The required spin-axis determination accuracy was 0.1 deg (1σ). The required spin rate determination accuracy was 10 percent.

The attitude was computed using single-frame analytic methods. The single-frame attitude solutions were then averaged. Single-frame attitude determination was performed using methods employing the following combinations of input data: the Sun angle/Earth-in rotation angle, Sun angle/Earth-out rotation angle, Sun angle/Earth width, Sun angle/midscan dihedral angle, Earth width/midscan dihedral angle, Sun angle/Earth-nadir-angle, and combinations of data in which Earth measurements were replaced by similar Moon measurements (Reference 3).

3.2.4 Interplanetary Monitoring Platform-8

The IMP-8 was launched in October 1973. IMP-8 was designed to study the solar and galactic cosmic radiation, solar plasma, solar wind, energetic particles, electromagnetic field variations, and the interplanetary magnetic field. The perigee height was 190,000 km.

The IMP-8 was a spin-stabilized mission. The attitude determination hardware consisted of an Adcole single-axis DSS and an optical telescope for horizon measurements. Due to its very high altitude the atmospheric height and the Earth oblateness impact on Earth-in and Earth-out

measurements were negligible, but unfortunately a poor alignment prevented the achievement of a superior measurement accuracy. The Sun sensor experienced a loss of accuracy because the least significant bit failed in a permanently "on" configuration.

The required spin-axis determination accuracy was 0.5 deg. The achieved spin rate varied between 12 and 68 rpm.

The attitude was computed using single-frame analytic methods. The single-frame attitude solutions were then averaged. Single-frame attitude determination was performed using methods employing the following combinations of input data: the Sun angle/Earth-in rotation angle, Sun angle/Earth-out rotation angle, Sun angle/Earth width, Sun angle/midscan dihedral angle, Earth width/midscan dihedral angle, Sun angle/Earth-nadir angle, and similar methods and methods replacing the Earth measurements with similar Moon measurements (Reference 3).

3.2.5 International Sun-Earth Explorer-3

The ISEE-3 was launched on August 12 1978. ISEE-3 studied the magnetosphere, the interplanetary space, and the interactions between them. The mission perihelion was at 0.973 AU, the mission aphelion was at 1.007 AU, and the orbit was contained in the ecliptic plane.

ISEE-3 was a spin-stabilized mission. The nominal spin axis had a right ascension of 270 deg and a declination of 67 deg. The angular momentum associated with a wheel-mounted horizon sensor (scan wheel) was undesirable, therefore a Panoramic Attitude Sensor (PAS) was used instead (Reference 3) for Earth-in, Earth-out, Moon-in, and Moon-out measurements (Reference 20). The PAS was used only in the near-Earth part of the spacecraft orbit. Two FSSs complemented the PAS.

The required spin axis determination accuracy was 1 deg (1σ). The nominal spin rate was 20 rpm ± 11 percent.

The attitude was computed using single-frame analytic methods. The single-frame attitude solutions were then averaged. The attitude determination methods used were the Sun angle/Earth-in rotation angle, Sun angle/Earth-out rotation angle, Sun angle/Earth width, Sun angle/midscan dihedral angle, Earth width/midscan dihedral angle, Sun angle/Earth-nadir angle, and similar methods and methods replacing the Earth measurements with similar Moon measurements (Reference 3 and 21). The various attitude determination methods used agreed within 1.0 deg (1σ); therefore, the attitude uncertainty based on flight data was 1.0 deg.

3.2.6 International Ultraviolet Explorer

The IUE was launched on February 14, 1978. The mission objective was to study the ultraviolet spectra of stellar sources. IUE was a spin-stabilized mission during the early mission stage.

Although IUE was spin-stabilized, the spin axis orientation was variable. The spinning-mode attitude determination hardware consisted of a spinning-mode DSS and a PAS. In addition, the

FSSs were considered to be used as a backup in the event of a spinning-mode DSS failure. Due to the spacecraft geometry, while in spinning mode, the Sun entered the FSS FOVs only at certain times; therefore, the FSSs could not be used as a primary Sun angle data source. In addition, when a test was performed to determine the FSS data quality, the measurement standard deviation exceeded 10 deg, proving the FSSs were not reliable in spinning mode. The cause of this large measurement uncertainty was not determined (Reference 22).

In spinning mode, the required attitude determination uncertainty was 1.0 deg. The achieved accuracy was 0.6 deg. The nominal spin rate was 60 rpm ± 10 percent (Reference 23). The achieved spin rate determination accuracy was 0.2 percent.

The attitude was determined using several single-frame methods (see Section 4.2.1) and a batch least-squares fit method. The results were consistent within 0.6 deg.

3.2.7 Geostationary Operational Environmental Satellite-3

The Geostationary Operational Environmental Satellite (GOES)-3 was launched on April 9, 1975. The GOES series of spacecraft is a joint effort of NASA and the National Oceanic and Atmospheric Administration (NOAA) to provide systematic worldwide weather coverage. The transfer to a geosynchronous orbit was designed to be accomplished in stages.

GOES-3 was a spin-stabilized satellite in geostationary orbit. Its spin axis was in the orbit plane during transfer orbit and along the negative orbit normal during normal mission operations. The spin mode attitude determination hardware consisted of two V-slit Sun sensors and five BHSs (Reference 24).

The required spin-axis determination accuracy (1σ) was 1.5 deg. The target spin rate was 100 rpm.

The attitude was determined using the usual single-frame determination methods, the results of which were refined by block averaging (References 3 and 24).

3.2.8 GOES-5

GOES-5 was launched on May 22, 1981, as part of a series of spacecraft in a joint effort of NASA and NOAA to provide systematic worldwide weather coverage. The transfer to a geosynchronous orbit was designed to be accomplished in stages.

As in the case of GOES-3, GOES-5 was a spin-stabilized satellite in geostationary orbit. Its spin axis was in the orbit plane during transfer orbit, and along the negative orbit normal during normal mission operations. The spin mode attitude determination hardware consisted of two V-slit Sun sensors and two BHSs (Reference 25).

In spin mode, the required attitude determination accuracy (1σ) was 0.7 deg. The target spin rate was 100 rpm.

The attitude was determined using the usual single-frame determination methods, the results of which were refined by block averaging (References 3 and 25).

3.2.9 Atmospheric Explorer-3

The AE-3 was launched on December 16, 1973. The mission objective was to measure the energy input into the upper atmosphere by monitoring the composition, density, and temperature of neutral and charged particles; the ultraviolet radiation level, principally from the Sun; the spectral distributions; and line intensities. The initial orbit had a perigee of 153.0 km, an apogee of 4295.2 km, and an inclination of 68.1 deg.

AE-3 was either three-axis or spin-stabilized during different portions of the mission. Nominally, the spin axis had to be maintained within 2 deg of the orbit normal.

The attitude determination hardware consisted of two wheel-mounted HSs, one BHS, a spin-mode DSS, and a TAM. Both wheel mounted HSs were located on the spin axis while the BHS was placed on the spacecraft circumference.

While in spin-stabilized mode, the spin rate was set to values between 1 and 8 rpm. The required attitude determination accuracy was 1 deg (1σ).

The attitude was determined using the usual single-frame methods followed by averaging (Reference 26).

3.2.10 Small Astronomy Satellite-2

SAS-2 was launched on November 15, 1972. The SAS-2 mission was to observe the cosmic gamma ray sources.

SAS-2 was a spin-stabilized mission (Reference 27). The attitude determination hardware consisted of an N-slit star sensor, a single-axis DSS, and a TAM. The spacecraft was cylindrical in shape and the symmetry axis was also the spin axis. The N-slit star sensor and the DSS were mounted on the spacecraft circumference in a plane perpendicular to the spin axis.

The required right ascension and declination accuracy was 1 deg (1σ). The accuracy attained using the N-slit star sensor and the DSS was 0.33 deg for right ascension and 0.26 deg for declination. The accuracy attained using magnetometer data only was 0.7 deg for both right ascension and declination.

The attitude was determined using single-frame methods followed by averaging.

3.2.11 Italian Industrial Operations Research Satellite

The Italian Industrial Operations Research Satellite (SIRIO) was launched on August 25, 1977. SIRIO was a super-high-frequency communication satellite.

SIRIO was a spin-stabilized mission (Reference 28). Its attitude determination hardware consisted of two solar planar field sensors (SPFs), two solar V-beam sensors (SVBs), and two BHSs. An SPF and SVB pair provided the Sun angle with respect to the spin axis and an associated time signal. Therefore, it functioned like a V-slit Sun sensor.

The required attitude accuracy was 1 deg; the attained value was 0.1 deg. The achieved spin-rate determination accuracy was 0.22 percent.

The attitude was determined using standard single-frame methods followed by averaging.

Section 4. Mission Experience

Attitude accuracy descriptions in this section are arranged first by mission type. Section 4.1 describes three-axis-stabilized spacecraft while Section 4.2 covers spin-stabilized spacecraft. Within each section the subsections are arranged by sensor pair—each section describes the attitude accuracy achieved using a particular pair of sensors.

In Sections 4.1 and 4.2, figures are presented to provide a quick, visual means of assessing attitude accuracies. Figures are presented that contain data for each sensor pair, giving the achieved accuracies for the various missions studied. These results are brought together and summarized in an additional summary figure for each section.

Where they are available, the figures include values of the required attitude accuracies. These required accuracies are based on the use of the most accurate pair of sensors so that for cases in which the attitude accuracy using a less accurate pair of sensors is displayed, the required accuracy is usually much lower than the achieved accuracy.

4.1 Attitude Accuracies of Three-Axis-Stabilized Spacecraft

Attitude accuracies for three axis-stabilized spacecraft are generally reported as the accuracy of rotation about each of the body axes. The body axes are defined in mission-specific ways and reference should be made to Section 3 for the definition of the axes for each mission studied. Earth-referenced spacecraft do have a fairly consistent set of axis definitions based on the normal mission orientation relative to the Earth. For Earth-referenced spacecraft, the yaw axis is normally defined along the nadir, the pitch axis along the negative orbit normal, and the roll axis as the cross product of these two (approximately in the direction of the spacecraft velocity).

Many three-axis-stabilized spacecraft use IRUs for attitude propagation. In this study, when attitude determination with a pair of sensors is described, IRU measurements are normally used as well. AEM/HCMM, AEM-2/SAGE, SEASAT-1, DE-2, and SAMPEX had no IRUs so attitude determination for these satellites did not employ gyro measurements. Information on the use of IRUs is noted in these sections only if it is unusual or significant.

Two special cases are also included: OBC attitudes and attitudes determined using TAMs as the only attitude sensors. OBC attitudes are generally computed using the most accurate sensor set available by the OBC. They are described separately from the other attitudes because the attitudes are normally obtained using a Kalman filter, whereas ground solutions are usually obtained using a batch least-squares procedure. As the differences in data treatment are sufficiently large, OBC attitudes are described separately in the section corresponding to the sensor pair used but are plotted as separate values in the figures corresponding to the sensor pair used by the OBC.

TAMs are unusual in that the vector they produce changes its direction in GCI and Earth-centered coordinates, and the vector can point in virtually any direction relative to the spacecraft body. For this reason TAM measurements, together with gyro information, are often used as the basis of single-sensor, three-axis attitude determination. TAM-only attitudes are included as a separate section.

The main results are presented in a series of graphs. There is a graph for the case with two FHSTs, with an FHST and a FSS, and with only TAM data. Results for the other combinations of sensors are displayed in graphs showing pairs including an HS and one other sensor, and a TAM and one other sensor. Each of these graphs displays one or more values for each mission for which data exist. Where possible, separate values are given for attitude uncertainties corresponding to rotations about the roll, pitch, and yaw attitude axes. Where separate values are given, the top-most value is for roll, the middle value is for pitch, and the lowest value is for yaw. If only some of these axes can be given, then the axes are individually labeled.

The results presented are generally determined differently for active and inactive missions. For inactive missions, the only information available is in reports of mission attitude performance. The best estimate determined from mission reference documents is given. Often attitude accuracies must be inferred from reports on sensor performance (since sensor performance may be attitude-accuracy dependent). Data from inactive missions, especially ones that have been inactive for a considerable period of time, may be less reliable than the results for active missions because of inconsistency in the reference sources consulted and methods used for attitude-accuracy estimation.

For active missions, information from mission reports can often be supplemented or even replaced by direct measurements of the spacecraft data and the attitudes determined from these data. The most accurate pair of sensors is considered a reference pair. Attitude uncertainty for the reference pair is determined by statistically combining the measured uncertainty of the attitude at epoch (from the ADS) with known uncertainties that are not included in the ADS attitude uncertainties. The ADS uncertainties chiefly reflect the effects of measurement noise and must be combined with terms reflecting the effects of postcalibration alignment uncertainties, FOV variances, and other parameter uncertainties to provide a more accurate estimate of attitude determination accuracy.

Once reference attitudes have been determined using the most accurate sensor pair, they can be used to estimate the error of less accurate attitudes computed using a less accurate sensor pair. The attitude uncertainty of the less accurate case is determined by statistically combining the rms attitude residual (between the reference and less accurate attitudes) with the uncertainty in the reference attitude. Attitude accuracies of this sort are presented below.

In some cases the reference attitude is not significantly more accurate than the attitude calculated using a different sensor pair. In these cases, comparison with the reference attitude does not give accurate estimates of attitude error, so the attitude accuracy is estimated for these sensors using the same method of estimation as for the reference pair.

Mission descriptions for the missions studied are found in Section 3.1. All attitude error values listed in this section are those achieved in normal flight circumstances—when the sensors were not affected by anomalous error sources. The effect of such error sources on sensor accuracy is presented in Section 2; the effect of increased sensor errors on attitude determination is analyzed in Section 5. Each sensor is described in the first subsection in which it is used as a primary sensor: the FHST in Section 4.1.1; the FSS in Section 4.1.2; the HS in Section 4.1.3; the TAM in Section 4.1.4; and the DSS in Section 4.1.7.

4.1.1 Attitude Accuracies Using Two FHSTs

Because FHSTs are often the most accurate sensors used by satellites for attitude determination, the FHST attitudes are normally the best estimate of the true spacecraft attitude and are used to compute the reference attitude. For this reason, it is impossible to measure the difference between the FHST-only attitude and the reference attitude. Estimates of the FHST-only attitude accuracy can best be obtained by statistically combining the known uncertainties in FHST measurements. These uncertainties include

- Alignment uncertainties—systematic errors whose uncertainties are treated as random errors of normal distribution for computing attitude uncertainty.

- Sensor noise—given in terms of the noise equivalent angle (NEA). The NEA for standard FHSTs is about 12 arc sec and is treated as a random error of normal distribution.

- FOV calibration variation—for standard FHSTs, about 10 arc sec. These are systematic errors for any single location in the FOV but are treated as random errors of normal distribution for measurements at varying positions across the FOV.

- Timing error—the uncertainty in position in the FOV due to uncertainty in the time of the FHST measurement. This error arises from a ± 50-msec sensor timing uncertainty. It occurs only in spacecraft during attitude motions and is transformed from a 50-msec time uncertainty with a uniform distribution to an equivalent attitude uncertainty with a normal distribution in a manner dependent on the FHST geometry relative to the spacecraft motion.

Most of the above sensor errors are observed directly as position errors across the FOV. They contribute directly to uncertainties in attitude rotations perpendicular to the sensor boresight. The component of measurement uncertainties of a single FHST, corresponding to rotations about the boresight, can be estimated as the measurement uncertainties across the FOV (as enumerated above) divided by the sine of the angle between the observation and the rotation vector (in this case the boresight). With an FOV of radius 4 deg, these errors are larger by at least a factor of 14 than the errors in other directions.

With two FHSTs used for attitude determination, the sensor boresights are normally separated by a significant angle. Using such a geometry, the contribution of the inaccurate measurement

component of each tracker to the attitude and attitude error is supplemented by the more accurate contributions from the other sensor.

Attitude solutions using two FHSTs are often computed both by a ground ADS and one on board the spacecraft. Ground systems most often use a batch least-squares method for solution and usually solve for average gyro biases as part of the state vector. OBC systems usually use a Kalman filter and solve for an instantaneous gyro bias as part of the state vector. Because the ground ADS can usually use a much larger volume of data than can the OBC ADS, ground solutions may be more accurate than OBC solutions. OBC solutions may be more accurate if the ground solutions do not determine gyro biases, if the gyro biases vary significantly within the time covered by the ground solution data batch, or if more data are available to the OBC than to the ground ADS.

Depending on mission design and sensor placement, data from FHSTs may be limited by the FHSTs being occulted by the Earth during part of each orbit. FHST data availability may also be reduced by interference from the Sun, the Moon, and the Earth limbs. Some evidence suggests a slight degradation of FHST sensor accuracy while the spacecraft is in the SAA.

Figure 4-1 shows the estimated attitude accuracies for a number of missions that use two FHSTs for ground attitude determination. These include the active missions UARS and EUVE and the inactive missions SMM and MAGSAT. For EUVE, separate attitude accuracies were determined for the spacecraft in its two mission modes: rotating at 3 rpo about its *X*-axis and inertially pointed. The results shown are estimates of the accuracies obtained using all known significant error sources. Although they are minimum estimates of the actual attitude uncertainties, they are probably near the actual values because the error sources that are not included are almost certainly small.

Figure 4-1 also includes the estimated attitude accuracies for a number of missions using two FHSTs for OBC attitude determination. In some cases corresponding to active missions, a range of accuracies is shown. This range was determined using the ground attitude solution (where it is more accurate than the OBC solution—ground solution accuracies are shown in the same figure) as truth and determining the statistical deviations of the OBC attitude over a significant span (usually about one orbit) from the ground solution.

Of the active missions, EUVE had the most stringent attitude accuracy requirements and results. Although the sensors and sensor placement were similar for UARS and EUVE, EUVE was able to achieve significantly higher attitude accuracy through more accurate calibration and higher data volume.

At 3 rpo, the EUVE OBC achieved attitude accuracies superior to the ground system because the OBC Kalman filter included a gyro bias at each time step while the ground batch least-squares system solved for a single average bias over the batch. At 3 rpo the EUVE gyros were in high-rate mode and in this mode the gyro bias uncertainty produces a major contribution to the attitude uncertainty. Because the Kalman filter better represents the bias, this error is

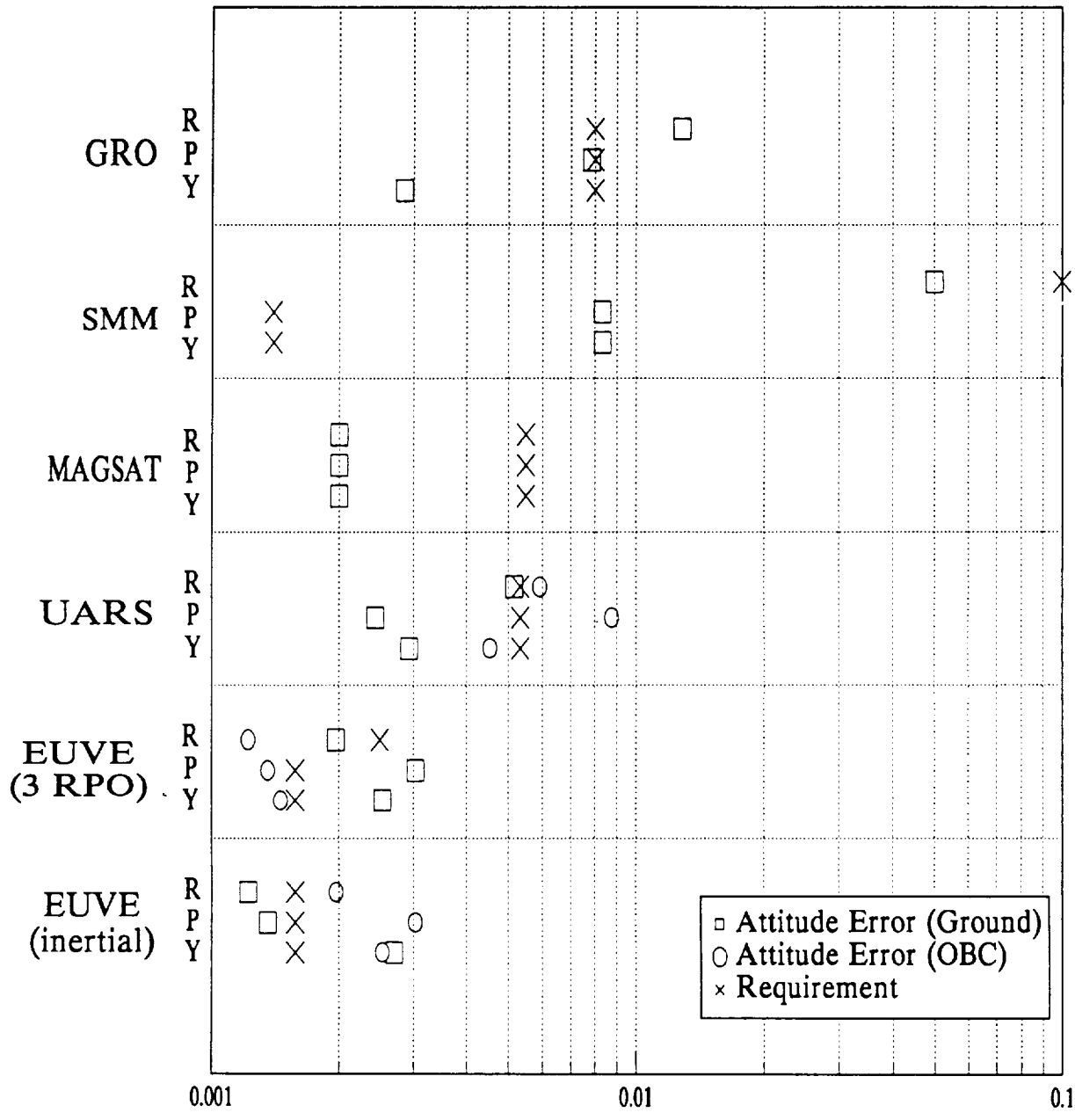

Figure 4-1. Attitude Accuracies (1σ) Using Two FHSTs

minimized. In inertial mode, the gyros were in low-rate mode, and their contribution to attitude uncertainty was smaller than at 3 rpo. The GRO attitude uncertainties are somewhat larger than those of other active missions. This slightly greater inaccuracy may be attributed to several causes:

- At the time for which the attitudes were determined the FHST2 scale factor drift was significant and uncertainties in the scale factor result in contributions to the attitude error computed by both the ground and OBC ADS.

- The compensation for the FHST2 scale factor change was performed differently for the ground and OBC ADS, resulting in an additional contribution to the attitude residuals and thus to the measured attitude error.

- The ground system does not solve for gyro bias as part of the state function in the ADS so any bias drift or fluctuation will result in additional attitude errors in the ground system.

4.1.2 Attitude Accuracies Using FSS and FHST

Attitude accuracies using one FSS and one FHST are included for the following missions: UARS, EUVE, TOPEX, SMM, GRO, and MAGSAT. Of these, GRO, UARS, EUVE, and TOPEX are active missions for which flight data were analyzed for this study (see Section 3.1 for additional information on TOPEX) to determine attitude accuracies, and SMM and MAGSAT are inactive missions for which attitude accuracies have been estimated from reports. Separate information is provided for EUVE in 3 rpo and inertial modes. SMM used a very accurate FPSS, and TOPEX used a CST, which has an accuracy comparable to the standard FHST.

The star trackers used on most of these missions are described in Section 3.1. TOPEX has star trackers that differ from other missions. They are CCD star trackers, produced by HDOS. These CCD star trackers, in contrast to most CCD trackers to be used in upcoming missions, have very similar characteristics to those of the NASA standard FHSTs, so they are grouped with them. They can track only one star at a time (in contrast to most other CCD star trackers), and their accuracy is rated at 10 arc sec (significantly less accurate than most CCD star trackers and comparable to FHST accuracy). One CST failed early in the TOPEX mission, so the CST plus FSS configuration was used for primary attitude data.

Attitudes using one FSS and one FHST are not usually determined as primary attitude solutions if two FHSTs are available, but they may be used if an FHST fails or if Earth occultation or Sun or Moon interference prevents the use of one of the FHSTs. The FSS may also be used in the primary attitude determination for inertial attitudes in which no guide star is in the FOV of one of the FHSTs. The SMM mission used an extremely accurate FSS (with a smaller FOV) as a primary sensor, and for this mission the FSS/FHST pair provided the reference attitude and the OBC attitude.

The standard FSS is manufactured by Adcole and has a square FOV 64 deg on a side. These FSSs normally provide a single-observation sensor accuracy of about 1 arc min. The ultimate accuracy of these sensors appears to be limited by the precision with which the transfer function represents the conversion of counts to angles. In two cases, calibration of the coefficients in the transfer function did not improve sensor accuracy. The 1-arc min sensor error appears to depend chiefly on the position in the FOV at which a measurement is made and has never been explicitly corrected. Some missions have flown Sun sensors with different accuracies. Attitudes using an FHST and an FSS exhibit the accuracy of the FHST in directions except that around the boresight of the FHST. The attitude accuracy in this direction is usually limited by the FSS accuracy supplemented by the FHST's accuracy around its boresight.

The amount of FSS data is limited by mission design and Earth occultation. Although the FOV is large, the Sun will take only about 15 minutes to pass through it for a typical near-Earth orbit, Earth-pointing satellite (e.g., UARS and TOPEX). For inertial-pointing satellites, the mission design may ensure that the Sun is potentially in the FOV at all times, but Earth occultation can remove Sun visibility during approximately one-third of the orbit. EUVE in 3 rpo mode and SMM had their Sun sensors pointed near the Sun at all times. Sun sensor measurements may also show errors when the Sun is near the Earth limb due to atmospheric refraction effects. This effect was evident for the EUVE mission and the degraded observations had to be eliminated from attitude determination.

Figure 4-2 shows the estimated attitude accuracies for a number of missions using one FSS and one FHST for attitude determination. The attitude accuracies for the active missions are obtained from comparisons of the two-FHST attitude with the FSS/FHST attitude.

For EUVE, there were significant differences in attitude accuracy using this sensor pair when the spacecraft rotated at 3 rpo compared with when it was inertially fixed. At 3 rpo, the single FHST used detects several stars, each of which provides an independent vector measurement. These vectors can be used together to obtain an attitude independent of the FSS data. The attitude accuracies at 3 rpo are comparable (slightly worse because only one FHST is used) to those using two FHSTs. When inertially fixed, the FHST views a single-star vector, and a three-axis attitude solution requires the additional use of the less accurate FSS data resulting in less accurate attitude solutions. The effect of sensor geometry can be seen by comparing the EUVE inertial attitude accuracies using FHST1 and the FSS with those using FHST2 and the FSS. The Sun-star angle when FHST2 was used was closer to 90 deg than when FHST1 was used, so the attitude errors are smaller in the former case.

For GRO the attitude accuracies are affected by the same factors described in Section 4.1.1. The effect of the FHST2 scale factor drift can be clearly seen by comparison of the FHST1 plus the FSS results with the FHST2 plus the FSS results. For all axes the measured attitude error is larger when FHST2 was used than when FHST1 was used. Although some of this shift could be due to a geometrical effect, its consistency for all axes indicates that a large portion of it is probably due to the incomplete compensation of scale factor drift.

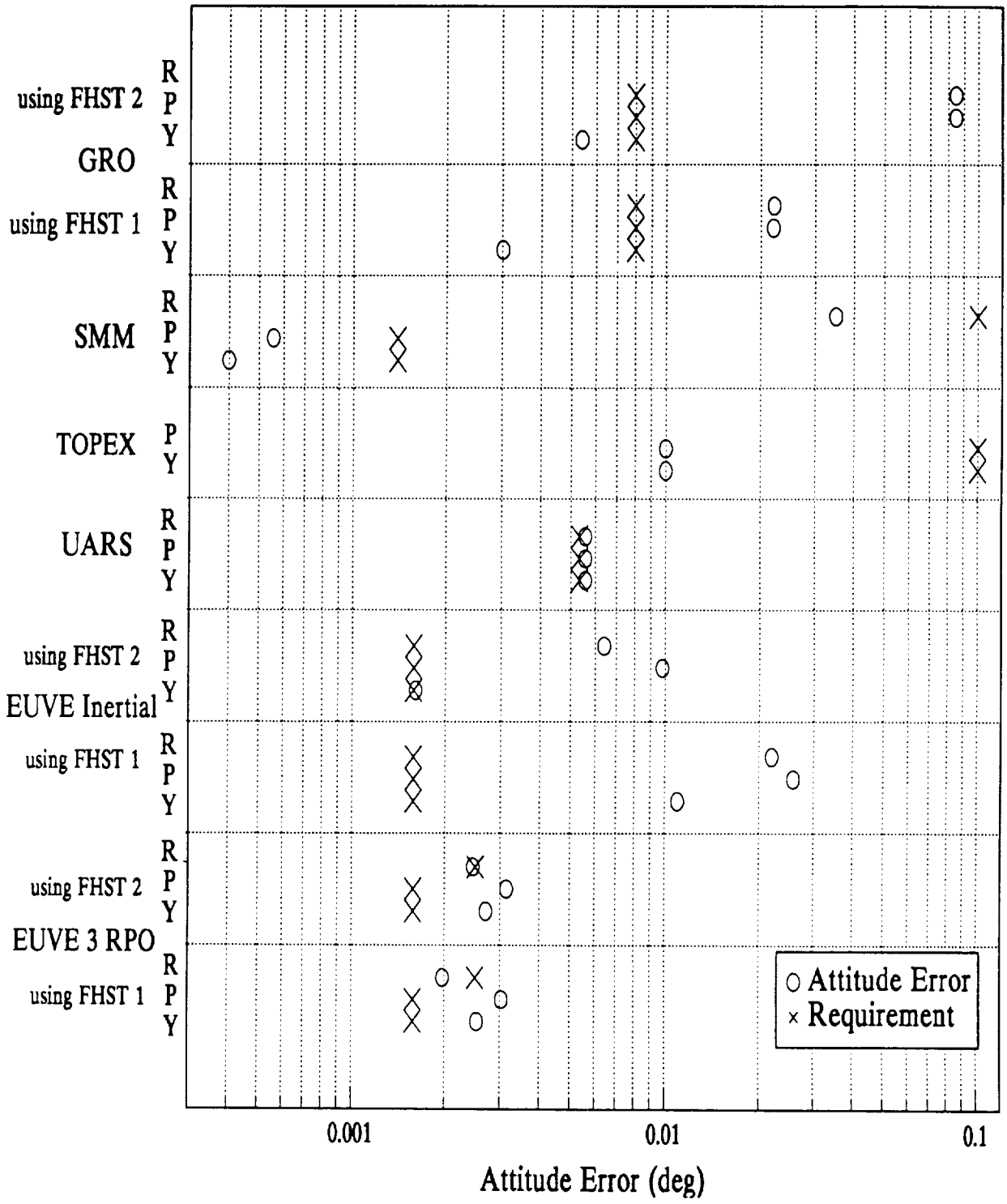

Figure 4-2. Attitude Accuracies (1σ) Using an FHST and an FSS

For SMM the attitude accuracy is significantly lower about the roll axis than about the other two axes. This result arises from the use of an extremely accurate FSS that is pointed along the roll axis.

4.1.3 Attitude Accuracies Using FHST and HS

Attitude accuracies using one FHST and a HS are available only for UARS.

HSs are occasionally used to supplement an FHST when no data are available from more accurate sensors. Because HSs determine the Earth direction relative to the spacecraft body, and the range of Earth angles that HSs can detect is limited, they are most often used in Earth-pointing spacecraft for which the Earth direction is nearly constant throughout the mission.

The most important error source affecting the HS were the measurement biases. Because these biases were produced mainly by misalignments, in-flight alignment is recommended (Reference 3 presents a comprehensive method for evaluating the biases).

HSs measure the emission of light (generally in the infrared region of the spectrum) from the stratosphere. As the sensor rotates, the rotation angle at which this light suddenly increases or decreases is processed to determine a horizon-crossing angle. Earth-in and Earth-out horizon crossings are processed to determine the width and/or center of an Earth chord. The ends of this chord are assumed to be at a nominal height above the surface of the Earth, and the width and/or center of the chord are interpreted in roll and pitch angles. The major uncertainty in HS output derives from the uncertainty in the height at which horizon crossing is detected. The horizon-crossing height is a function of atmospheric temperature at about 30 km above the surface. This temperature depends on latitude, time of year, and weather.

For some spacecraft ground systems, the systematic effects of latitude and time of year have been largely removed for ground attitude determination by an HRMU. Without an HRMU, HS sensor measurements are generally accurate to about 0.5 deg. The HRMU can improve accuracy to about 0.25 deg (Reference 4).

Ground-determined attitudes using HS data can be improved by a judicious choice of data-data may be taken chiefly from equatorial regions where horizon height effects are minimal. HS sensor accuracies are also dependent on the particular HS design, HS mounting on the spacecraft, mission altitude, and inclination of the orbit. HSs for different missions may, therefore, vary considerably in sensor measurement accuracy and in the accuracy of attitudes determined using their data. HSs of a design that decreases horizon height effects have recently been flown on the NOAA-10 spacecraft and are expected to be flown on the Tropical Rainfall Measuring Mission (TRMM) in the near future.

HS data are normally available throughout an entire orbit because the Earth is always visible from the spacecraft. On occasion, when the Sun is near the horizon observed by the HS, measurements may be corrupted. Figure 4-3 shows the estimated accuracies for missions using one HS and an additional sensor for attitude determination. The results for UARS with an HS

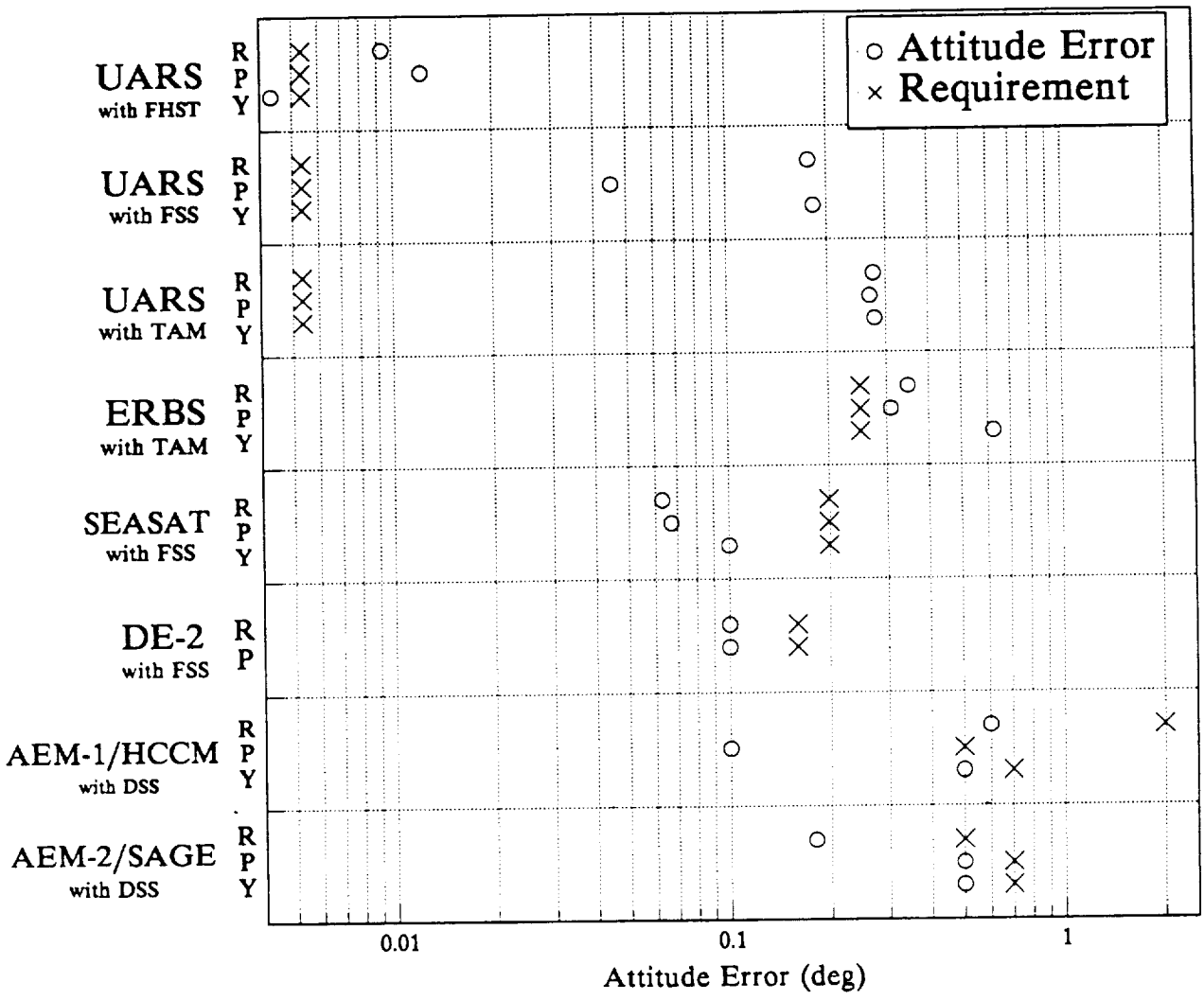

Figure 4-3. Attitude Accuracies (1σ) Using an HS and Another Sensor (FHST, FSS, DSS, or TAM)

and an FHST are included in this figure. The results are only slightly degraded from those for UARS using an FHST and an FSS. Because UARS rotates at 1 rpo and several stars are viewed during each orbit, the FHST is the major contributor to the attitude accuracy, and the HS has little effect.

4.1.4 Attitude Accuracies Using FHST and TAM

Attitude accuracies using one FHST and one TAM are included for the UARS and EUVE, both active missions. Results are included for EUVE in both 3 rpo and inertial modes.

TAMs are seldom used to supplement an FHST—they are used only when no data are available from more accurate sensors. TAM sensor accuracies are limited by the accuracy of the reference vector (from a model of the Earth's magnetic field at the spacecraft position), by local magnetic fields due to residual magnetization of the spacecraft and operation of spacecraft magnetic torquers (which are used to dump accumulated angular momentum), and often by the digitization of the magnetometer measurements.

The effect of residual magnetic fields can be minimized by solving for a TAM bias either separately from or together with the attitude solution. The reference magnetic field is normally modeled for ground solutions using a spherical harmonic expansion on the spacecraft position and time. The coefficients of this expansion change with time and are periodically updated (about every 5 years). The expansion may be truncated to save resources but is usually continued out to the sixth or eighth order. Even higher order expansions are becoming available. The accuracy of this expansion is no better than about ± 1 mG at near-Earth-spacecraft altitudes and can be considerably worse if the expansion is truncated before the sixth order.

TAM data are measurable at all points in the spacecraft orbit and for near-Earth spacecraft are the most reliable source of three-axis attitude information, but their limited accuracy precludes using them when accurate attitudes are required. Figure 4-4 shows the estimated attitude accuracies for a number of missions using a TAM and one other sensor. Data for UARS and EUVE using a TAM and an FHST are included in this figure.

As with the FSS and FHST pair and the HS and FHST pair the attitude accuracy using a TAM and FHST is not far degraded from that using an FHST only in the cases where the spacecraft is rotating (UARS and EUVE in 3 rpo mode). In strong contrast, the attitude accuracy of EUVE in inertial mode is degraded by about two orders of magnitude from the attitude accuracy of EUVE using the same sensors but rotating at 3 rpo.

4.1.5 Attitude Accuracies Using FSS and HS

Attitude accuracies using one FSS and one HS are included for UARS, DE-2, and SEASAT-1. Of these, UARS is an active mission, whereas SEASAT-1 and DE-2 are inactive missions for which the accuracies have been estimated from postlaunch reports. HSs are occasionally used to supplement FSS data when no data are available from more accurate sensors. Section 4.1.3 contains more details about HSs.

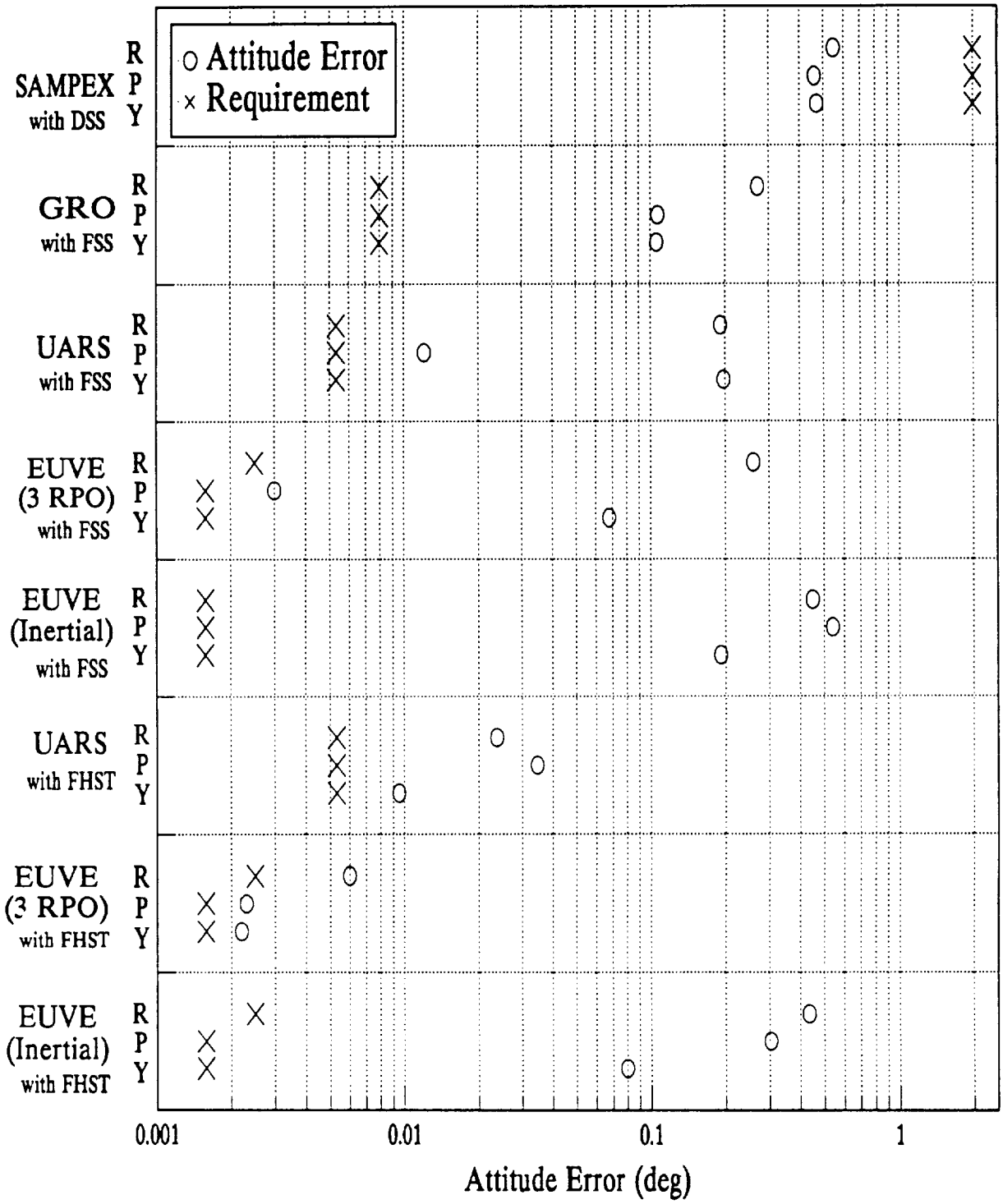

Figure 4-4. Attitude Accuracies (1σ) Using a TAM and Another Sensor (FHST, FSS, or DSS)

Some of the properties of FSSs are described in Section 4.1.2 and those of HSs in Section 4.1.3. This combination of sensors is not used for fine attitude determination if FHST data are available. FSSs are most useful as primary attitude sensors in missions with attitudes fixed with respect to the Sun, whereas HSs are used almost exclusively in Earth-pointing missions. As a result, mission plans do not, in general, provide primary attitude determination using this sensor combination. This pair of sensors can be used in case of failure of the primary attitude sensors. Nevertheless, some missions such as SEASAT-1 used them as primary attitude determination sensors. The attitude determination results are included in Figure 4-3.

4.1.6 Attitude Accuracies Using One FSS and One TAM

Attitude accuracies using one FSS and one TAM are included for UARS and EUVE, both of which are active missions. Data for EUVE are included in both its 3-rpo mode and its inertial mode.

The results are included in Figure 4-4. The FSS observations provide only a single accurate vector for EUVE in 3-rpo mode because the rotation is about the sunline so the observed Sun vector remains fixed with respect to the spacecraft body. This clearly also applies to EUVE in inertial mode. UARS, in contrast, rotates about its pitch axis; therefore, even though the Sun is visible only for at most a quarter of each orbit, the Sun position changes relative to the body, and Sun data affects the UARS attitude accuracy about all three axes.

4.1.7 Attitude Accuracies Using One DSS and One HS

Attitude accuracies using one DSS and one HS are included for the AEM-1/HCMM and AEM-2/SAGE, both of which are inactive missions for which the accuracies have been estimated from postlaunch reports. The HS and DSS have similar accuracies and were frequently paired on missions with less stringent attitude determination requirements.

DSSs generate an output, which is a digital representation of the angle between the sunline and the normal to the sensor face (Reference 1). The Sun image illuminates a pattern of slits. The slits are divided into a series of rows with a photocell beneath each row. Because the photocell voltage is proportional to cos θ (θ = Sun angle), a fixed threshold is inadequate for determining the voltage at which a bit is turned "on". This is compensated for by the use of the automatic threshold adjust (ATA) slit, which is half the width of the others. Consequently, the ATA photocell output is half that from any other fully lit photocell independent of θ, as long as the Sun image is narrower than any reticle slit. A bit is turned "on" if its photocell voltage is greater than the ATA photocell voltage and, consequently, "on" denotes that a reticle slit is more than half illuminated (independent of the Sun angle). The sign bit or the most significant bit determines which side of the sensor the Sun is on. The encoded bits provide a discrete measure of the linear displacement of the Sun image relative to the sensor center line or null. Several codes are used, including V-brush and Gray. The Gray code is the most widely used because Gray encoded data are less susceptible to corruption due to reticle pattern imperfection or stray light interference. Nevertheless, regardless of the encoding scheme used, in some particular situations, strong stray light can corrupt the DSS data (Reference 29). The DSSs usually have

several offset fine bits used by an integrator circuit to provide increased resolution (otherwise limited to 0.5 deg, the Sun angular diameter). By combining the output of two or three offset bit patterns in an interpolation circuit, 0.25-deg, or 0.125-deg accuracy can be attained. Two-axis DSSs, the most common digital sensors used on three-axis-stabilized spacecraft, consist of two single-axis units mounted at right angles yielding 64-by-64-deg or 128-by-128-deg FOVs. Full sky coverage can be obtained by using five or more 128-by-128-deg sensors. Section 4.1.3 contains more details about HSs.

The attitude accuracy study presented in the postlaunch reports (References 2 and 4) was performed using several orbits of data. The results are included in Figure 4-3.

The important error sources affecting the HS are described in Section 4.1.3.

4.1.8 Attitude Accuracies Using One DSS and One TAM

SAMPEX is included as an example of a mission using one DSS and one TAM. Although SAMPEX is an active mission, there were no other sensors available for comparison. SAMPEX attitudes were computed on the ground using these two sensors using attitude rates inferred from the changes in the attitude sensor data. The rate information was then used for attitude propagation.

The SAMPEX results are included in Figure 4-4.

4.1.9 Attitude Accuracies Using One HS and One TAM

Data for UARS and ERBS using one HS and one TAM are included. Because the HS and TAM have similar low to moderate inherent accuracies and are both limited to near-Earth missions, the HS does not add significant attitude information to that available from the TAM alone. Perhaps for this reason few missions used this sensor pair for attitude determination. The results for UARS and ERBS are included in Figure 4-3. Comparison with the results for TAM only (Figure 4-5) will show similar attitude accuracies.

4.1.10 Attitude Accuracies Using TAM Only

Attitude accuracies using TAM only are included for the following missions: UARS, EUVE, ERBS, AEM-1/HCMM, AEM-2/SAGE, and SEASAT-1. Of these, UARS, EUVE, and ERBS are active missions for which flight data were analyzed for this study to determine attitude accuracies, while HCMM, SAGE, and SEASAT are inactive missions for which attitude accuracies have been estimated from reports.

The attitude accuracy study presented in the postlaunch reports (References 2, 4, 5, and 7) was performed using several orbits of data. The attitude results are summarized in Figure 4-5.

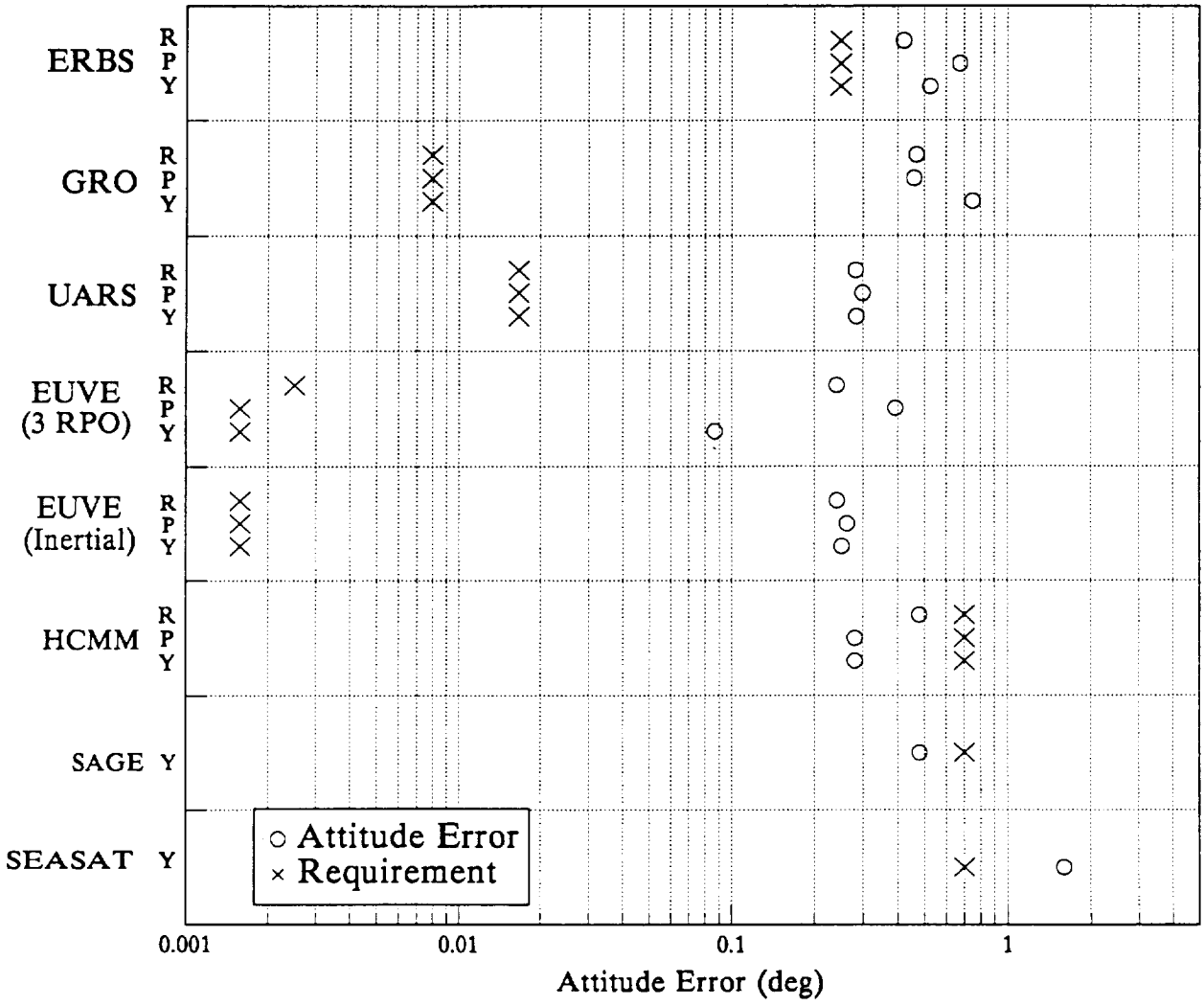

Figure 4-5. Attitude Accuracies (1σ) Using TAM Only

The observed biases included the instrument null error, spacecraft uncompensated field, internal alignment, and external alignment. The random errors included the telemetry noise, telemetry quantization error, and field model errors.

The most important error sources affecting the HCMM TAMs were the scale factor variations due to changes in the spacecraft magnetic field (see Reference 2). Scale factors and biases were periodically determined using DSS data and updated in the attitude determination system. In the absence of these scale factor and bias updates, the errors were on the order of a couple of degrees. The changes in the spacecraft magnetic field were due to transient magnetic fields in the science instruments.

The most important error sources for SAGE were also due to the science instruments. The spurious magnetic fields generated by them were very difficult to predict; therefore, the magnetometers could not be calibrated. The magnetometer data were useless when the science instruments were used. Fortunately, these periods represented only about 10 percent of the total.

For EUVE, TAM biases, scale factors, and the effect of the magnetic torquer bars on the TAMs were determined during calibration. The factors had little effect on the TAM-only attitude accuracy.

On UARS, TAM biases were determined and monitored in the early mission stages, and no significant TAM bias changes were found.

The lack of attitude accuracy improvement after calibration on both UARS and EUVE is due perhaps to the relatively large data digitization of the TAM in the telemetry (8 mG) being the same size as the calibration corrections.

The achieved attitude accuracies are presented in Figure 4-5.

4.1.11 Summary of Three-Axis-Stabilized Attitude Accuracies

Figure 4-6 shows a summary of the ground-determined attitude accuracies for each of the sensor pairs described in greater detail above. In this figure, all of the missions with data available for particular pairs of sensors are gathered on a single horizontal level. Attitudes using different sensor pairs on the mission are represented throughout the graph by a common symbol. The values given for each spacecraft and attitude pair in Figure 4-6 are the rms of the uncertainties from all axes.

Note that for some spacecraft (e.g., SMM) the attitude uncertainties about particular axes are substantially different from those for the other two axes, so the average attitude uncertainties may not truly represent uncertainties on any particular axis.

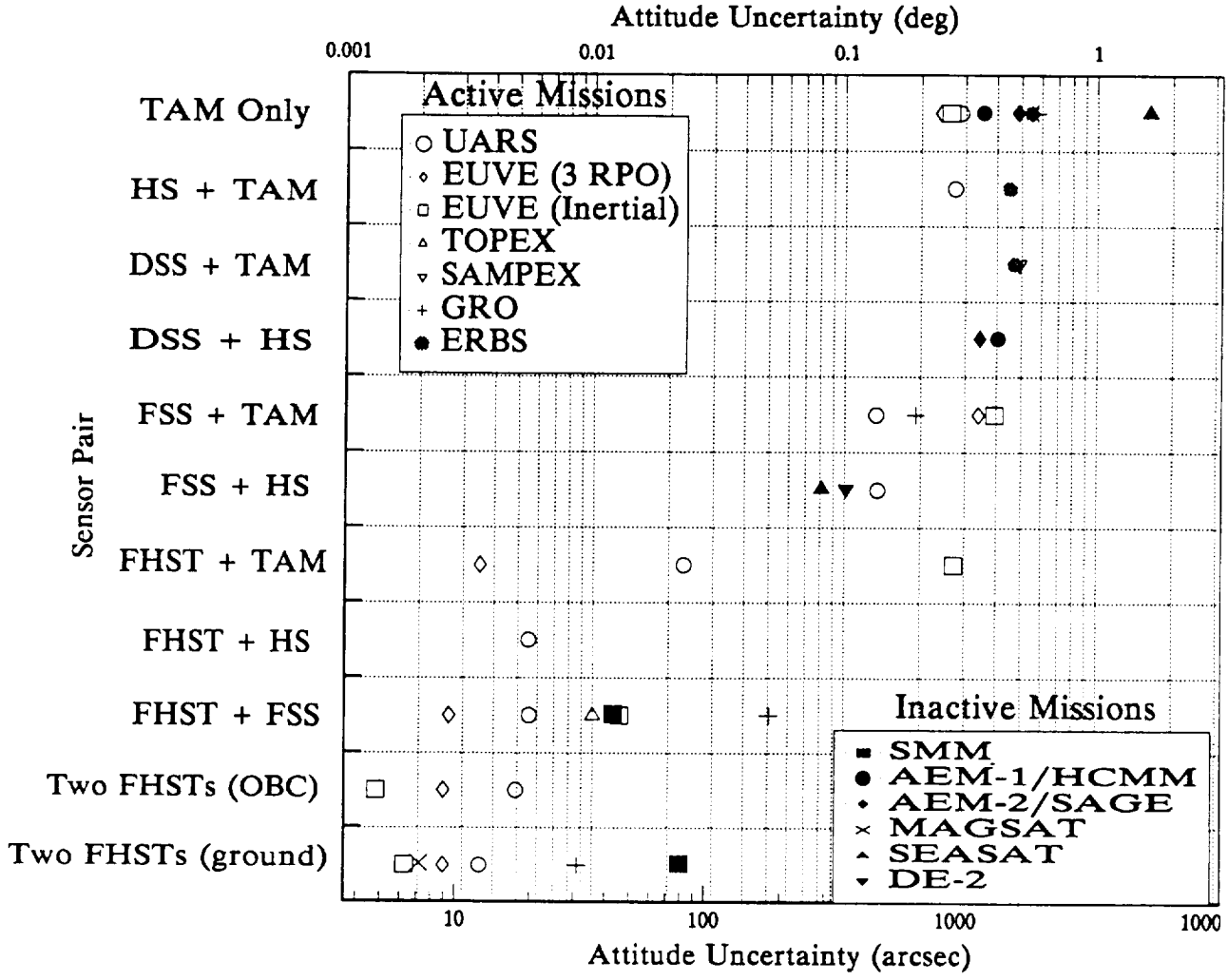

Figure 4-6. Summary of Three-Axis-Stabilized Attitude Accuracies (1σ)

4.2 Attitude Accuracies of Spin-Stabilized Spacecraft

This section includes plots of attitude accuracies for various sensor pairs used by spin-stabilized spacecraft. In each of these plots, the range of attitude accuracies and/or the mean attitude accuracy for various spacecraft using the specified sensor pair are given. Whenever possible, a range is given for each axis. In general, these spin-stabilized spacecraft did not have gyros, so the attitude determination methods used in these missions could not use gyro data. When the mission requirements were not satisfied by single-frame methods, a spacecraft dynamics model was used to propagate data to a common time.

4.2.1 Attitude Accuracy Using a Single-Axis DSS and an HS

Attitude accuracies using a single-axis spinning-mode Sun sensor and one spinning-mode Earth sensor are included for CTS, DE-1, IMP-8, IUE, and AE-3. All of these are inactive missions. The attitude accuracy data were taken from published reports (References 3, 12, 17, 18, 22, and 26).

The spinning-mode Sun sensor, spinning-mode Earth sensor pair is quite common. Each spinning-mode Sun sensor is divided into two parts (References 3 and 17): element A and element B. Element B senses the instantaneous angle of the projection of the sunline onto the rotating plane of the spacecraft. In each spin revolution, element A generates a reference pulse at the instant the rotating X_b - Z_b plane crosses the sunline. At this time, the angle read by element B is identical to the elevation angle of the Sun above or below the spacecraft spin plane X_b - Y_b. The sunline crossing signal provided by element A is also used for timing Earth horizon crossings, which are sensed by the spinning Earth sensors. This information can be used to calculate the rotation angle between the Sun direction and the nadir direction. The spinning-mode Earth sensors detect the exact time in each spin revolution that the centerline of their FOV crosses the sky-to-Earth boundary and the Earth-to-sky boundary. These two types of crossings are commonly named horizon-in and horizon-out crossings, respectively. They are detected by the sensors through the sharp change in infrared energy associated with them. The rigidly body-mounted HSs do not produce an angular velocity signal; otherwise, they are very similar to the wheel-mounted HSs described in Section 4.1.4.

Figure 4-7 shows the estimated attitude accuracies for a number of missions using one spinning-mode Sun sensor and one spinning-mode Earth sensor for attitude determination. The mission descriptions are found in Section 3.2.

4.2.2 Attitude Accuracy Using an FSS and an HS

Attitude accuracies using a spinning-mode FSS and one spinning-mode Earth sensor are included for the ISEE-3, an inactive mission. The attitude accuracy data were taken from published reports (Reference 20).

This sensor complement is similar to the one presented in Section 4.2.1 except that the FSS has better accuracy than the DSS.

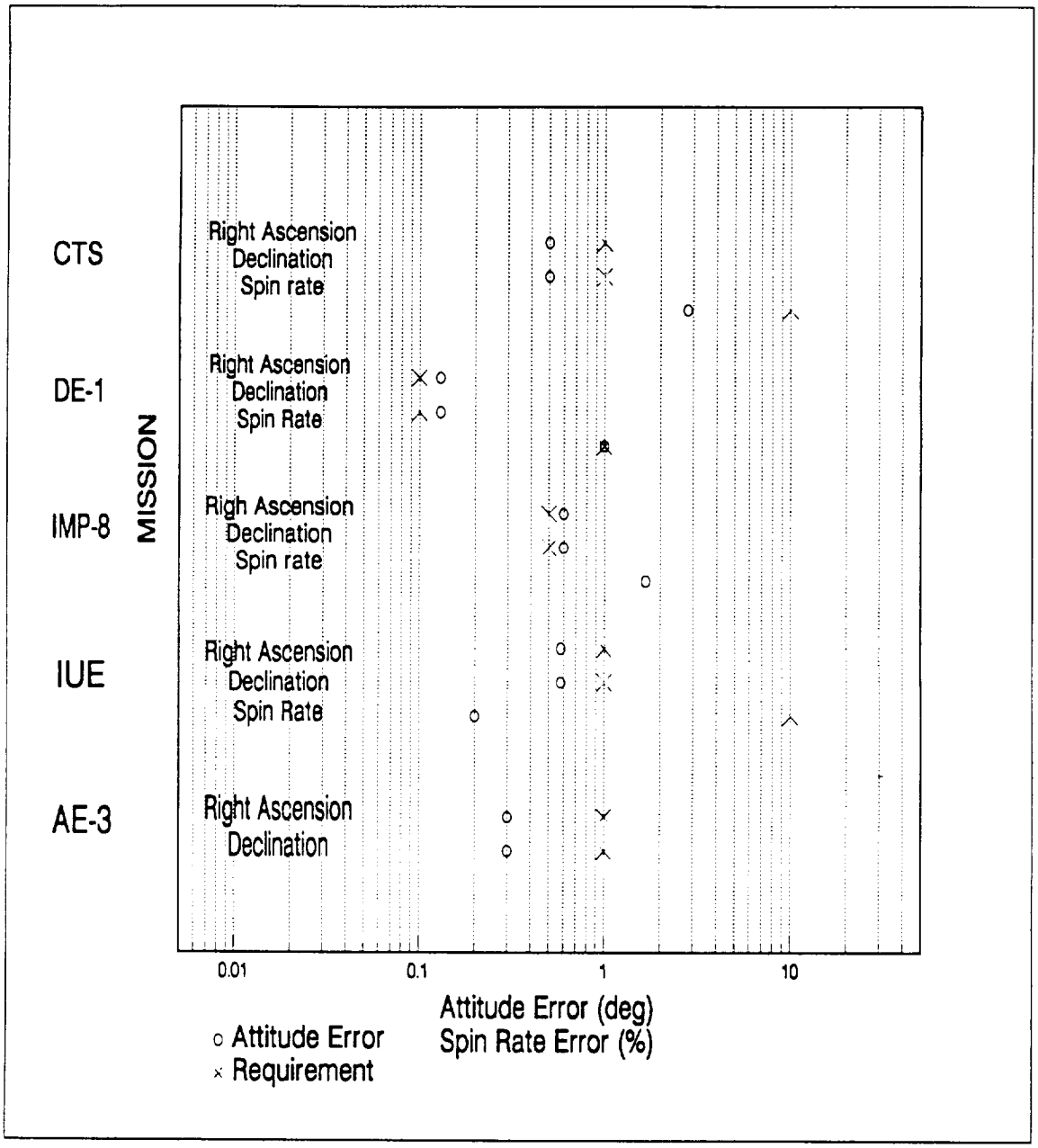

Figure 4-7. Attitude Accuracies (1σ) Using a DSS and an HS

The spinning-mode FSSs are similar to those used on board the three-axis-stabilized missions that are described in Section 4.1.3, except for the fact that the spinning-mode FSSs are single-axis instruments, equipped with a trigger element for Sun measurement timing.

Figure 4-8 shows the estimated attitude accuracies for ISEE-3 using one spinning-mode FSS and one spinning-mode Earth sensor for attitude determination. The mission description is found in Section 3.2.

4.2.3 Attitude Accuracy Using a Single-Slit Star Scanner and a Single-Axis DSS

Attitude accuracies using a spinning-mode Sun sensor and a single-slit star scanner are included for the inactive SSS-1 mission. The attitude accuracy data were taken from published reports (Reference 19).

The single-slit star sensor used by SSS-1 was a visible light photomultiplier with a single-slit focal plane reticle producing a fan shaped FOV (Reference 19). The plane of the fan included the spacecraft spin axis as well as the optical axis. As the optical FOV is swept across the sky by the spacecraft motion, the focused image of a star lies momentarily in the transparent focal plane slit, and starlight passes through to the photomultiplier behind the reticle. From this star transit the photomultiplier produces an analog pulse. If the star has a sufficiently bright magnitude, a threshold trigger will fire and the electronics will measure the entrance time, width, and amplitude of the star pulse. Due to the width of the slit (0.5 deg) the measurement uncertainty was higher than for usual slit star sensors.

The attitude determination accuracy obtained using this pair of sensors is presented in Figure 4-9. The mission descriptions are found in Section 3.2.

4.2.4 Attitude Accuracy Using a V-Slit Sun Sensor and an HS

Attitude accuracies using a V-slit Sun sensor and one spinning-mode Earth sensor are included for the GOES-3, GOES-5, and SIRIO missions. All are inactive missions. The attitude accuracy data were taken from published reports (References 24 and 25).

The V-slit Sun sensor, spinning-mode Earth sensor pair was common for the GOES satellite series. A V-slit Sun sensor normally contains two plane field (PF) sensors making an angle β with respect to each other (Reference 3). Each PF sensor has a planar FOV. Thus, the projection of the FOV onto the celestial sphere is a segment of a great circle. The sensor provides an event pulse whenever the FOV crosses the Sun. Therefore, the Sun angle, β, can be obtained directly from the measurements of the spin rate and the time interval between the two Sun-sighting events provided by the two PF sensors.

The attitude determination accuracy attained using this pair of sensors is presented in Figure 4-10. The mission descriptions can be found in Section 3.2.

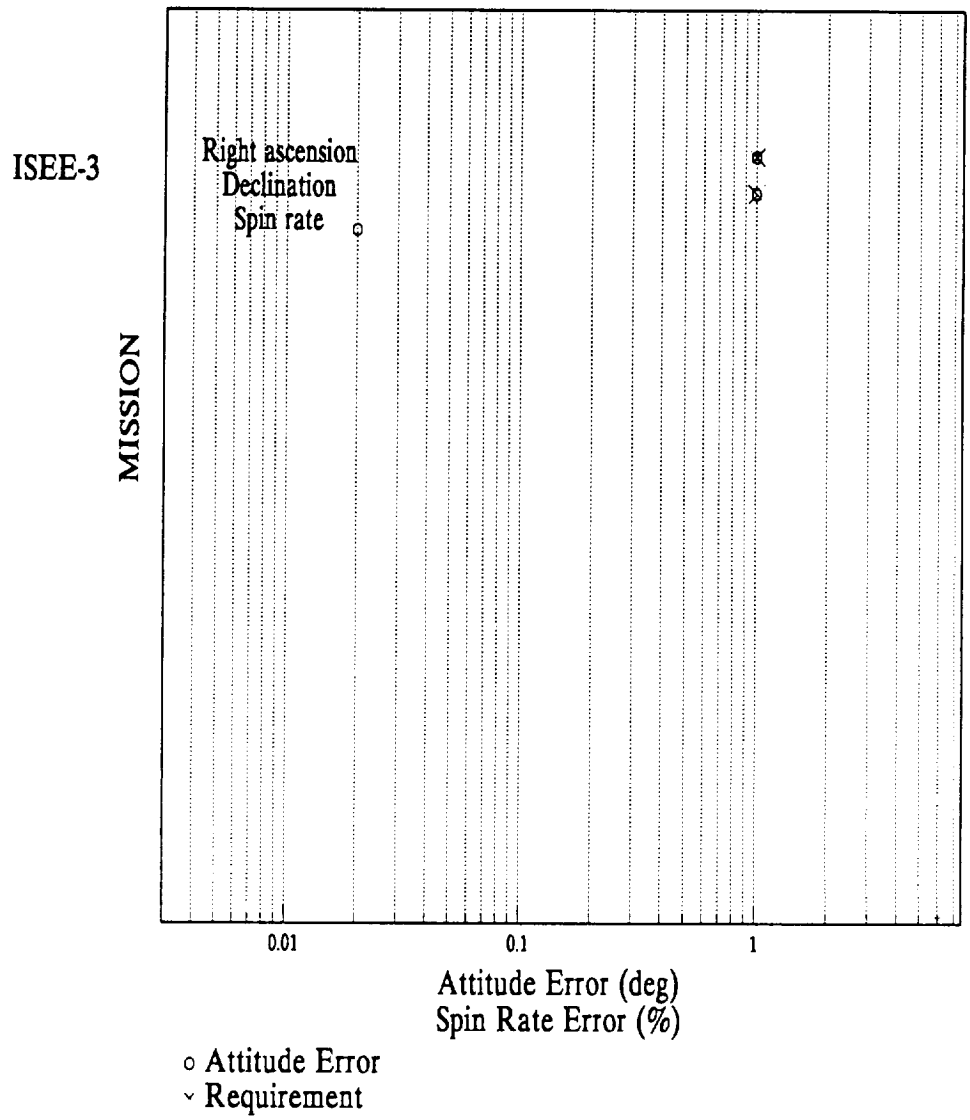

Figure 4-8. Attitude Accuracies (1σ) Using a Single-Axis FSS and an HS

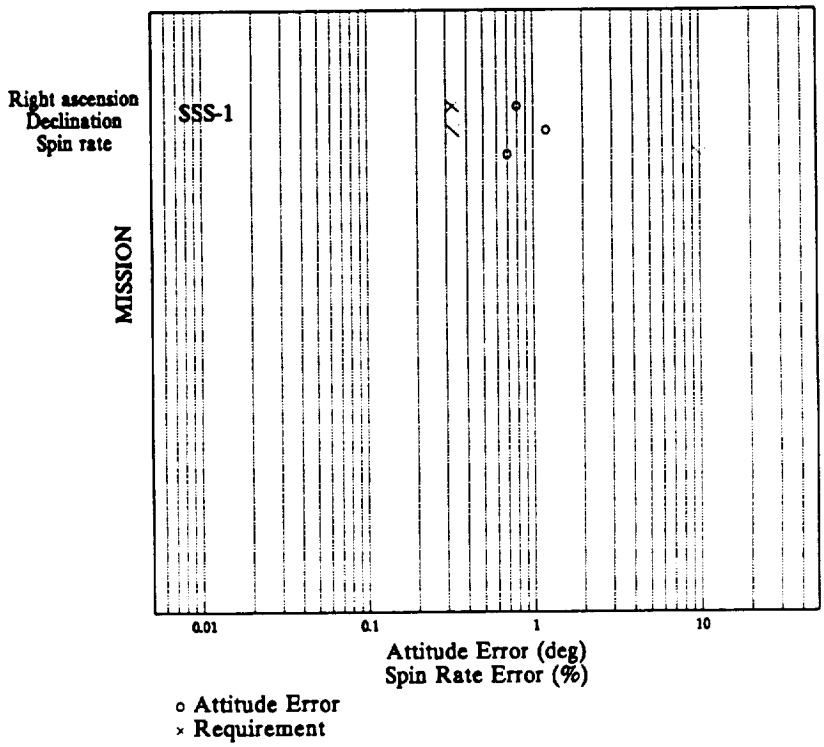

Figure 4-9. Spin-Axis Attitude Accuracies (1σ) Using a Single-Slit Star Scanner and a Single-Axis DSS

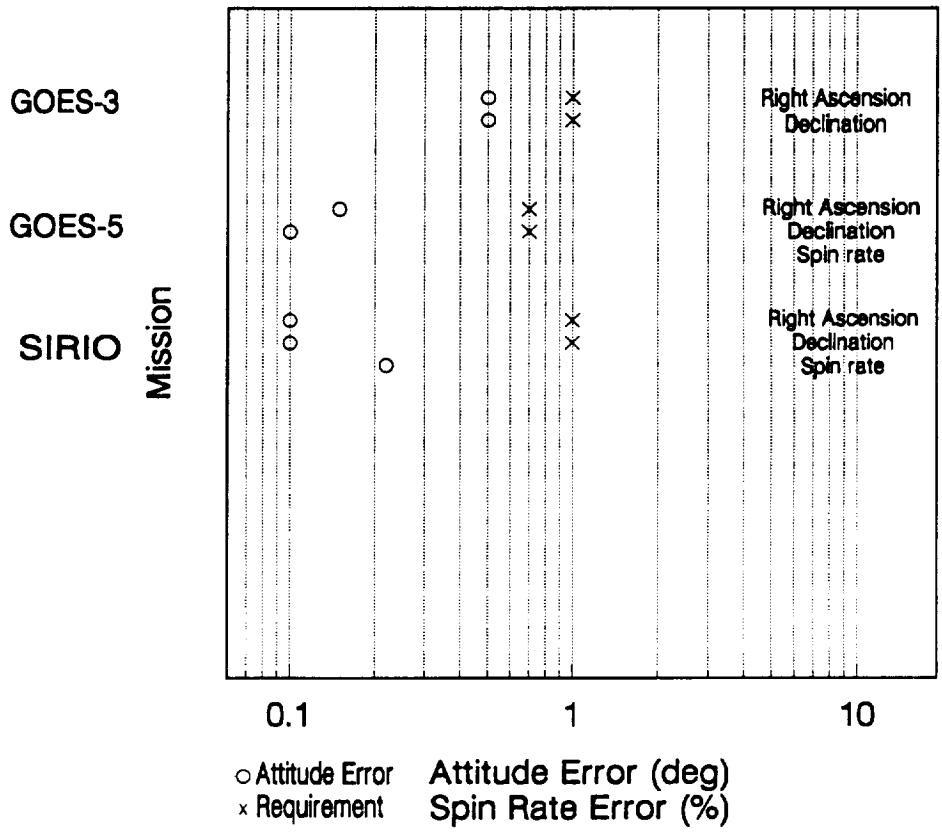

Figure 4-10. Spin-Axis Attitude Accuracies (1σ) Using a V-Slit Sun Sensor and an HS

4.2.5 Attitude Accuracy Using an N-Slit Star Scanner and a Single-Axis DSS

Attitude accuracies using an N-slit Star scanner and a single-axis DSS are included for the inactive SAS-2 mission. The attitude accuracies were taken from published reports (Reference 27).

The N-slit star scanner is similar in operation to the V-slit star scanner and provides a pulse when a star crosses a slit. The crossing time of the first is proportional to the star's azimuth angle (Reference 3). The elapsed time between the first and second crossing provides information about the star's elevation in the spacecraft frame of reference.

The attitude accuracy attained using this sensor pair is presented in Figure 4-11. The mission description can be found in Section 3.2.

4.2.6 Attitude Accuracy Using TAM Only

Attitude accuracies using TAM only are included for the inactive SAS-2 mission. The attitude accuracy data were taken from published reports (Reference 27).

On board the spinning satellites, the TAMs are not used as primary attitude determination instruments. Whenever they are included in the attitude determination hardware, they are intended to serve as a backup. Therefore, the available data referring to the attitude accuracy attained using TAMs only is limited.

The attitude accuracy attained using this sensor pair is presented in Figure 4-12. The mission description can be found in Section 3.2.

4.2.7 Summary of Spin-Stabilized Attitude Accuracies

Figure 4-13 shows a summary of the attitude accuracies for each of the sensor pairs described in greater detail above. In this figure, all the missions with data available for particular pairs of sensors are gathered on a single horizontal level. Attitudes using different sensor pairs on the mission are represented throughout the graph by a common symbol.

The attitudes represented in Figure 4-13 are rms values of right ascension and declination.

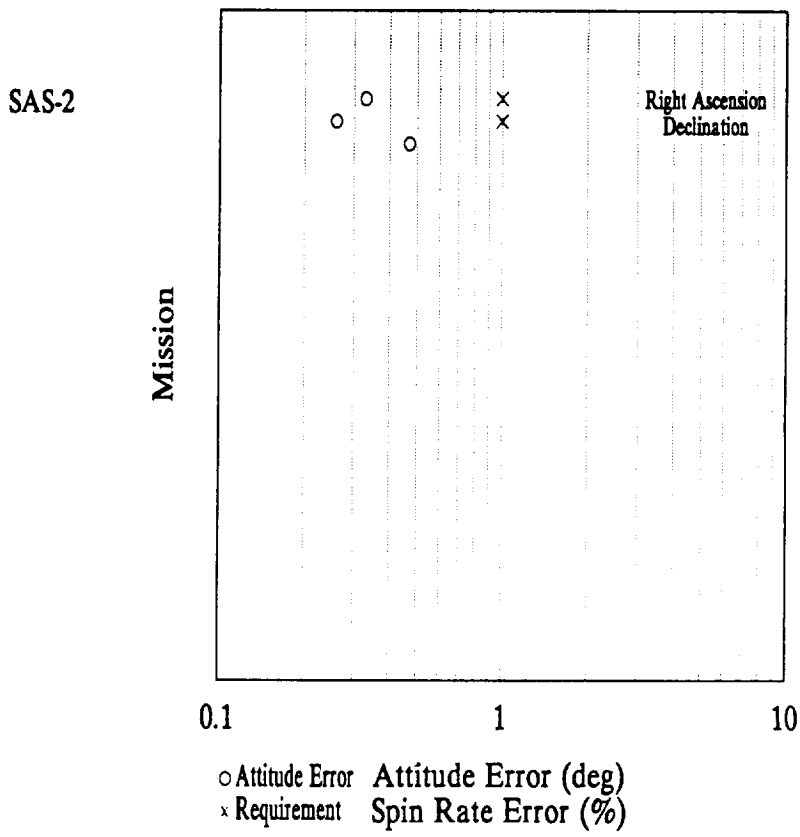

Figure 4-11. Spin-Axis Attitude Accuracies (1σ) Using a Multiple-Slit Star Scanner and a Single-Axis DSS

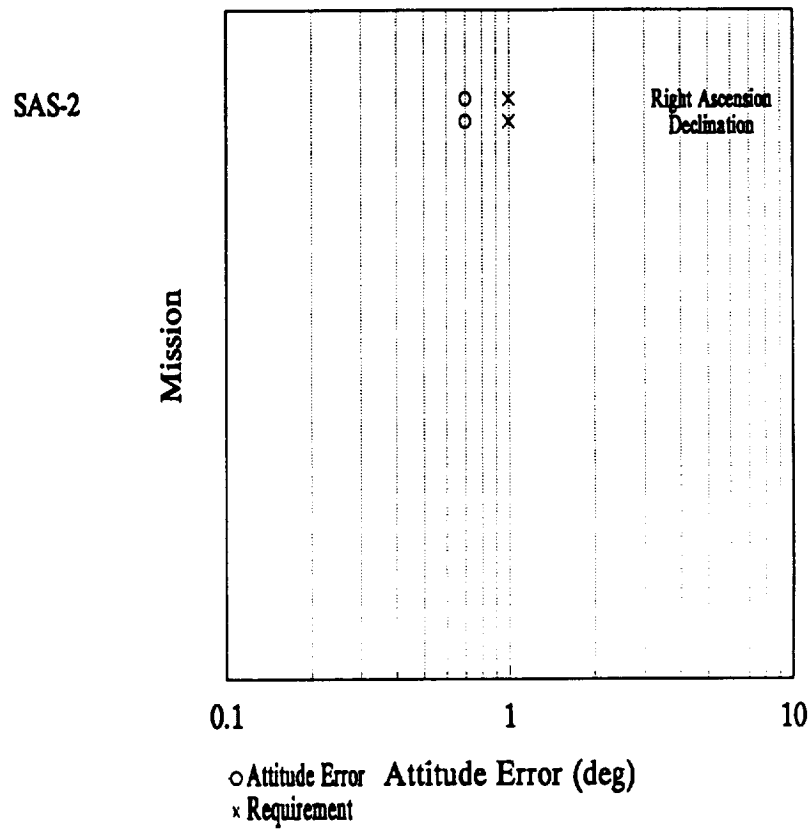

Figure 4-12. Single-Axis Attitude Accuracies (1σ) Using TAM Only

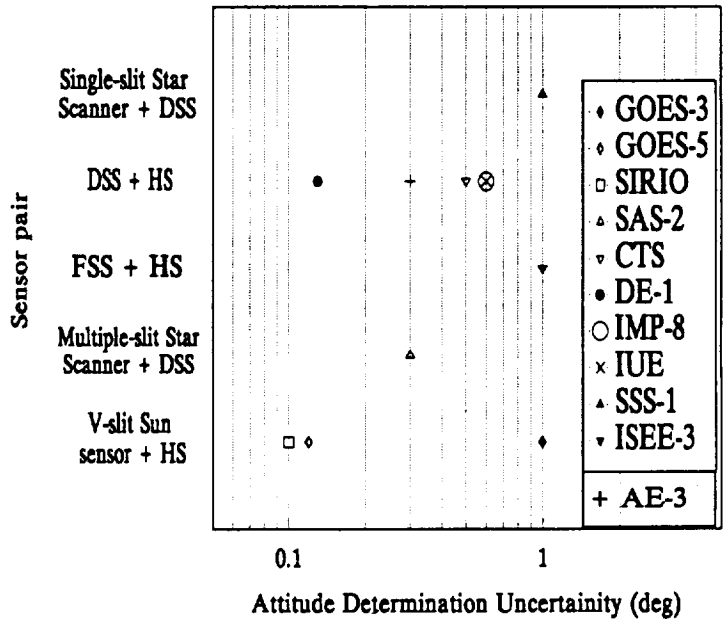

Figure 4-13. Summary of Spin-Stabilized Attitude Accuracies (1σ)

Section 5. The Effect of Sensor Accuracy Variations

The attitude sensors are subject to various external error sources (see Section 2.6 for more details) which may not be compensated for by normal calibration procedures. In some cases, these errors act like measurement biases that can be evaluated and compensated by using special calibration procedures. In other cases they increase the measurement noise. This Section presents the effect of sensor noise variation on attitude determination accuracy. Note that other error sources usually dominate the attitude uncertainty.

5.1 Three-Axis-Stabilized Spacecraft

For three-axis-stabilized spacecraft, the effect of increased sensor noise on attitude determination accuracy was modeled using ADEAS. The accuracy of one sensor was considered to be nominal, while the second sensor accuracy was varied over a broad range. Reference 30 contains information regarding ADEAS usage. ADEAS requires detailed mission characteristic data, therefore the results obtained are mission specific. However, if two spacecraft have similar sensor geometries, orbits, and attitudes, then their attitude determination accuracies can be assumed to be the same. If some of the mission characteristics are significantly different, then the ADEAS results included in this Section can provide only an initial evaluation. Table 5-1 presents the sensor pairs included and the main ADEAS NAMELIST values. Timespans of 10 minutes were considered. The attitude accuracies listed are those attained at the end of the timespan. Both sensor data rates were assumed to be approximately 15 seconds. The batch and the Kalman filter solutions were identical. The reference time and the orbit epoch were the same. The sensor orientation is referred to body frame. Unless otherwise specified, the right ascension of ascending node, the argument of perigee, and the mean anomaly are zero. Normally, CSSs are not used for attitude determination, therefore they were not included. CCDs were not included because of current ADEAS release limitations.

The noise of one sensor was assumed to be nominal, while the noise of the second sensor varied from 0.1 $\times$ nominal to 10 $\times$ nominal. To improve the clarity of plots and to avoid confusions, no sensor biases and misalignments were considered. For more information regarding biases and misalignments the reader should refer to the extensive literature on the subject (see, for example, Reference 3). Logarithmic scales were used on both axes to accommodate extended ranges. The sensor noise is expressed as a ratio between its actual and nominal values. The plots present the RMS of the three-axis attitude errors. The nominal sensor noise levels are listed in Table 5.2. Plots 5-1 through 5-4 were generated assuming the FHSTs tracked more than one star.

Table 5-1. Figure List, Sensor Complement, Orbit, and Attitude

Fig. no.	Sensor complement	Epoch time	Orbit elements	Body attitude	Sensor geometry	
					Euler seq.	Euler angles (deg)
1	Two FHSTs	800621.100000	a=6878.0 km, e=0.001, i=28.0 deg	Euler seq.:X,Y,Z; Euler angles (deg): 150.0, 0, 0	FHST 1 & 2: X, Z, X	FHST1: 102, 54, -20 FHST2: -102, 127, -20
2	FHST & FSS	800321.100000	a=6878.0 km, e=0.001, i=28.0 deg	Euler seq.:X,Y,Z; Euler angles (deg): 150., 0, 0	FHST: X, Z, X; FSS: Y, X, Z	FHST: 102, 54, -20 FSS: 90, 0, 0 (inertial); -90, 0, 0 (1 rpo)
3	FHST & HS	791031.000000	a=6833. km, e=0.016, i=97 deg, mean anomaly=90 deg	Euler seq.:X,Y,Z Euler angles (deg): 0, 0, 0	FHST: X, Z, X; HS: X, Y, Z	FHST: 102, 54, -20 HS: 90, 0, 0
4	FHST& TAM	791031.000000	a=6833. km, e=0.016, i=97 deg, mean anomaly=90 deg	No rotation	FHST: X, Y, Z; TAM: no rotation	FHST: 102, 54, -20
5	FSS & HS	780518.000000	a=7168. km, e=0.0008, i=108 deg, ra=302 deg, argument of perigee=90 deg	No rotation	FSS: Z, Y, Z HS: X, Y, Z	FSS: 270, 97, -90 HS: 64, 0, 0
6	FSS & TAM	790321.000000	a=6833, e=0.016, i=97 deg, mean anomaly=90 deg	no rotation	FSS: no rot.; TAM: X, Z, X	TAM: 90, 0, 0
7	DSS & HS	790422.000000	a=6978, e=0.001, i=55 deg	no rotation	DSS: Z, X, Z HS: X, Y, Z	DSS: -30, 133, -90 HS: -90, 0, 0
8	DSS & TAM	790422.000000	a=6978, e=0.001, i=55 deg	no rotation	DSS: Z, X, Z TAM: no rot.	DSS: -30, 133, -90
9	HS & TAM	790422.000000	a=6978, e=0.001, i=55 deg	no rotation	HS: X, Y, Z TAM: no rot.	HS: -90, 0, 0
10	TAM only	790422.000000	a=6978, e=0.001, i=55 deg	no rotation	TAM: no rot.	

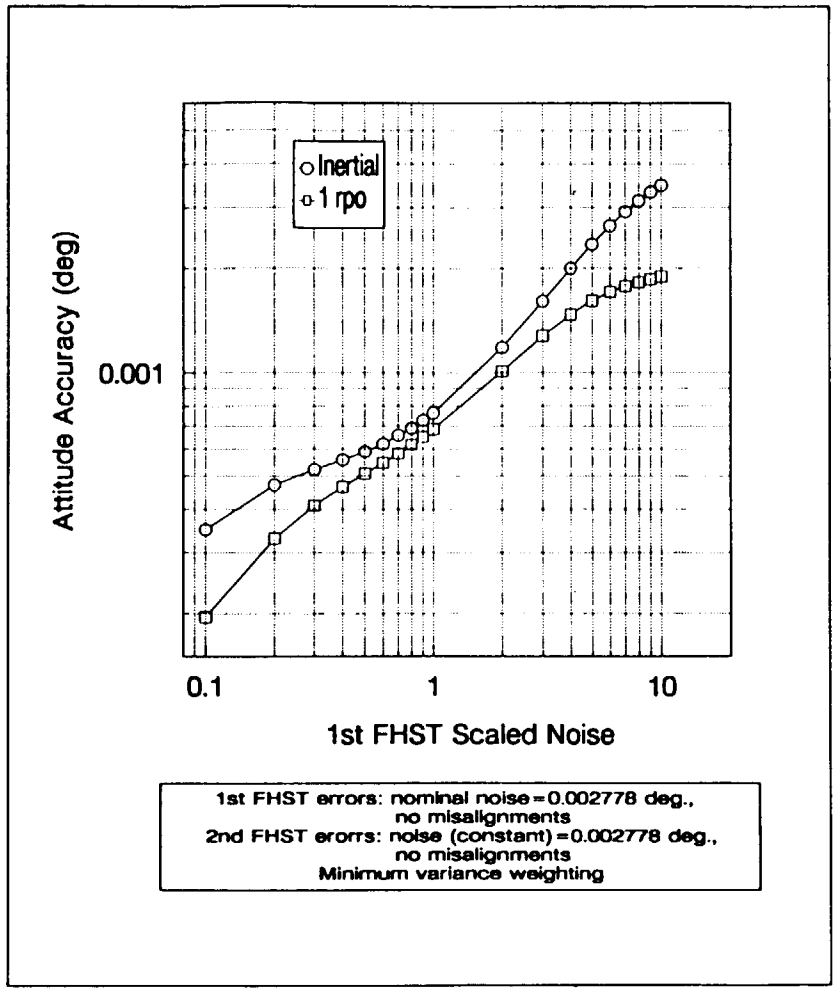

Figure 5-1. The Effect of Sensor Noise Variation on Attitude Determination Accuracy Using a Two-FHST Sensor Complements

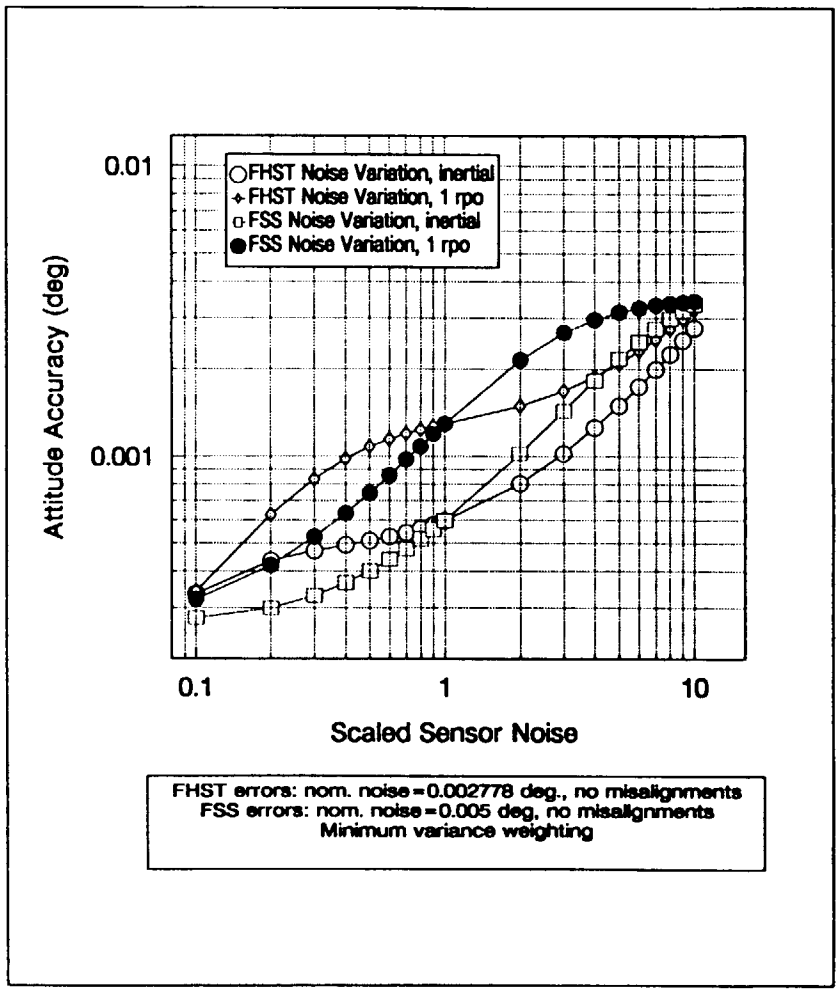

Figure 5-2. The Effect of Sensor Noise Variation on Attitude Determination Accuracy Using an FHST and FSS Sensor Complement

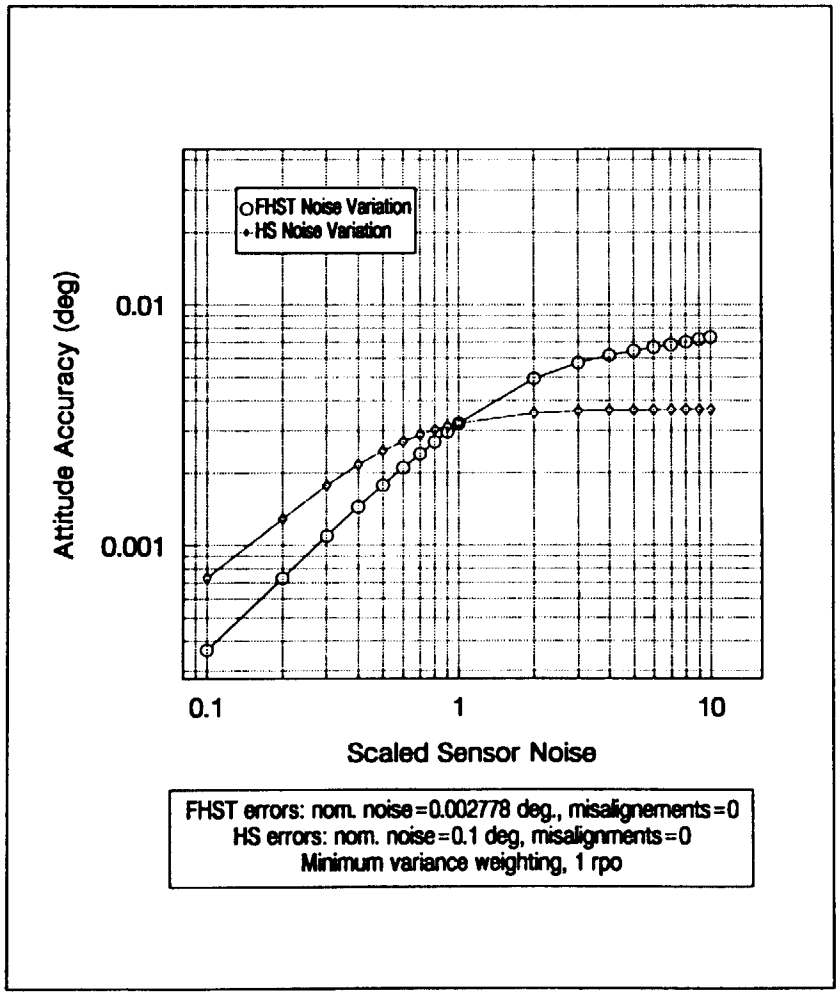

Figure 5-3. The Effect of Sensor Noise Variation on Attitude Determination Accuracy, FHST and HS Sensor Complement

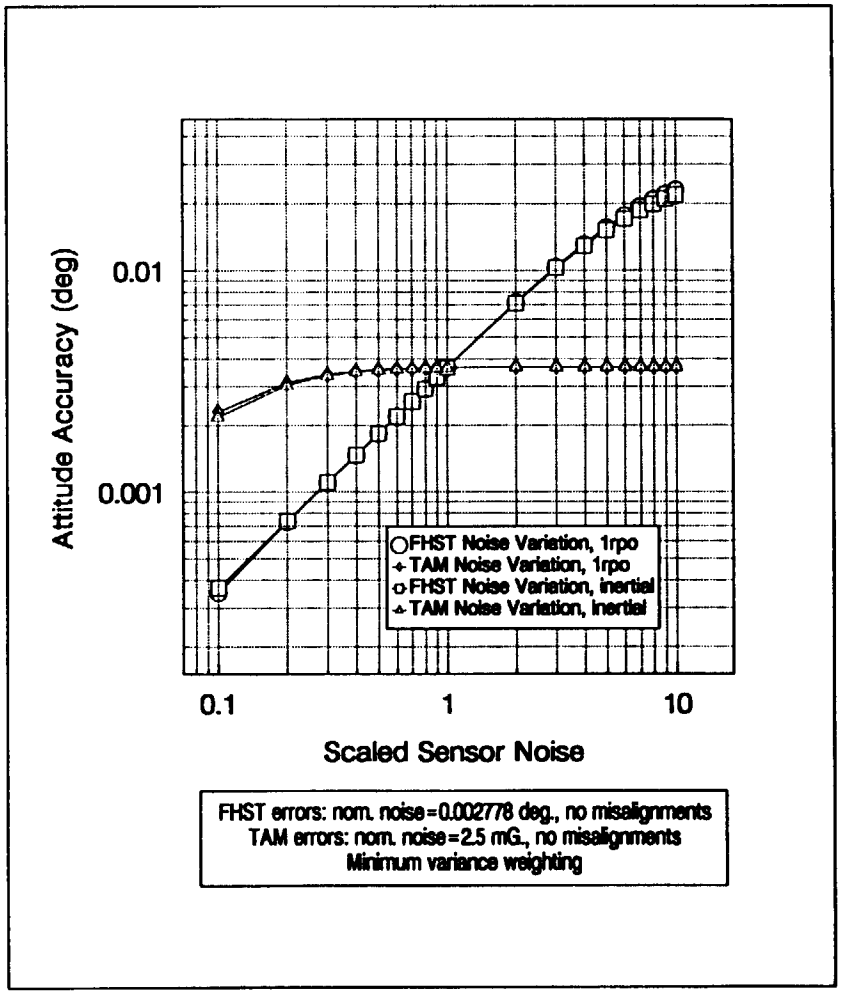

Figure 5-4. The Effect of Sensor Noise Variation on Attitude Determination Accuracy, FHST and TAM Sensor Complement

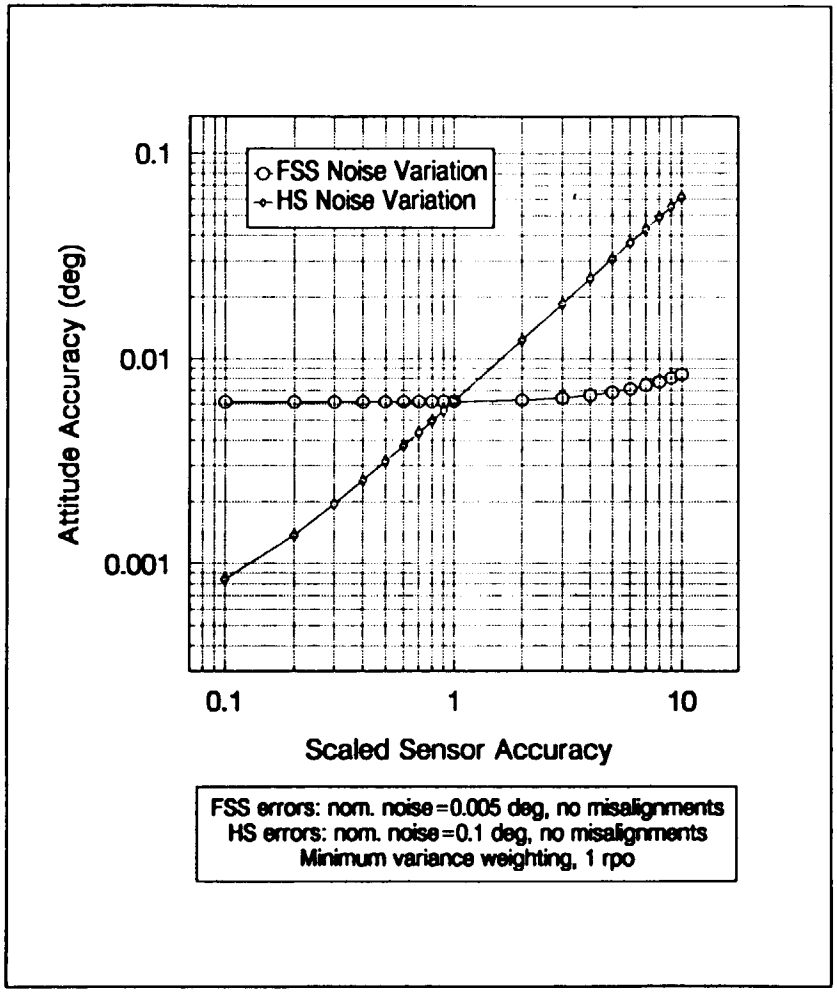

Figure 5-5. The Effect of Sensor Noise Variation on Attitude Determination Accuracy, FSS and HS Sensor Complement

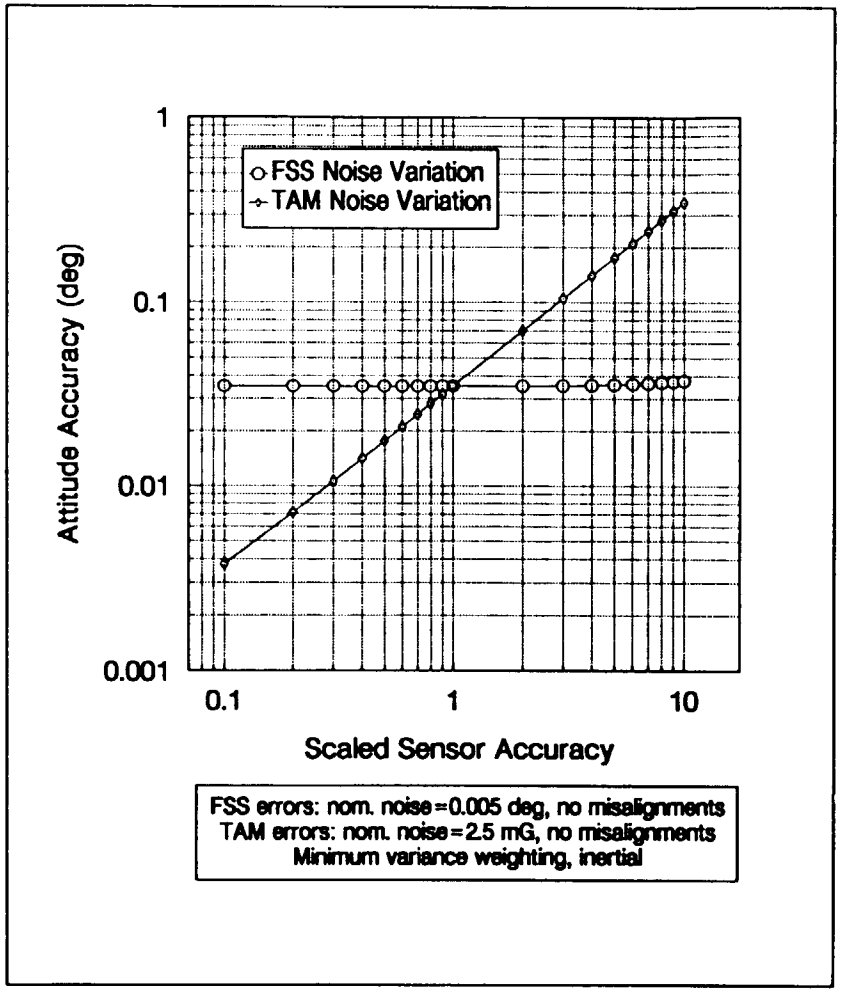

Figure 5-6. The Effect of Sensor Noise Variation on Attitude Determination Accuracy, FSS and TAM Sensor Complement

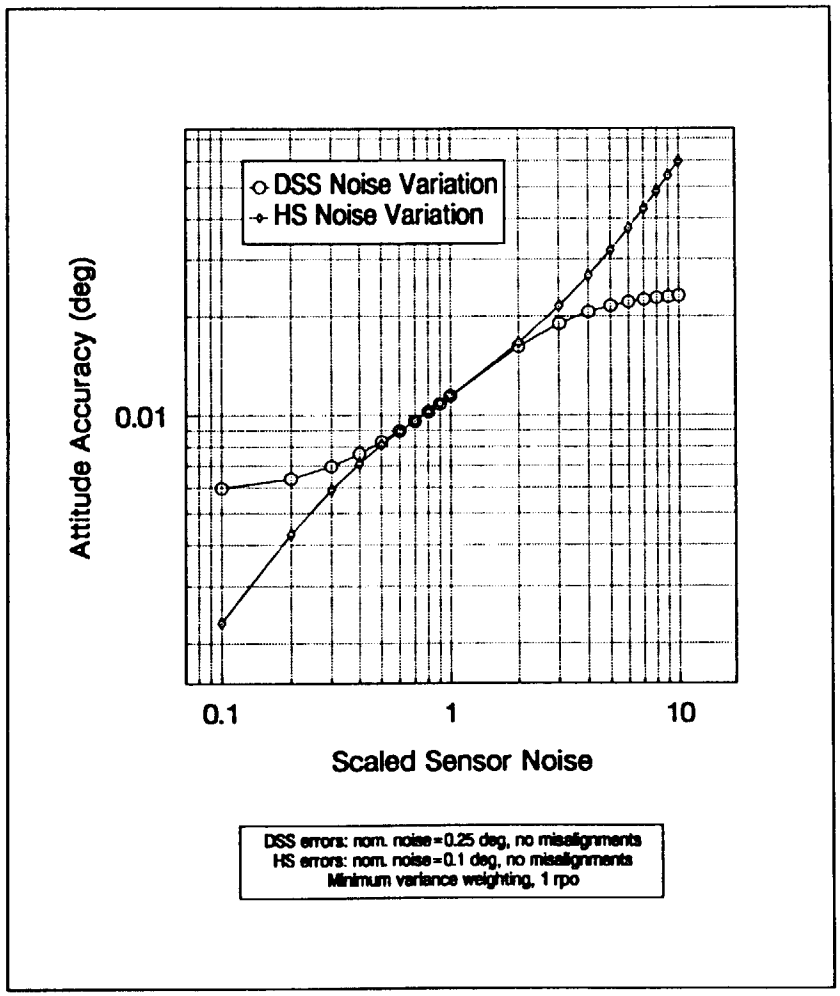

Figure 5-7. The Effect of Sensor Noise Variation on Attitude Determination Accuracy, DSS and HS Sensor Complement

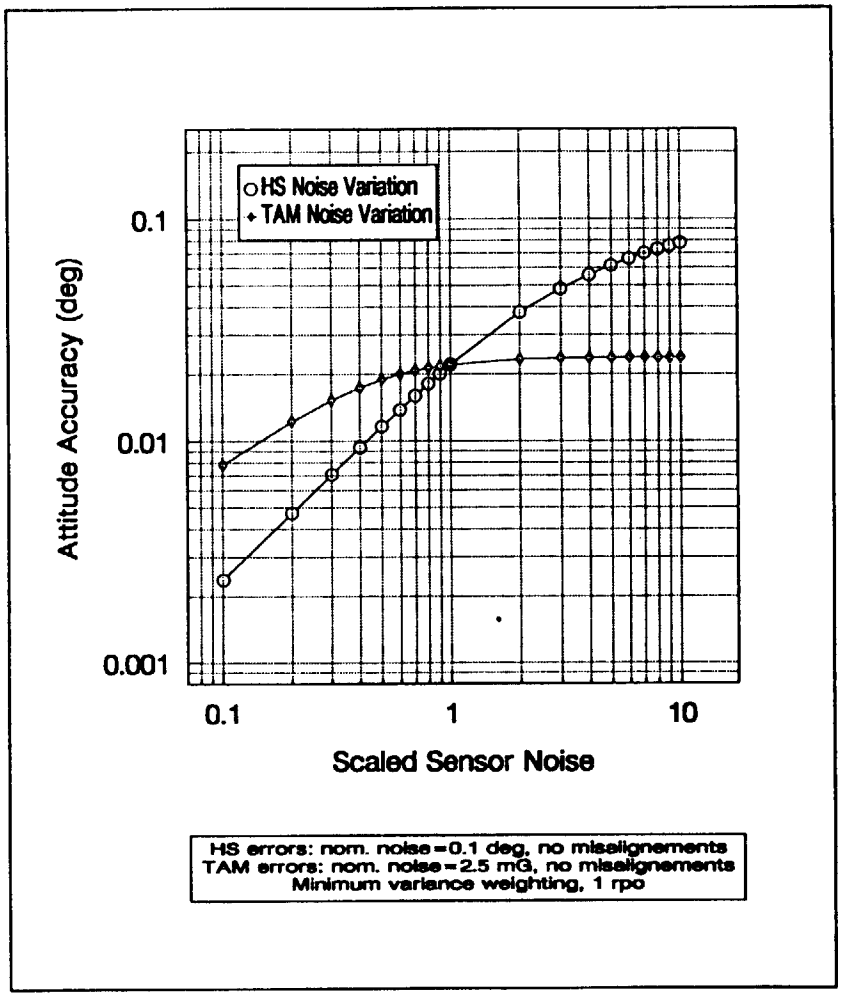

Figure 5-8. The Effect of Sensor Noise Variation on Attitude Determination Accuracy, HS and TAM Sensor Complement

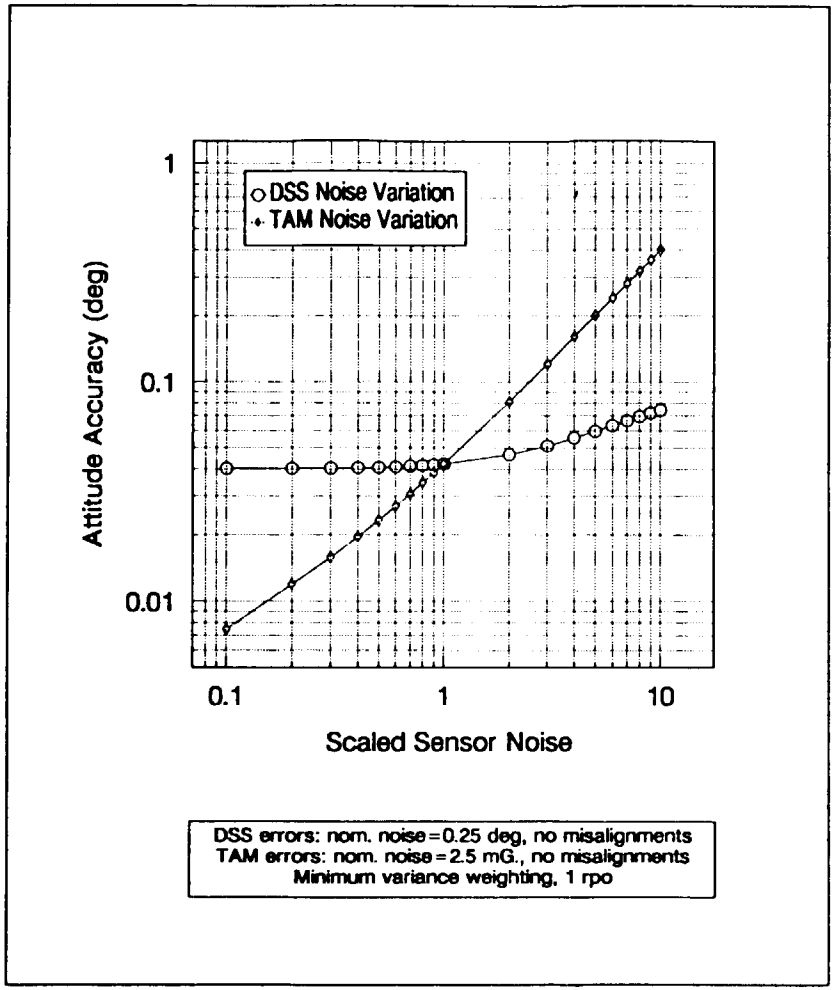

Figure 5-9. The Effect of Sensor Noise Variation on Attitude Determination Accuracy, DSS and TAM Sensor Complement

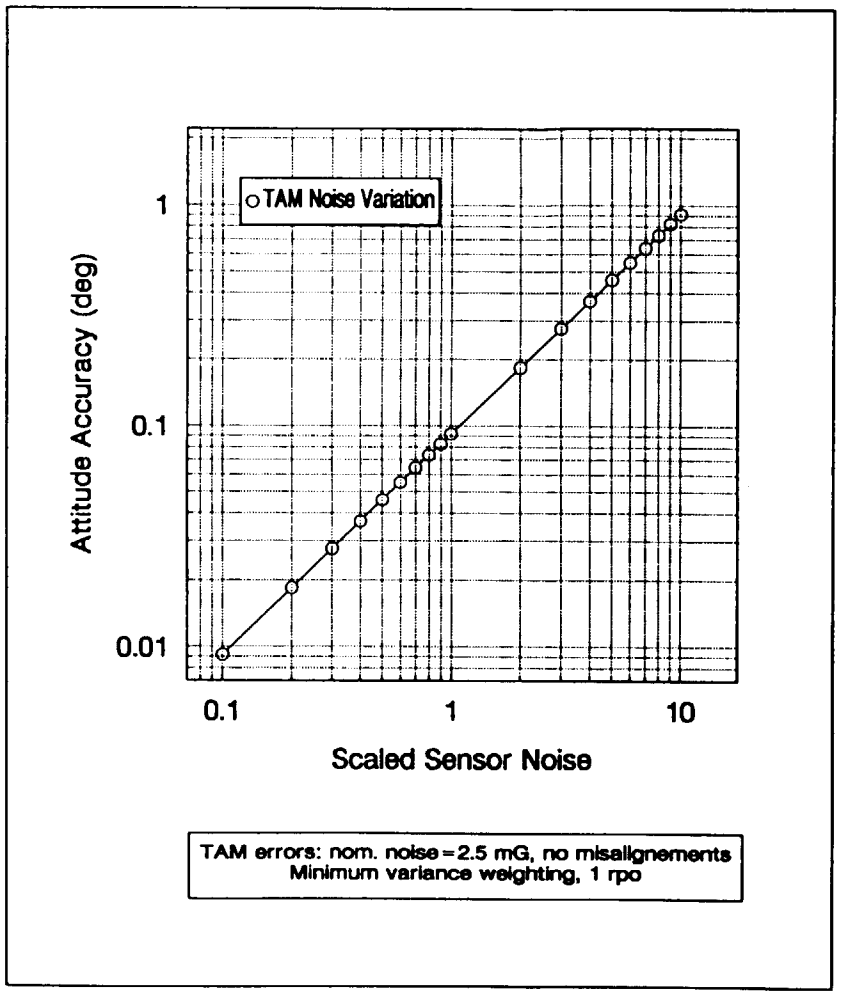

Figure 5-10. The Effect of Sensor Noise Variation on Attitude Determination Accuracy, Magnetometers Only

Table 5-2. Nominal Sensor Noise Levels (1σ)

Sensor	FHST	FSS	HS	DSS	TAM
Nominal noise level	10 arc sec	18 arc sec	0.1 deg	0.25 deg	2.5 mg

5.2 Spin-Stabilized Spacecraft

For spin-stabilized missions the ellipse method (Reference 3) was used. This is an analytical procedure for estimating the spin-axis orientation uncertainty in which each resulting ellipse is the locus of points having a specific error. The solutions are valid for attitude accuracies determined using single-frame methods. The attitude uncertainties are plotted as functions of measurement uncertainties including both the random and the systematic errors and the angle between the sensor.

The results of these studies may be used for qualitative estimation of attitude accuracies. They can provide useful information on how proposed sensor complements, sensor orientations, and noise levels will affect the attitude accuracy.

If the uncertainty in a transmitted measurement is due to either Gaussian-distributed random noise or any unknown systematic error that is assumed to have a Gaussian distribution, then contours of constant attitude uncertainty correspond to ellipses on the celestial sphere (Reference 3). Assuming unitary measurement densities, the semimajor and the semiminor axes can be expressed in terms of the measurement uncertainties U_1 and U_2 as

$$\sigma_1^2 = \frac{1}{2}\frac{U_1^2 + U_2^2}{\sin^2\theta}\left[1 + (1 - 4U_1^2U_2^2\sin^2\theta/(U_1^2 + U_2^2)^2)^{1/2}\right]$$

The boundaries of the error ellipses are lines of constant probability density. The uncertainty along any arbitrary axis is given by the perpendicular projection of the error ellipse onto that axis. A precise statement of the attitude uncertainty for Gaussian errors requires the specification of three independent numbers, e.g., the size and eccentricity of the error ellipse and the orientation of the long axis relative to some arbitrary direction. If it is desirable to use a single parameter to represent the attitude uncertainty, the radius of a circle with the same geometrical area as the error ellipse may be used. This radius is given by

$$U_{mean} = (\sigma_{max}\sigma_{min})^{1/2} = (U_1 U_2/\sin\theta)^{1/2}$$

Note that this representation gives a poor estimate when σ_{max} is much larger than σ_{min}. In such cases, it is better to represent the attitude uncertainty by σ_{max}.

When a pair of sensors is used and the correlation angle is 90 deg the single-frame attitude uncertainty can be estimated from Figure 5-11. This figure presents the variation of U_{mean} as a function of sensor measurement uncertainties. The measurement uncertainties are plotted along the *X*-and *Y*-axes using logarithmic scales. The attitude uncertainty is plotted along the *Z*-axis using a logarithmic scale. To aid in reading the plot, contour lines of equal height (*Z*) values were added. These are marked with dotted lines.

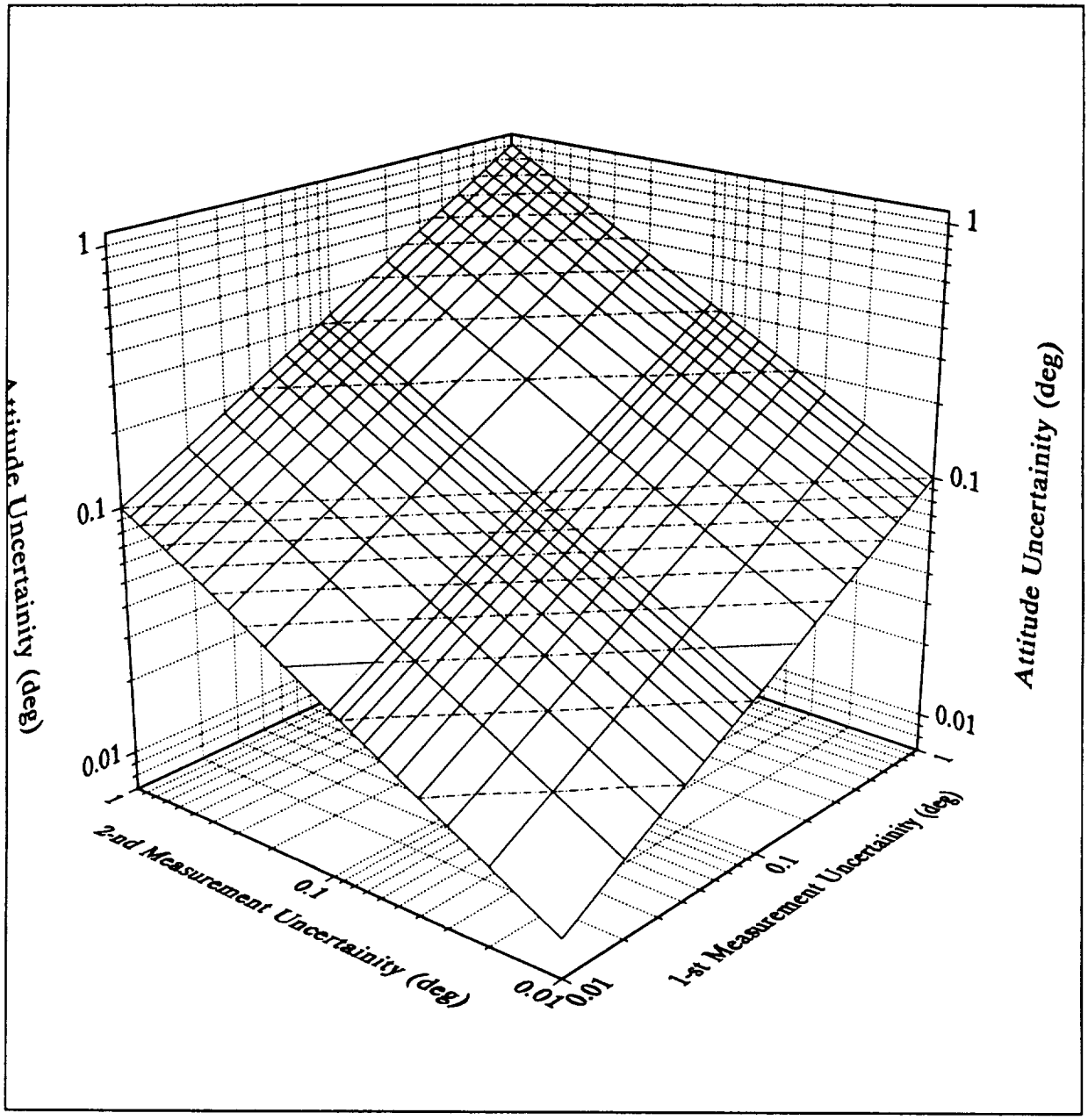

Figure 5-11. The Attitude Uncertainty U_{mean} (deg.) as a Function of Measurement Uncertainties (deg), Correlation Angle, θ = 90 deg.

As an example, consider the case with the first measurement uncertainty of 0.2 and the second of 0.05. The 0.2 value is associated with the auxiliary line located in the *X-Y* plane and intersecting the *X*-axis at the 0.2 tick, the 11th line. The 0.05 value is associated with the auxiliary line intersecting the *Y*-axis at the 0.05 tick, the fifth line. Each auxiliary line located in the *X-Y* plane has a corresponding one on the three-dimensional surface marked with a continuous line. On the three-dimensional surface, the 11th and 5th lines and the 0.1 contour height have a common intersection. This means the attitude uncertainty is 0.1 deg.

A separate plot of this sort would be necessary for each correlation angle, which is impractical to display in this document. To allow for a more concise presentation of the results, the number of independent variables was reduced by using the ratio of measurement uncertainties of the less accurate to the more accurate sensor as one independent variable. The angle between the measurements is a second independent variable and the ratio of the attitude uncertainty to the most accurate sensor measurement uncertainty is the dependent variable. This convention is used in the other figures. These figures may be scaled to actual attitude uncertainties multiplying the ratio by the actual measurement uncertainty of the more accurate sensor.

The correlation angles are plotted along the *X*-axis using a linear scale. The ratio of the measurement uncertainty of the least accurate sensor to that of the most accurate sensor is plotted along the *Y*-axis, using a logarithmic scale. The relative single-frame attitude uncertainty is plotted along the *Z*-axis using a logarithmic scale. Equal height contours (the dotted lines) are drawn on the surface. Figure 5-12 presents the scaled maximum attitude uncertainty associated with the semimajor error ellipse axis. Figure 5-13 presents the scaled U_{mean} values.

The following example clarifies the usage of these two figures. The example refers to Figure 5-12 but the procedure is similar for both figures. Assume that the first sensor measurement uncertainty is 0.1 deg, the second sensor measurement uncertainty is 0.3 deg, and the correlation angle is 18 deg. The measurement uncertainty ratio is therefore 3.0. The auxiliary line drawn on the surface that corresponds to this ratio is the third counting from the lower corner along the lower left surface edge (the edge is considered to be the first line). The auxiliary line corresponding to a correlation angle of 18 deg is the 37th counting from the lower corner, along the lower right surface edge. These two lines intersect between the third and fourth contours. Since the *Z*-axis scale is logarithmic, the height of the intersection point is about 3.3. Therefore, the ratio between the error ellipse semimajor axis, σ_{max}, and the uncertainty of the most accurate sensor is 3.3. This means that $\sigma_1 = 3.3 \times 0.1 = 0.33$ deg.

Single-frame results can be refined through averaging and systematic error estimation. If several frames are averaged and there are only random errors, the attitude uncertainty decreases as $U/N^{1/2}$, where U is the uncertainty presented in the plot and N the number of frames considered. The attitude should be either constant over the timespan considered or the spacecraft dynamics should be very well modeled and the measurements propagated to a common time. On the other hand, systematic errors are to be included in the state vector and determined using estimators, since these errors are not eliminated over multiple frames.

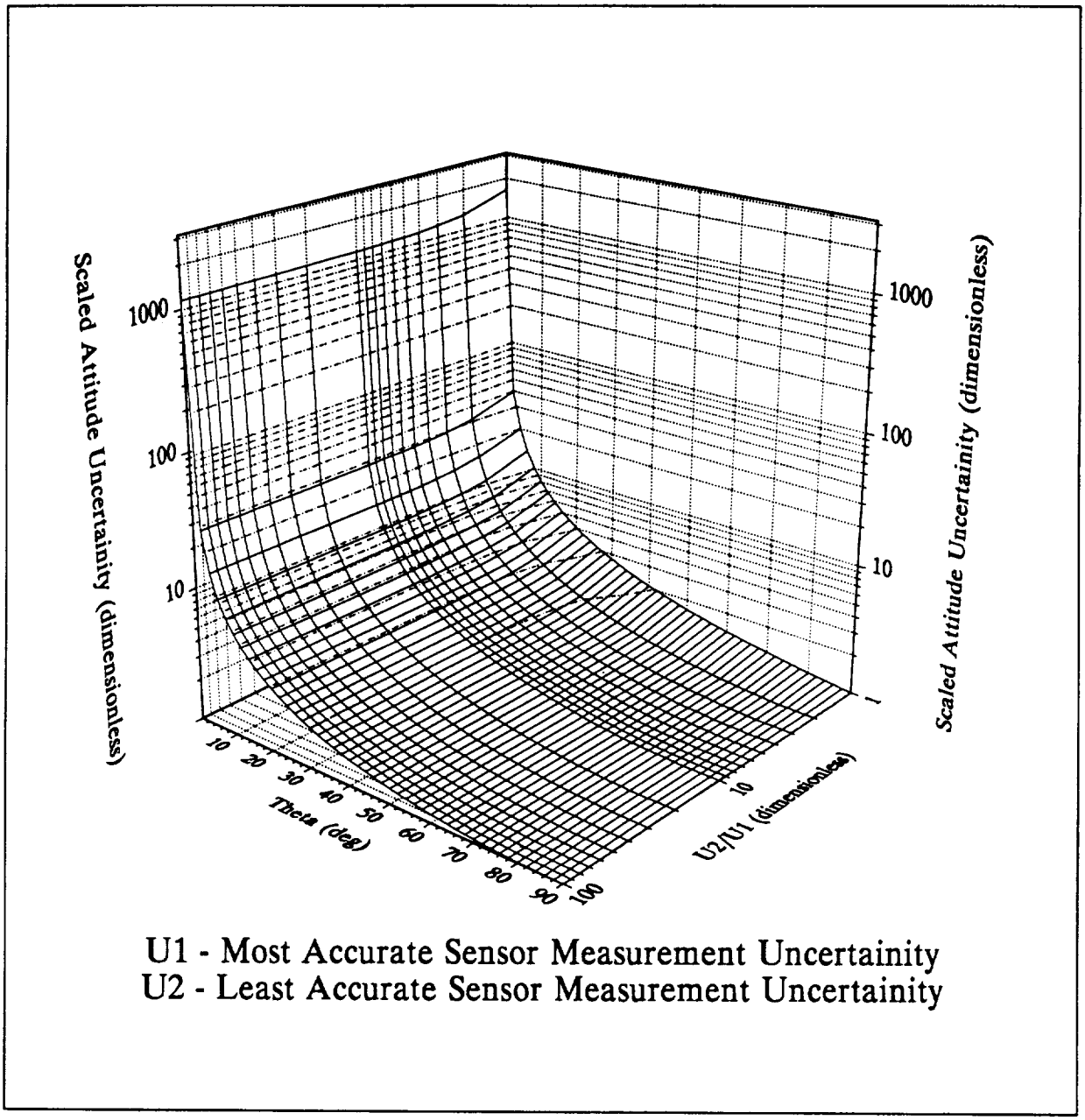

Figure 5-12. Scaled Maximum Attitude Uncertainty, σ_{max}/U_2 as a Function of the Correlation Angle (deg) and the Measurement Uncertainties Ratio

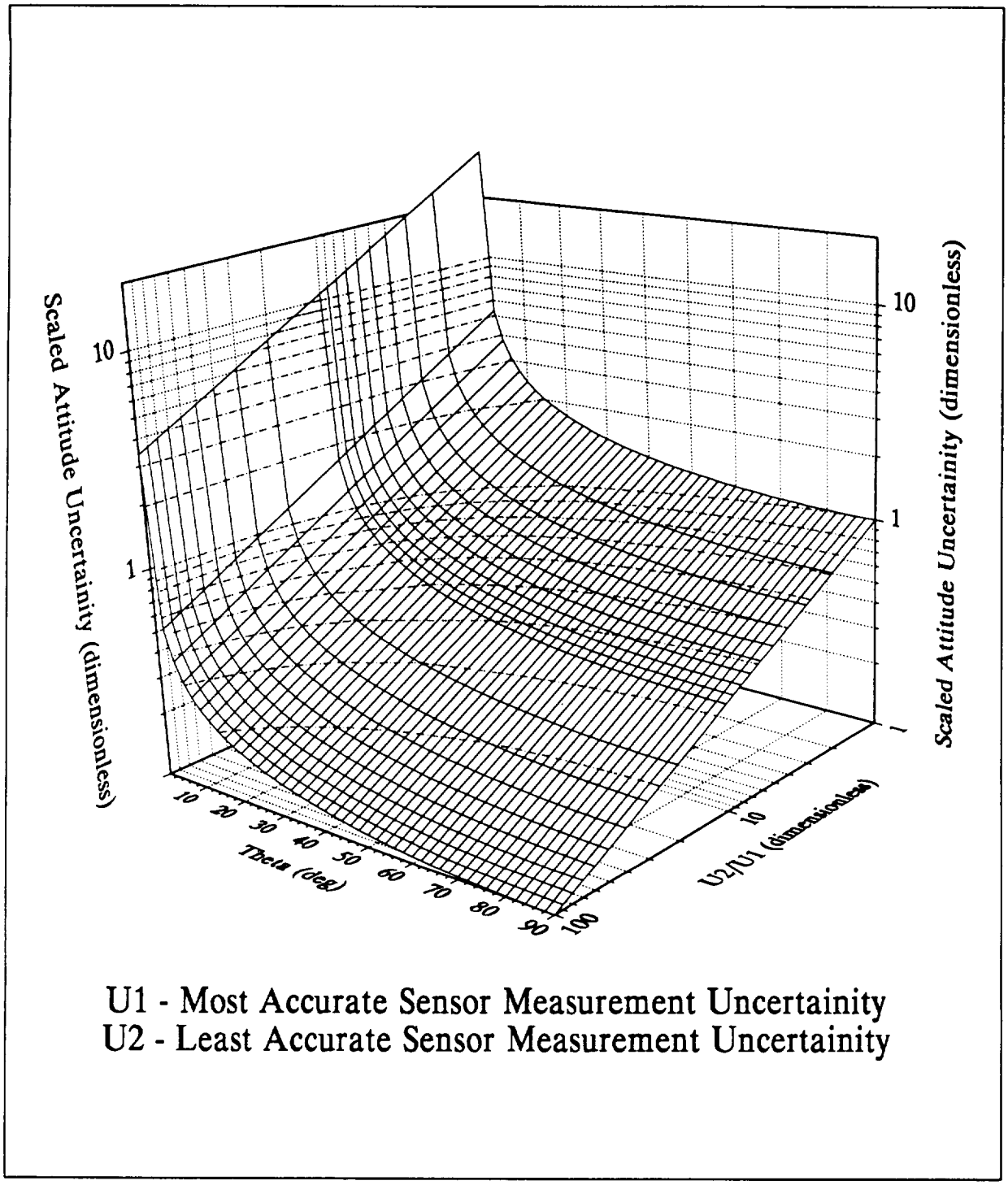

Figure 5-13. Scaled Attitude Uncertainty U_{mean}/U_2 as a Function of the Correlation Angle, θ (deg) and the Measurement Uncertainties Ratio

Section 6. Summary and Conclusions

The attitude determination accuracy survey included 11 spin-stabilized and 12 three-axis-stabilized missions. The three-axis-stabilized missions that were included are DE-2, ERBS, EUVE, GRO, HCMM, MAGSAT, SAGE, SAMPEX, SEASAT, SMM, TOPEX, and UARS. The spin-stabilized missions that were included are AE-3, CTS, DE-1, GOES-3, GOES-5, IMP-8, ISEE-3, IUE, SAS-2, SIRIO, and SSS-1.

These missions used a wide variety of attitude sensors. The sensors used by the three-axis-stabilized missions include the FHST, FSS, DSS, HS, and the TAM. Most of the recent three-axis-stabilized missions use IRUs to propagate measurement data. The attitude sensors used by the spin-stabilized missions surveyed include the single- and multi-slit star scanners, spin mode DSS, spin mode FSS, BHS, and TAM.

The overall accuracy of spin-mode sensors used ranges from 0.05 to about 1 deg. For the three-axis-stabilized missions the accuracy ranges from 0.001 to about 1 deg. The most accurate sensors used on board the three-axis-stabilized missions are the FHST, the related CCD, and the FSS. These instruments achieve high accuracy but at high cost.

Because sensors commonly used on three-axis-stabilized missions are more accurate than those used on spin-stabilized missions, three-axis-stabilized missions can achieve better attitude determination accuracies. For spinning missions, the attitude determination accuracy ranges from 0.1 to 1 deg. For three-axis-stabilized missions the attitude determination accuracy ranges from 0.001 to 2 deg.

Glossary

ADEAS	Attitude Determination Error Analysis System
ADS	Attitude Determination System
AE	Atmospheric Explorer
AEM	Applications Explorer Mission
ASTRA	Advanced Star Tracker
ATA	automatic threshold adjust
AU	Astronomical Unit
BASD	Ball Aerospace Division (now BECD)
BBRC	Ball Brothers Research Corporation (now BECD)
BECD	Ball Electro-optics/Cryogenics Division
BHS	body-mounted horizon scanner
CCD	charge-coupled device
COBE	Cosmic Background Explorer
CSS	coarse Sun sensor
CST	CCD star tracker
CTS	Communications Technology Satellite
DE	Dynamics Explorer
DFSS	digital fine Sun sensor
DSS	digital Sun sensor
ERBS	Earth Radiation Budget Satellite
ESA	Earth sensor assembly
EUVE	Extreme Ultraviolet Explorer
FDD	Flight Dynamics Division
FHST	fixed-head star tracker
FOV	field of view
FPSS	fine-pointing Sun sensor
FSS	fine Sun sensor
GCI	geocentric inertial (coordinate system)
GHz	Gigahertz
GOES	Geostationary Operational Environmental Satellite
GRO	Gamma Ray Observatory
GSFC	Goddard Space Flight Center
HCMM	Heat Capacity Mapping Mission
HDOS	Hughes Danbury Optical Systems
HRMU	Horizon Radiance Modeling Utility
HS	horizon scanner
HST	Hubble Space Telescope
IMP	Interplanetary Monitoring Platform
IRU	inertial reference unit
ISEE	International Sun-Earth Explorer
IUE	International Ultraviolet Explorer
JPL	Jet Propulsion Laboratory

kW	kilowatt
MACS	Modular Attitude Control System
MAGSAT	Magnetic Satellite Mission
mG	Milligauss
MMS	multimission modular spacecraft
MTA	magnetic torquer assembly
NASA	National Aeronautics and Space Administration
NEA	noise equivalent angle
NOAA	National Oceanic and Atmospheric Administration
OA	Office of Applications
OA	Orbit Adjust
OBC	onboard computer
OCS	orbital coordinate system
PAS	Panoramic Attitude Sensor
PF	plan field
POSEIDON	TOPEX/Poseidon (See TOPEX)
PSS	platform Sun sensor
QUEST	quaternion estimator
RMS	root mean square
rpm	revolutions per minute
rpo	revolutions per orbit
SAA	South Atlantic Anomaly
SAGE	Stratospheric Aerosol and Gas Experiment
SAMPEX	Solar, Anomalous, and Magnetospheric Particle Explorer
SAS	Small Astronomy Satellite
S/C	spacecraft
SEASAT	Ocean Studies Satellite
SES	static Earth sensor
SIRIO	Italian Industrial Operations Research Satellite
SMM	Solar Maximum Mission
SOHO	Solar and Heliospheric Observatory
SPF	solar planar field sensor
SSPP	Solar-Stellar Pointing Platform
SSS	Small Scientific Satellite
SSW	sudden stratospheric warming
STS	Space Transportation System
SVB	solar-V beam sensor
SWAS	Submillimeter Wave Astronomy Satellite
TAM	three-axis magnetometer
TOPEX	Ocean Topography Experiment (TOPEX/Poseidon)
TRMM	Tropical Rainfall Measuring Mission
TWT	travelling wave tube
UARS	Upper Atmosphere Research Satellite
USGS	United States Geological Survey
XTE	X-Ray Timing Explorer

References

1. Computer Sciences Corporation, CSC/SD-77/6017UD1, *Applications Explorer Mission-A/ Heat Capacity Mapping Mission (AEM-A/HCMM) Attitude System Functional Specifications and Requirements*, R. Byrne, J. S. Legg, J. W. Wood, et al., January 1977

2. ———, CSC/TM-78/6221, *Applications Explorer Missions-A/Heat Capacity Mapping Mission (AEM-A/HCMM) Postlaunch Report*, D. Niebur, F. Baginski, and R. Byrne, September 1978

3. J. R. Wertz, ed., *Spacecraft Attitude Determination and Control*, Dordrecht: D. Reidel Publishing Company, 1985

4. Computer Sciences Corporation, CSC/TR-84/6008, *Infrared Horizon Sensor Modeling for Attitude Determination and Control*, T. H. Lee, M. C. Phenneger, S. P. Singhal, and T. Stengle (GSFC), November 1984

5. ———, CSC/TR-79/6008, *SEASAT-1 Postlaunch Attitude Analysis*, S. Bilanow, K. W. Chan, G. F. Manders, and M. C. Phenneger, June 1979

6. ———, CSC/TM-79/6073, *AEM-B/SAGE Attitude Analysis*, C. B. Spence, G. Lerner, D. Niebur, et al., March 1979

7. ———, CSC/TM-79/6223, *Application Explorer Missions-2/Stratospheric Aerosol and Gas Experiment (AEM-2/SAGE) Postlaunch Report*, D. P. Niebur, September 1979

8. ———, CSC/TM-81/6043, *MAGSAT Infrared Horizon Scanner Data Evaluation Report*, S. Bilanow, March 1981

9. ———, CSC/SD-78/6077UD1, *MAPS/MAGSAT Attitude System Functional Specifications and Requirements*, M. B. Baker, R. N. Collier, Y. S. Hoh, et al., September 1978

10. ———, CSC/TM-81/6036 *High Precision Attitude Determination for MAGSAT*, G. Abshire, R. McCutcheon, G. Meyers, et al., April 1981

11. Goddard Space Flight Center, Flight Dynamics Division, FDD/553-90/016, *Solar Maximum Mission (SMM), Summary of Operational Attitude Support*, D. S. Pitone (CSC), prepared by Computer Sciences Corporation, April 1990

12. OAO Corporation, *Dynamics Explorer - A and - B Attitude System Functional Specification and Requirements*, December 1979

13. Computer Sciences Corporation, CSC/TR-85/6703, *Earth Radiation Budget Satellite (ERBS) Attitude Support Postlaunch Report*, E. Burges, R. Pendley, and J. Rowe, August 1985

14. ———, CSC/SD-82/6013, *Earth Radiation Budget Satellite (ERBS) Attitude Ground Support System (AGSS) Functional Specifications and Requirements*, B. Fang, K. Liu, M. Radomski, and S. Smith, September 1982

15. Goddard Space Flight Center, Flight Dynamics Division, 554-FDD-91/114R0UD0, *Gamma Ray Observatory (GRO), Flight Dynamics Analysis Team Support, Postlaunch Report*, L. Kulp (CSC), prepared by Computer Sciences Corporation, February 1992

16. Computer Sciences Corporation, CSC/TR-89/6022, *Gamma Ray Observatory (GRO), Flight Dynamics Support System Specifications, III. Mathematical Specifications, Revision 1*, L. Snyder, March 1989

17. ———, CSC/TM-76/6001 *Communications Technology Satellite (CTS) Attitude Analysis and Support Plan*, M. Joseph, J. Oehlert, G. Page et al., February 1976

18. ———, CSC/TM-76/6104 *Communications Technology Satellite (CTS) Postlaunch Report*, P. M. Smith and G. K. Tandon, May 1976

19. ———, CSC/TR-73/6022 *Evaluation of SSS-1 Star Sensor Attitude Determination*, D. F. Alderman, B. M. Beard, H. S. Gotts, and J. E. Kronenfeld, September 1973

20. ———, CSC/TM-79/6061 *ISEE-3 Attitude Postlaunch Report*, P. Batay-Csorba and J. N. Rowe, April 1979

21. ———, CSC/TR-78/6012, *International Sun-Earth Explorer-C (ISEE-C) Attitude Analysis and Support Plan*, J. N. Rowe, P. A. Batay-Csorba, S. K. Hoven, G. Repass (GSFC), May 1978

22. ———, CSC/TM-78/6072, *IUE Attitude Analysis Postlaunch Report*, S. Bilanow, W. Boughton, C. Hsieh, and J. McEnnan, March 1978

23. ———, CSC/TM-77/6305, *International Ultraviolet Explorer Attitude Analysis and Support Plan*, D. R. Sood, December 1977

24. ———, CSC/TM-78/6198 *Flight Dynamics Postflight Report for the Geostationary Operational Environmental Satellite-3 (GOES-3)*, W. Boughton, D. Haley, September 1978

25. ———, CSC/TM-81/6149, *Geostationary Operational Environmental Satellite-5 (GOES-5) Attitude Postlaunch Report*, S. Bilanow, H. L. Hallock, R. McCuthcheon, et al., July 1981

26. ———, CSC/TM-75/6004 *Horizon Sensor Behavior of the Atmosphere Explorer-C Spacecraft*, C. F. Gartrell, M. E. Plett, and K. S .Liu, May 1975

27. ———, CSC/TM-74/6158, *SAS-2 Attitude Processing Study*, V. Norrod, May 1978

28. ———, CSC/TM-77/6264, *SIRIO Attitude Analysis Postlaunch Report*, L. C. Chen, J. J. McEnnan, October 1977

29. Goddard Space Flight Center, Flight Dynamics Division, FDD/554-90/121, CSC/TM-90/6103 *Study of the Earth Albedo Interference on Sun Sensors*, H. Arabshahi (CSC), D. Brasoveanu (CSC), and M. Phenneger (CSC), prepared by Computer Sciences Corporation, September 1990.

30. Computer Sciences Corporation, CSC/SD-88/6004 *Attitude Determination Error Analysis System (ADEAS) Release 4 User's Guide*, D. Dortenzo, M. Nicholson, M. Regardie, October 1988

REPORT DOCUMENTATION PAGE

Form Approved
OMB No. 0704-0188

1. AGENCY USE ONLY *(Leave blank)*	2. REPORT DATE	3. REPORT TYPE AND DATES COVERED
	October 1994	Technical Memorandum

4. TITLE AND SUBTITLE

Spacecraft Attitude Determination Accuracy From Mission Experience

5. FUNDING NUMBERS

550

6. AUTHOR(S)

D. Brasoveanu, J. Hashmall, and D. Baker

7. PERFORMING ORGANIZATION NAME(S) AND ADDRESS (ES)

Goddard Space Flight Center
Greenbelt, Maryland 20771

8. PEFORMING ORGANIZATION REPORT NUMBER

95B00001

9. SPONSORING / MONITORING ADGENCY NAME(S) AND ADDRESS (ES)

National Aeronautics and Space Administration
Washington, DC 20546-0001

10. SPONSORING / MONITORING ADGENCY REPORT NUMBER

NASA TM-104613

11. SUPPLEMENTARY NOTES

Brasoveanu and Hashmall: Computer Sciences Corporation, Lanham, Maryland;
Baker: Goddard Space Flight Center, Greenbelt, Maryland

12a. DISTRIBUTION / AVAILABILITY STATMENT

Unclassified - Unlimited
Subject Category 18

Availability: NASA CASI (301)621-0390.

12b. DISTRIBUTION CODE

13. ABSTRACT *(Maximum 200 words)*

This document presents a compilation of the attitude accuracy attained by a number of satellites that have been supported by the Flight Dynamics Facility (FDF) at Goddard Space Flight Center (GSFC). It starts with a general description of the factors that influence spacecraft attitude accuracy. After brief descriptions of the missions supported, it presents the attitude accuracy results for currently active and older missions, including both three-axis stabilized and spin-stabilized spacecraft. The attitude accuracy results are grouped by the sensor pair used to determine the attitudes. A supplementary section is also included, containing the results of theoretical computations of the effects of variation of sensor accuracy on overall attitude accuracy.

14. SUBJECT TERMS

Accuracy, AE, AEM/HCMM, AEM/SAGE, Attitude, CTS, DE, ERBS, EUVE, GOES, GRO, IMP, ISEE, IUE, MAGSAT, SAMPEX, SAS, Satellite, SEASAT, Sensor accuracy, Sensor pair, SIRIO, SMM, Spin-stabilized, SSS, Three-axis stabilized, TOPEX/POSEIDON, UARS

15. NUMBER OF PAGES

107

16. PRICE CODE

17. SECURITY CLASSIFICATION OF REPORT	18. SECURITY CLASSIFICATION OF THIS PAGE	19. SECURITY CLASSIFICATION OF ABSTRACT	20. LIMITATION OF ABSTRACT
Unclassified	Unclassified	Unclassified	UL